Functional neuroimaging in dementia

Janne Papma

The research described in this thesis was financially supported by Hersenstichting Nederland, Alzheimer Nederland and Stichting Dioraphte.

Financial support for the printing of this thesis was kindly provided by:
Erasmus University Rotterdam
Alzheimer Nederland
Pfizer B.V.
Nutricia Advanced Medical Nutrition
Novartis Pharma B.V.
Internationale Stichting Alzheimer Onderzoek
Theater Veder

Cover & Layout: N. Vermeulen, S. Vinke, Ridderprint BV, Ridderkerk, the Netherlands
Cover photo: Kim van Dijk, Kim van Dijk photography
Printed by: Ridderprint BV, Ridderkerk, the Netherlands
ISBN: 978-90-5335-605-0

Functional Neuroimaging in Dementia

Functionele Neuro-imaging in Dementie

Proefschrift

ter verkrijging van de graad van doctor aan de
Erasmus Universiteit Rotterdam
op gezag van de
rector magnificus

Prof.dr. H.G. Schmidt

en volgens besluit van het College voor Promoties.

De openbare verdediging zal plaatsvinden op
7 december 2012 om 9.30 uur

door

Jacomina Maria Papma
geboren te Noordoostpolder

PROMOTIECOMMISSIE

Promotoren
Prof.dr. P.J. Koudstaal
Prof.dr. J.C. van Swieten

Overige leden
Prof.dr. W.J. Niessen
Prof.dr. S.A.R.B. Rombouts
Prof.dr. G.J. Biessels

Copromotoren
Dr. N.D. Prins
Dr. M. Smits

CONTENTS

PUBLICATIONS AND MANUSCRIPTS BASED ON THE STUDIES DESCRIBED IN THIS THESIS

Chapter 2.1

Papma JM, Smits M, Mattace Raso FU, Niessen WJ, de Koning I, Koudstaal PJ, van Swieten JC, Prins ND. Clinical applicability of 'mild cognitive impairment due to AD' and vascular mild cognitive impairment. Submitted.

Chapter 2.2

Papma JM, Smits M, de Koning I, Mattace Raso FU, van der Lugt A, Vrooman HA, van Swieten JC, Koudstaal PJ, van der Veen FM, Prins ND. Cerebral small vessel disease influences encoding in MCI: an episodic memory related fMRI study. J Alzheimers Dis; Major revision.

Chapter 2.3

Papma JM, den Heijer T, de Koning I, Mattace Raso FU, van der Lijn F, van der Lugt A, van Swieten JC, Koudstaal PJ, Smits M, Prins ND. The influence of cerebral small vessel disease on default mode network deactivation in mild cognitive impairment. Neuroimage Clin; Major revision.

Chapter 2.4

Papma JM, de Groot M, de Koning I, Mattace Raso FU, van der Lugt A, Vernooij MW, Niessen WJ, van Swieten JC, Koudstaal PJ, Prins ND, Smits M. Cerebral small vessel disease affects white matter microstructure in mild cognitive impairment. Hum Brain Mapp; Major revision.

Chapter 3.1

Papma JM, Seelaar H, de Koning I, Hasan D, Reijs AEM, Valkema R, Prins ND, van Swieten JC. Episodic memory impairment in frontotemporal dementia: a ^{99m}Tc-HMPAO SPECT study. Curr Alzheimer Res 2012; Published online 2012 Sep 25.

Chapter 3.2

Seelaar H, Papma JM, Garraux G, de Koning I, Reijs AEM, Valkema R, Rozemuller AJM, Salmon E, van Swieten JC. Brain perfusion patterns in familial frontotemporal lobar degeneration. Neurology 2011; 77(4): 384-392.

Chapter 3.3

Chiu WZ, Papma JM, de Koning I, Donker Kaat L, Seelaar H, Reijs AEM, Valkema R, Hasan D, Boon AJW, van Swieten JC. Midcingulate involvement in progressive supranuclear palsy and tau-positive frontotemporal dementia. J Neurol Neurosurg Psychiatry 2012; 83(9): 910-915.

Chapter 1

General Introduction

Dementia is a devastating disease for both patient and caregiver, as there is little or no treatment available and the usual progressive nature will eventually lead to a total dependence and a drastic shortening of life span. Current estimates indicate that worldwide around 35.6 million people live with dementia, a number that is anticipated to double every 20 years up to 115.4 million dementia cases in 2050 (WHO, 2012). This tremendous rise in dementia will become one of the largest public health problems this century (WHO, 2012), which emphasizes the importance of research regarding pathophysiological processes underlying dementia. The aim of this thesis was to increase knowledge on brain functioning in dementia and its prodromal stage by means of functional neuroimaging.

Dementia is a clinical syndrome that is defined as a deterioration of cognitive functions and activities of daily living. This syndrome can be caused by several neurodegenerative disorders and brain diseases, of which Alzheimer's disease (AD) is the most common cause, representing 60-70 percent of all elderly dementia cases (Jellinger, 2006; WHO, 2012; McMurtray et al., 2005), and a third of dementia cases with a young onset (Harvey et al., 2003). In elderly, vascular dementia (VaD) is the second most common dementia subtype, yet prevalence estimates differ across studies as a consequence of the fact that cerebrovascular pathology often co-occurs with other pathology types, in particular AD (Jellinger, 2006). The second most common cause of young onset dementia is frontotemporal dementia (FTD), estimated to account for about 15 percent of young onset cases (Ratnavalli et al., 2002; WHO 2012; EUROCODE, 2006), disregarding the fact that FTD patients tend to be misdiagnosed during life (Jellinger, 2006). Years before the actual diagnosis of dementia, pathophysiological changes can already become clinically manifest. Mild cognitive impairment (MCI) is a clinical concept that aims to identify individuals at this prodromal dementia stage, characterized by cognitive impairment without interference with normal daily activities.

Early identification of causes of dementia as well as the development of biomarkers becomes increasingly important with emerging disease modifying treatment and increasing knowledge regarding the prognosis of specific dementia subtypes. Early identification however is hampered, first, by a lack of knowledge concerning the effects of pathologic subtypes either in isolation or co-existing, and second, by the fact that various disorders that cause dementia may overlap with respect to clinical and cognitive symptoms. Functional neuroimaging can aid in addressing these kind of issues, as it has the great advantage that it allows to investigate early alterations in brain functioning, even before structural changes become apparent. Functional MRI (fMRI) is at present the most used functional neuroimaging technique in research settings. This technique allows assessing brain activation by detecting associated changes in blood flow. When

neural activity increases there is increased demand of oxygen, provided by a local blood flow increase. These local changes in -oxygenated- blood flow can be detected using a blood oxygenation level-dependent, BOLD, contrast. By the performance of standardized cognitive tasks during fMRI scanning we can subsequently study and localize transient brain activation directly resulting from a specific cognitive event. Another functional neuroimaging technique with well established diagnostic value is perfusion single-photon emission computed tomography (SPECT). Using the ^{99m}Tc-HMPAO tracer one can assess blood flow, which is tightly coupled to local brain metabolism and energy use. Quantitative assessment of neural activity and neural metabolism can aid in unraveling the functional substrates of overlapping symptomatology and identification of the functional role of certain pathologic subtypes in a clinical syndrome.

Using functional neuroimaging techniques, the aim of this thesis was twofold:

1. To study the effects of cerebral small vessel disease on brain functioning as well as on structural connectivity in mild cognitive impairment, using task based fMRI and diffusion tensor imaging. (Chapter 2)
2. To study patterns of impaired brain perfusion underlying cognitive symptoms in early onset AD, FTD and progressive supranuclear palsy, using perfusion SPECT. (Chapter 3)

Chapter 2 studies the influence of cerebral small vessel disease (CSVD) on neural functioning and structural connectivity in MCI. CSVD is a condition affecting the microvessels supplying the white matter and subcortical grey matter regions, which can be assessed on conventional MRI as white matter hyperintensities and lacunar infarcts. While in MCI, CSVD is associated with cognitive impairment and even disease progression, the mechanisms through which CSVD influences clinical and cognitive symptomatology are still largely unknown. **Chapter 2.1** introduces the concepts and terminology of MCI and vascular cognitive impairment, and discusses the applicability of recently proposed criteria for prodromal AD and prodromal VaD. In **Chapter 2.2** and **Chapter 2.3** I studied the influence of CSVD in MCI on neural functioning by means of task based fMRI. **Chapter 2.4** focuses on the effects of CSVD on the normal appearing white matter in MCI, in particular the normal appearing white matter of tracts important for neural network functioning.

Chapter 3 studies patterns of impaired brain perfusion underlying cognitive symptoms in early onset AD, FTD and progressive supranuclear palsy (PSP). Early discrimination between these neurodegenerative conditions during life is hampered by the fact that clinical and cognitive symptomatology can overlap. Quantitative analysis of brain

perfusion SPECT enables us to establish the underlying functional substrates of specific symptomatology in these disorders. **Chapter 3.1** addresses the functional substrate of episodic memory impairment in the behavioral variant of FTD. Brain perfusion patterns in pathological subtypes of FTD are investigated in **Chapter 3.2.** Finally, **Chapter 3.3** focuses on the role of functionally affected brain regions in cognition in PSP in comparison with FTD patients.

In **Chapter 4** I reflect on the main findings, discuss methodological considerations and speculate on the implications of the results and finally give suggestions for future directions of functional neuroimaging in dementia.

REFERENCES

Alzheimer's disease International factsheet, *The Prevalence of Dementia Worldwide* (2008).

EUROCODE: Report of WP7 2006. Prevalence of dementia in Europe. Alzheimer Europe, 2006

Harvey RJ, Skelton-Robinson M, Rossor MN. The prevalence and causes of dementia in people under the age of 65 years. J Neurol Neurosurg Psychiatry 2003; 74: 1206-1209.

Jellinger KA. Clinicopathological analysis of dementia disorders in the elderly-an update. J Alzheimers Dis 2006; 9: 61-70.

Ratnavalli E, Brayne C, Dawson K, Hodges JR. The prevalence of frontotemporal dementia. Neurology 2002; 58: 1615-1621.

World Health Organization 2012. *Dementia: a public priority*

Chapter 2

Functional and structural neuroimaging in mild cognitive impairment

Chapter 2.1

Clinical applicability of 'mild cognitive impairment due to AD' and vascular mild cognitive impairment

Janne M. Papma
Marion Smits
Francesco U. Mattace Raso
Wiro J. Niessen
Inge de Koning
Peter J. Koudstaal
John C. van Swieten
Niels D. Prins

Submitted

Chapter 2.2

Cerebral small vessel disease influences encoding in MCI: an episodic memory related fMRI study

Janne M. Papma
Marion Smits
Inge de Koning
Francesco U. Mattace Raso
Aad van der Lugt
Henri A. Vrooman
John C. van Swieten
Peter J. Koudstaal
Frederik M. van der Veen
Niels D. Prins

Journal of Alzheimer's disease; Major revision.

Chapter 2.3

The influence of cerebral small vessel disease on default mode network deactivation in mild cognitive impairment

Janne M. Papma
Tom den Heijer
Inge de Koning
Francesco U. Mattace Raso
Fedde van der Lijn
Aad van der Lugt
John C. van Swieten
Peter J. Koudstaal
Marion Smits
Niels D. Prins

Neuroimage clinical; Major revision

ABSTRACT

Introduction

Cerebral small vessel disease (CSVD) is thought to contribute to cognitive dysfunction in patients with mild cognitive impairment (MCI). Recent evidence suggests that in healthy elderly CSVD impairs brain deactivation and functional connectivity. The objective of the present study was to examine the effects of CSVD on brain (de)activation in patients with MCI using task based functional MRI (fMRI).

Methods

We included 42 patients with MCI and 25 controls. MCI patients were subdivided into those with (n = 16) and without CSVD (n = 26). All participants underwent a physical and neurological examination, neuropsychological testing, structural MRI, and fMRI during a working memory paradigm.

Results

MCI patients with and without CSVD had a similar neuropsychological profile and task performance during fMRI, but differed with respect to underlying brain (de)activation patterns. MCI patients with CSVD showed impaired deactivation in the precuneus/posterior cingulate cortex, a region known to be involved in the default mode network. In MCI patients without CSVD, brain activation depended on working memory load, as they showed relative 'hyperactivation' during vigilance, and 'hypoactivation' at a high working memory load condition in working memory related brain regions.

Discussion

The observed differences in brain activation and deactivation between MCI patients with and without CSVD, who had a similar 'clinical phenotype', supports the view that, in patients with MCI, different types of pathology can contribute to cognitive impairment through different pathways. We present evidence that the potential underlying mechanisms of CSVD affecting cognition in MCI may be through network interference.

INTRODUCTION

Mild cognitive impairment (MCI) is a clinical construct that classifies individuals with cognitive impairment and high risk of dementia (Albert et al., 2011; DeCarli, 2003; Petersen, 2004). While MCI is a heterogeneous condition, it was found that Alzheimer's disease (AD) and Vascular dementia (VaD) are the most common clinical endpoints, and consequently either Alzheimer pathology, cerebral vascular pathology, or a combination of the two, underlie the great majority of MCI cases (Meyer et al., 2002; Mitchell and Shiri-Feshki, 2009; Petersen et al., 2001). The most common type of cerebrovascular pathology is cerebral small vessel disease (CSVD), which can be visualized on MRI as white matter hyperintensities (WMH) and lacunar infarcts (Pantoni, 2010). In MCI patients, CSVD has been associated with cognitive deficits, including reduced mental processing speed, impaired executive functioning, and deficits in working and episodic memory (Galluzzi et al., 2005; Luchsinger et al., 2009; Nordahl et al., 2005; Nordlund et al., 2007; Villeneuve et al., 2011). Whereas Alzheimer pathology is known to cause cognitive deficits by affecting cortical brain regions, the mechanisms through which CSVD contributes to cognitive impairment are still a matter of debate. It has been postulated that the link between CSVD and cognitive impairment lies in frontal lobe functioning, CSVD causing cognitive impairment through disconnection of cortico-striatal loops resulting in frontal lobe dysfunction (Cummings, 1993; Pugh and Lipsitz, 2002; Tullberg et al., 2004). This hypothesis is supported by results from a recent task based functional MRI (fMRI) study in healthy elderly with CSVD, that showed an association between the extent of vascular burden, reduced neural activation and lower functional connectivity in the prefrontal cortex (Mayda et al., 2011). While the analyses in this study were limited to frontal regions of interest (ROI) and effects of CSVD on neural functioning in the rest of the brain remained unclear, the study does postulate a relationship between structural white matter integrity and neural network functioning underlying cognitive deterioration. Several recent studies have examined this relationship within the default mode network (DMN) (Damoiseaux and Greicius, 2009), a network of brain regions including the medial prefrontal cortex, posterior cingulate cortex (PCC)/precuneus, hippocampus and anterior cingulate cortex (ACC), found to be actively suppressed, i.e. deactivated, during the performance of cognitive tasks (Buckner et al., 2008; Greicius et al., 2003; Raichle et al., 2001).

The objective of this study was to examine the role of CSVD on brain functioning in MCI. For this purpose we assessed fMRI activation as well as deactivation patterns during an n-back working memory paradigm in MCI patients with and without CSVD as well as elderly controls. This paradigm is heavily dependent upon the frontal lobe (Braver et al., 1997), and was previously found to be effective in examining deactivation within the DMN

in MCI (Kochan et al., 2010). We hypothesize that through the interference with structural connectivity, CSVD interferes with network functioning, in particular the DMN. To address this hypothesis we examined deactivation in MCI patients with CSVD, MCI patients without CSVD and controls by means of ROI analysis. This ROI analysis was based on deactivation within controls, restricted to a priori defined regions known to be involved in the DMN, the medial prefrontal cortex, PCC/precuneus, hippocampus and ACC (Buckner et al., 2008; Greicius et al., 2003; Raichle et al., 2001).

METHODS

Participants

We recruited MCI patients, aged 65 years or older, from outpatient clinics of the departments of Geriatrics and Neurology of the Erasmus MC – University Medical Center Rotterdam, the Netherlands, and 7 surrounding hospitals on the basis of criteria for MCI by Petersen (2004; Petersen and Morris, 2005). These criteria include: 1) presence of cognitive complaint by patient or relatives; 2) impairment in one or more cognitive domains; 3) preserved overall general functioning, with possible increased difficulty in the performance of activities of daily living; and 4) absence of dementia according to the DSM-IV or NINCDS ADRDA criteria for dementia. We screened 57 MCI patients for study eligibility. Exclusion criteria were a history of a neurological or psychiatric disorder negatively affecting cognition (e.g. major stroke, cerebral tumor or depression) and contraindication for MRI (e.g. metal implants, claustrophobia). After the initial screening we invited 55 MCI patients to participate in the present study. All patients underwent a standardized work-up, including physical and neurological examination, extensive neuropsychological assessment and structural and functional MRI scanning. After the MRI examinations, we excluded 2 patients due to physical inability or refusal to undergo MRI when presented with the MRI scanner, 1 MCI patient because of excessive head movement (movement more than 1 voxel, 3mm), 2 patients with vision problems, and 8 patients based on insufficient fMRI task performance (as described below). We included the remaining 42 patients in our analyses. Controls (n = 25; 65 years or older) were either relatives of MCI patients, or were recruited through advertisement in the Erasmus MC. The same in- and exclusion criteria applied to the controls, except that controls did not have cognitive complaints and a neuropsychological profile within normal boundaries. Controls underwent the exact same work-up as the MCI patients. All participants gave written informed consent to our protocol that was approved by the medical ethics committee of the Erasmus MC.

Structured interview

We collected data on demographics, general functioning, activities of daily living and vascular risk factors by means of a structured interview. Level of education was assessed with a Dutch education scale ranging from 1 (less than 6 years elementary school) to 7 (academic degree) (Verhage, 1964). We defined hypertension as a systolic blood pressure ≥ 160 mm Hg or diastolic blood pressure ≥ 90 mm Hg or the use of antihypertensive medication.

Neuropsychological assessment

Trained neuropsychologists administered a standardized battery of neuropsychological tests to all participants. The battery included the MMSE as a global cognitive screening method; the Dutch version of the Rey Auditory Verbal Learning Test, i.e. the 15-word verbal learning test (15-WVLT) and the stories of the Rivermead Behavioural Memory Test (RBMT) to assess memory; the Trail Making Test (TMT) part A and Stroop II as measures of cognitive processing speed; the TMT part B, Stroop III, the modified Wisconsin Card Sorting Test (WCST), and a phonological fluency task to assess executive functioning; the Boston Naming Test (BNT; 60 items version) and semantic fluency tasks (animals and occupations) to measure word finding difficulties and lexical retrieval; the subtest Block Design of the Wechsler Adult Intelligence Scale III and clock drawing to assess visuo-spatial and visuo-constructive ability. For every neuropsychological test we calculated z-scores, using the mean and standard deviation of the test scores from the control group (z-score = individual test score minus mean divided by the standard deviation). Subsequently, we constructed composite scores for the following cognitive domains: memory (15 WVLT and RBMT immediate recall and delayed recall), information processing speed (TMTA and Stroop II), executive functioning (TMTB and Stroop III), and language (BNT and semantic fluency tasks). Visuo-spatial skills and visuo-constructive ability are represented by a single neuropsychological test, and consisted of z scores of respectively the Block Design test and clock drawing test. We defined impairment in a cognitive domain as a z-score of -1.5 below the mean score of controls in that domain.

MRI acquisition protocol

We performed structural and functional MR imaging on a 3.0T MRI scanner with an 8-channel head coil (HD platform, GE Healthcare, Milwaukee, US). High resolution 3 dimensional (3D) inversion recovery fast spoiled gradient recalled T1-weighted structural MRI was acquired in the axial plane with the following parameters: repetition time (TR) = 10.4 ms, echo time (TE) = 2.1 ms, inversion time (TI) = 300 ms, flip angle 18°, acquisition matrix 416x256, field of view (FOV) = 250x175 mm^2. We acquired 192 slices with a slice thickness of 1.6 mm with 0.8 mm overlap in a total acquisition time of 4:57 min. T2-fluid attenuated inversion

recovery (FLAIR) images were obtained with the following parameters: TR = 8000 ms, TE = 120 ms, TI = 2000 ms, acquisition matrix 256x128 mm^2, FOV = 210x210 mm^2. We acquired 64 contiguous slices with a slice thickness of 2.5 mm in a total acquisition time of 3:13 min. Whole brain functional MRI images were obtained with a single shot T2* weighted echo-planar imaging (EPI) sequence sensitive to *blood oxygenated level dependent* (BOLD) contrast with the parameters: TR = 2500 ms, TE = 30 ms, flip angle 75°, acquisition matrix 64x96, FOV = 250x250 mm^2. We acquired 32 contiguous slices with a slice thickness of 3.5 mm. The total acquisition time was 6:43 min. Functional data acquisition included 5 dummy scans, which we discarded from further analysis.

Visual assessment of lacunar infarcts and WMH on MRI

A neurologist (NDP), experienced in the assessment of CSVD on MRI, assessed lacunar infarcts and WMH through visual inspection of the 3D T1-weighted and T2-FLAIR MRI images, blinded for clinical information. We used the semi-quantitative rating scale of Fazekas to rate the presence and severity of WMH and recorded the number of lacunar infarcts on MRI (Fazekas et al., 2002). Lacunar infarcts were defined as subcortical infarcts smaller than 20 mm in size (Fisher et al., 1982). Based on the definition used in other studies (Frisoni et al., 2002; Nordlund et al., 2007), we defined the presence of CSVD as the presence of severe WMH (Fazekas score 2 or higher) affecting both posterior and anterior white matter regions, and/or the presence of two or more lacunar infarcts on MRI. We subsequently classified MCI patients as MCI patients with CSVD (n = 16), or MCI patients without CSVD (n = 26).

Automated MRI tissue segmentation and volumetric analysis of WML and hippocampi

Based on intensities of the 3D T1-weighted and T2-FLAIR MRI scans, we used a validated k-nearest neighbour classifier to automatically classify tissues into cerebrospinal fluid, grey matter, normal appearing white matter and WMH (de Boer et al., 2009; Vrooman et al., 2007). The hippocampus was segmented using the 3D T1-weighted image by means of an automated method as described previously (den Heijer et al., 2010; van der Lijn et al., 2008). Briefly, the two most important components of this method are a statistical intensity model and a spatial probability map. The intensity model describes the typical intensities of the hippocampus and the background. The spatial probability map is derived from the registration of multiple atlases and contains the probability of being part of the hippocampus for every voxel. A single rater (TdH), blinded for clinical information, visually inspected the results of all automated hippocampal segmentations, and where necessary manually corrected these using FSLView. To account for differences in head size, we divided all measured volumes by total intracranial volume (TIV).

Functional MRI paradigm

We used a visual n-back task to engage working memory (Owen et al., 2005; Smits et al., 2009). Participants received instructions and practiced the task 30 minutes prior to MRI scanning. Within the scanner visual stimuli were presented onto a back-projection screen, using Presentation software (version 14.4, Neurobehavioral Systems Inc, Albany, CA, US). The screen was visible within the scanner with a mirror mounted on the head coil. External triggering by the MR system ensured synchronization of the stimulus presentation and precise recording of task performance and response times. Participants responded with a button press, which was recorded using MR-compatible fibre optic response buttons. We implemented the n-back task as a block design consisting of 3 active conditions with increasing working memory load: 0-back (vigilance), 1-back (low working memory load), 2-back (high working memory load), and a rest condition. During the rest condition no visual stimuli were presented (black screen), and participants were instructed to keep their eyes open. The condition and rest blocks were preceded by a visual instruction of 3 s, and each block lasted 30 s. Active conditions consisted of 10 stimuli (numbers 0-9), with an inter-stimulus interval of 3 s, during which 3 or 4 'hit' stimuli had to be identified. Each active block was presented 3 times, intermixed and counterbalanced with 4 rest conditions.

Functional MRI behavioral data analysis

Behavioral data consisted of task performance and reaction time (RT). Similar to Snodgrass and Corwin (1988) we defined hit rate (H) as the probability of correct response, *P* (H/total possible hits), and false alarm rate (FA) as the probability of false alarm *P* (FA/total possible non-hits). Task performance was subsequently calculated for the separate conditions (0-back, 1-back, 2-back) using d prime, a measure of sensitivity to true-positive items (Snodgrass and Corwin, 1988). In addition we calculated the index Performance *Pr* = H – FA, where *Pr* = 1 reflects perfect performance and *Pr* = 0 reflects chance performance (Langeslag et al., 2009). Eight MCI patients (3 without CSVD and 5 with CSVD) with an average *Pr* < 0.5 were excluded from our fMRI analyses to ensure that differences in brain activation were related to pathological changes instead of performance-related variability (Price and Friston, 1999), and we based the analyses on the remaining 42 MCI patients and 25 controls in our fMRI analyses.

Functional MRI data analysis

We analyzed fMRI data using Statistical Parametric Mapping software (SPM5; Wellcome Department of Cognitive Neurology, London, UK), implemented in Matlab R2009b (Mathworks, Natick, MA, USA). On an individual level, we spatially realigned all functional images using a rigid body transformation, and coregistered these images to the individual's

T1-weighted image. To normalize functional and anatomical images we performed a unified segmentation/normalization procedure to standard brain space defined by the Montreal Neurological Institute (MNI) as provided within SPM5 (Ashburner and Friston, 2005). Functional images were resampled into 3x3x3 mm^3 voxels and spatially smoothed with a 10 mm full width half maximum Gaussian kernel. We calculated individual statistical parametric maps using the general linear model. Our design matrix included the rest condition, the active conditions, the instruction, a high-pass filter of 128 s and individual movement parameters to account for residual effects of head movement. At a single-subject level we contrasted BOLD response during vigilance (0-back), low (1-back) and high (2-back) working memory load against baseline 'rest' activity. These contrasts were entered into second level one-sample and two sample t-tests, examining both activation and deactivation within and between groups. In addition to these analyses we created a flexible factorial model with group (controls, MCI patients with CSVD and MCI patients without CSVD) x working memory load (vigilance, low and high working memory load). We examined the main effect of working memory load on fMRI BOLD response, as well as interaction effects between controls and MCI patient groups.

Results for within group analyses, both activation and deactivation results, were thresholded at $p < 0.05$ family wise error (FWE) correction for multiple comparisons. Since at this stringent threshold no deactivation was seen in patient groups, we further explored within group deactivation results at a more lenient threshold of $p < 0.001$, not corrected for multiple comparisons, with at least 20 contiguous voxels. We focused our between group analyses, main effect and interaction analyses, on regions of interest (ROIs) that were shown to be relevant to activation during nonverbal n-back tasks in a meta-analysis study of Owen et al. (2005). These regions include the lateral premotor cortex, the cingulate gyrus, the dorsolateral prefrontal cortex and the inferior parietal lobule. We used the WFU Pickatlas toolbox (Wake Forest School of Medicine, Winston Salem), to create 4 masks containing the bilateral ROIs. Reported results of activation in between group analyses and main or interaction analyses survived FWE correction for multiple comparisons within the ROIs using small volume correction (Friston, 1997; Worsley et al., 1996), or within the entire brain for regions not a priori specified.

For exploration of the deactivation results, we created a ROI based on the within group analysis in controls and a priori selected regions known to be involved in the default mode network. We created a mask of the a priori defined regions using WFU Pickatlas. In addition, we identified clusters of deactivation within the 0-back, 1-back and 2-back conditions in controls, by contrasting them vs. the rest condition ($p < 0.001$ not corrected for multiple comparisons). We created one single mask of these regions using an AND function in MarsBar 0.41 (Marseille Boîte À Région d'Intérêt), in which we also included the a priori selected regions. The resulting deactivation ROI included therefore only

those regions known to be involved in the DMN, and deactivated during all conditions in controls (Figure 4 a). Within this ROI we extracted mean beta values and subsequently exported these to SPSS (version 17.0 for Windows, Chicago, Ill. U.S.A.) for further analyses. Anatomical labelling of significantly activated clusters was performed using WFU Pickatlas.

Statistical analysis

We compared demographic, neuropsychological, imaging characteristics and mean beta values using SPSS. Differences between groups on continuous variables were assessed with analysis of variance (ANOVA) and post hoc independent sample t-tests. Non parametric data were compared using Kruskal-Wallis, followed by Mann-Whitney *U* tests. Between group analyses of nominal variables were performed by means of Chi-square tests. We performed a group (controls, MCI patients with CSVD, MCI patients without CSVD) x load (0-back, 1-back, 2-back) ANOVA for the fMRI behavioral measures d prime and RT as well as mean beta values from the deactivation ROI. Post hoc two sample t-tests were performed to further investigate the significant results for d prime, RT and mean beta values. In all of the above mentioned statistical analyses a p value <0.05 was considered statistically significant.

RESULTS

Characteristics

Characteristics of MCI patients and controls are listed in table 1. The percentage of women was lower in MCI patients without CSVD relative to controls, and hypertension was more often present in MCI patients with CSVD and healthy controls as compared with MCI patients without CSVD.

Table 1 Characteristics of controls and MCI patients with and without cerebral small vessel disease

	Controls (n = 25)	MCI total group (n = 42)	MCI with CSVD (n = 16)	MCI without CSVD (n = 26)
Age, years	71.6 (5.2)	73.4 (4.4)	74.3 (4.4)	72.8 (4.4)
Sex, women (%)	11 (44.0)	8 (19.0)[a]	5 (31.3)	3 (11.5)[a]
Education	5.5 (1.2)	5.4 (1.2)	5.6 (1.2)	5.3 (1.2)
MMSE	28.8 (1.2)	27.2 (2.0)[a]	27.2 (1.8)[a]	27.2 (2.1)[a]
Hypertension, prevalence (%)	17 (68.0)	24 (57.1)	14 (93.3)	10 (38.5)[a,b]
Smoking, prevalence (%)*	15 (60.0)	30 (71.4)	14 (87.5)	16 (61.5)
APOE -/ε4, prevalence (%)†	6 (28.6)	21 (53.8)	10 (71.4)	11 (44.0)[a]

Values are unadjusted means (standard deviation) or number of participants (percentages). MCI: mild cognitive impairment. CSVD: cerebral small vessel disease. MMSE: mini mental state examination.
* Prevalence current and former smoking. † Missing data for 4 controls, 2 MCI patients with CSVD and 1 MCI patient without CSVD. Differences between groups by means of independent sample t-test or Chi-Square test: [a] p <0.05 compared with controls [b] p <0.05 compared with MCI patients with CSVD.

Neuropsychological test results

Table 2 summarizes the neuropsychological test results. After correcting for age, sex and education, MCI patients with and without CSVD showed a cognitive profile with memory impairment as the most prominent finding. In addition, MCI patients with and without CSVD performed worse on executive functioning relative to controls. MCI patients without CSVD performed worse on tasks for language as compared with both controls and MCI patients with CSVD. Other cognitive domains revealed no differences between MCI patients with and without CSVD.

Table 2 Neuropsychological test results for controls and MCI patients with and without cerebral small vessel disease

	Controls (n = 25)	MCI with CSVD (n = 16)	MCI without CSVD (n = 26)
Memory	0.00 (0.72)	-1.74 (0.74)[a]	-1.69 (0.70)[a]
Processing speed	0.00 (0.87)	-0.68 (1.07)	-0.54 (1.00)
Executive function	0.00 (0.90)	-0.94 (1.40)[a]	-0.88 (1.43)[a]
Language	0.00 (0.71)	-0.63 (0.83)	-1.41 (1.34)[a,b]
Visuospatial ability	0.00 (1.00)	-0.35 (1.32)	-0.54 (1.13)
Visuoconstructive ability	0.00 (1.00)	-0.73 (1.10)	-0.36 (1.70)

Values are unadjusted z-score means (standard deviation). MCI: mild cognitive impairment. CSVD: cerebral small vessel disease. Differences between groups were calculated by means of ANCOVA corrected for age, sex and education: [a] $p < 0.05$ compared with controls [b] $p < 0.05$ compared with MCI patients with CSVD.

Structural MRI measures

According to the classification used, MCI patients with CSVD had higher Fazekas scores, higher incidence of lacunar infarcts and showed greater WMH volumes, relative to TIV as well as volume in ml, compared with MCI patients without CSVD and controls (table 3). In addition, both MCI patients with and without CSVD had lower hippocampal volumes than controls.

fMRI task performance

Task performance, characterized by d prime and RT, was influenced by working memory load, with lower d prime scores and longer RT at high working memory load (main effect for task d prime $F(2,195) = 50.3$, $p < 0.001$; main effect for task RT; $F(2,195) = 22.0$, $p < 0.001$. Task performance differed between controls and MCI patient groups, independent of working memory load (main effect for group d prime $F(2,195) = 3.8$, $p = 0.023$; main effect for group RT $F(2,195) = 4.3$, $p = 0.015$). There were no significant interaction effects. The significant main effect for group seemed to be driven by significantly worse performance during the low (1-back) working memory load condition in MCI patients without CSVD relative to controls (d prime 1-back: $p = 0.014$; RT 1-back: $p = 0.013$).

Table 3 MRI characteristics for controls and MCI patients with and without cerebral small vessel disease

	Controls (n = 25)	MCI with CSVD (n = 16)	MCI without CSVD (n = 26)
WMH Fazekas score*	0 (0; 1)	2 (2; 2)[a]	1 (0; 1)[b]
Lacunar infarcts, prevalence (%)	2 (8.0)	7 (43.8)[a]	3 (11.5)[b]
Gray matter	41.3 (3.2)	39.8 (3.0)	40.7 (2.4)
White matter	37.9 (0.2)	35.8 (2.5)[a]	36.7 (2.3)[b]
WMH, volume in ml*	15.1 (11.8; 22.8)	30.8 (23.9; 40.9)[a]	16.0 (10.7; 20.9)[b]
WMH*	1.4 (1.1; 2.2)	2.8 (2.6; 3.7)[a]	1.3 (1.0; 1.6)[b]
Left hippocampus	0.29 (0.03)	0.26 (0.03)[a]	0.24 (0.04)[a]
Right hippocampus	0.28 (0.03)	0.26 (0.03)[a]	0.25 (0.03)[a]

Values are unadjusted means (standard deviations) or number of participants (percentages). MCI: mild cognitive impairment. CSVD: cerebral small vessel disease. * median (interquartile range). Gray matter, white matter and white matter hyperintensities, left and right hippocampal volumes are proportions of total intracranial volume. Differences between groups by means of ANCOVA corrected for age and sex, Mann-Whitney *U* test or Chi Square tests: [a] $p < 0.05$ compared with controls [b] $p < 0.05$ compared with MCI patients with CSVD.

MCI patients without CSVD did not differ from controls on the 0-back (d prime 0-back: p = 0.674; RT 0-back: p = 0.170) or 2-back condition (d prime 2-back: p = 0.076; RT 2-back: p = 0.103). MCI patients with CSVD did not differ from controls on the 0-back, 1-back or 2-back condition (d prime 0-back: p = 0.765; RT 0-back: p = 0.253; d prime 1-back: p = 0.112; RT 1-back: p = 0.262; d prime 2-back: p = 0.348; RT 2-back p = 0.123). MCI patients with and without CSVD showed similar task performance (d prime 0-back: p = 0.933; RT 0-back: p = 0.886; d prime 1-back: p = 0.514; RT 1-back: p = 0.239; d prime 2-back: p = 0.569; RT 2-back: p = 0.776).

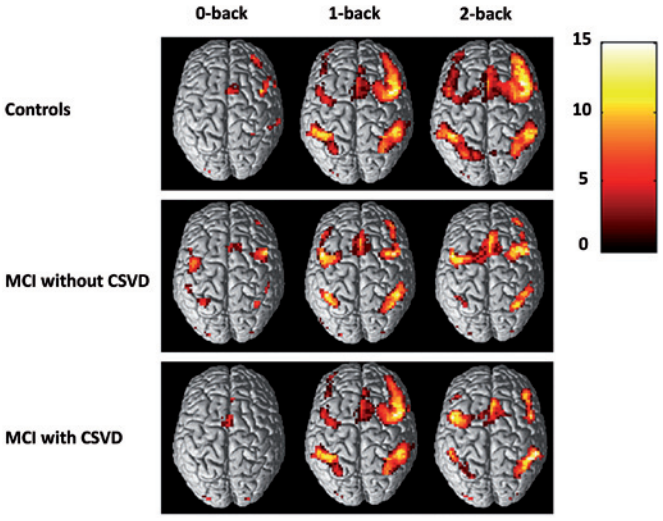

Figure 1 Within group fMRI *activation* results for different levels of working memory load (0-back versus rest; 1-back versus rest, 2-back versus rest), results displayed at p <0.05 FWE correction for multiple comparisons.

fMRI BOLD – task related activation

Vigilance, low and high working memory load conditions activated a wide network of regions that was similar in controls and patient groups and included: bilaterally the middle, medial, and inferior frontal lobe, the inferior and superior parietal lobe and the inferior occipital lobe (Figure 1), activated regions consistent with previous fMRI studies using an n-back working memory paradigm (Owen et al., 2005).

Table 4 Between group analyses

	Cluster size	MNI coordinates			T value
		X	Y	Z	
0-back; MCI without CSVD > Controls					
Inferior parietal lobule R	201	45	-42	42	5.96
		36	-57	42	3.99
Middle frontal gyrus L	100	-30	0	51	5.01
Middle frontal gyrus R	134	30	3	51	4.76
		27	24	48	3.46
Inferior parietal lobule L	98	-42	-51	48	4.45
2-back; Controls > MCI without CSVD					
Middle frontal gyrus R	17	42	39	30	4.07

Results at p <0.05 FWE small volume correction.

We found no difference in brain activation between controls and MCI patients with CSVD for different levels of working memory load. Relative to controls, MCI patients without CSVD showed significant increased activation, 'hyperactivation', during vigilance (0-back) bilaterally in the inferior and middle frontal gyrus (Figure 2 A, table 4); and less activation, 'hypoactivation', during high working memory load (2-back) in the right middle frontal gyrus (Figure 2 B, table 4). A direct comparison between the two MCI patient groups revealed no significant differences for various levels of working memory load.

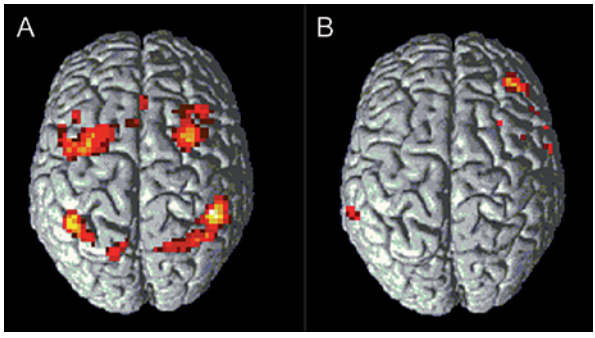

Figure 2 A) Activation in 2 sample t-test MCI without CSVD > Controls during vigilance (0-back versus rest). B) Activation in 2 sample t-test Controls > MCI without CSVD during high working memory load (2-back versus rest). Results displayed at p <0.001, not corrected for multiple comparisons, for illustrative purposes.

Main effect analyses for working memory load in a 3 x 3 flexible factorial model revealed the same extensive networks of regions found in the within group analyses; and showed increased activation with increasing working memory load (results not shown). Results of interaction analyses are summarized in table 5. When examining group x load interactions we found that controls showed a significantly larger increase in activation with increasing levels of working memory load (2 back > 0-back and 2-back > 1-back) when compared with MCI patients without CSVD in bilateral regions involved in the n-back task, including the bilateral inferior parietal lobule, the bilateral middle and superior frontal gyrus and the anterior cingulate gyrus (Owen et al., 2005). Vice versa, the interaction contrasts of MCI patients without CSVD versus controls yielded no significant results. These results support the findings of 'hyperactivation' at vigilance and 'hypoactivation' at high working memory load encountered in between group analyses in MCI patients without CSVD. When we examined interaction effects between the two patient groups we encountered a significant effect for the anterior cingulate gyrus, for the contrast (MCI with CSVD > MCI without CSVD) x (2-back > 1-back). This implies a difference in working memory load dependent fMRI response in MCI patients without CSVD as compared with MCI patients with CSVD. We found no significant interaction effects between controls and MCI patients with CSVD.

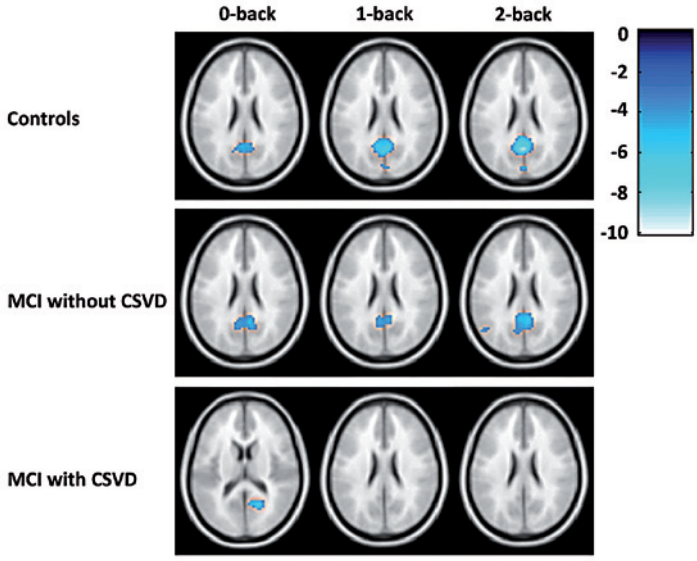

Figure 3 Within group fMRI *deactivation* results for different levels of working memory load (0-back versus rest; 1-back versus rest, 2-back versus rest), results displayed at p <0.001, not corrected for multiple comparisons.

Table 5 MNI coordinates interaction contrasts for controls and MCI patient groups with and without CSVD

	Cluster size	MNI coordinates			T value
		X	Y	Z	
(Controls > MCI without CSVD) x (2-back > 0-back)					
Inferior parietal lobule R	79	48	-63	39	4.61
Inferior frontal gyrus L	23	-45	48	-3	4.00
Middle frontal gyrus R	71	30	15	42	3.99
Middle frontal gyrus L	18	-36	21	45	3.61
Inferior parietal lobule L	11	-51	-39	42	3.22
(Controls > MCI without CSVD) x (2-back > 1-back)					
Cingulate gyrus L	280	-12	24	39	4.16
Middle frontal gyrus L		-27	18	45	3.80
Superior frontal gyrus L		-12	39	36	3.75
Anterior cingulate gyrus L		-21	45	9	3.65
Anterior cingulate gyrus L	57	-6	33	9	4.01
Medial frontal gyrus R	425	15	30	45	3.96
Superior frontal gyrus R		18	48	30	3.84
(MCI with CSVD > MCI without CSVD) x (2-back > 1-back)					
Anterior Cingulate gyrus L+R	25	0	21	21	3.48

Results at p <0.05 FWE small volume correction.

fMRI BOLD – task induced deactivation

We found within group task induced deactivation within the precuneus/PCC in controls during low and high working memory load conditions when thresholded at p <0.05 FWE correction for multiple comparisons. At a more lenient threshold of p <0.001, not corrected for multiple comparisons, MCI patients without CSVD showed deactivation in the precuneus/PCC during all working memory load conditions, with additional deactivation of the medial frontal gyrus in MCI patients without CSVD (Figure 3, table 6). MCI patients with CSVD, showed task-induced deactivation in the PCC during vigilance, but no deactivation during low and high working memory load conditions (Figure 3). We used a ROI analysis of deactivated regions within the DMN in controls to further explore these differences in task-induced - within group - deactivation. The resulting ROI comprised the precuneus/PCC region (Figure 4 A, B). A group x working memory load ANOVA, revealed a significant main effect for group for this ROI (p = 0.008), without a significant main effect for working memory load or a significant interaction effect. Concentrating on the two MCI patient groups, we found a trend for the main effect of group (p =0.098). Post hoc, mean beta values differed between controls and MCI patients with CSVD during the 2-back condition in the precuneus/PCC region (p = 0.028).

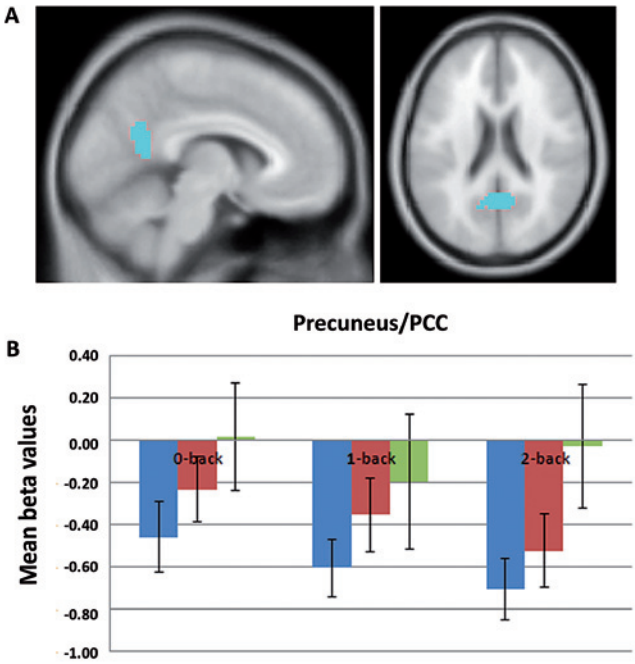

Figure 4 A) ROI analysis, obtained with AND function of 0-back, 1-back and 2-back contrast in controls in conjunction with a priori defined DMN ROI. B) Chart diplays group differences in mean beta values for the ROI.

DISCUSSION

In the present fMRI study we examined differences in brain activation and deactivation during a working memory task in MCI patients with and without CSVD and controls. We found evidence for impaired task induced brain deactivation in a region known to be involved in the default mode network in MCI patients with CSVD. MCI patients without CSVD showed 'hyperactivation' during vigilance, and 'hypoactivation' at high working memory load.

We found a similar cognitive profile in MCI patients with and without CSVD with memory impairment as the most prominent finding, and additional executive functioning problems. MCI patients without CSVD performed worse on language related tasks when compared with MCI patients with CSVD and controls. The presence of CSVD is typically associated with a prominent dysexecutive cognitive syndrome and memory deficits to a far lesser extent (Nordahl et al., 2005; Prins et al., 2005), as specifically frontal circuits are thought to be affected by white matter lesions and lacunar infarcts (Cummings, 1993; Pugh and Lipsitz, 2002). In this context, memory impairment has been explained as the result of diminished executive control, leading to working memory deficits, in turn affecting memory functioning (Nordahl et al., 2005).

Table 6 Within group deactivation results

	Cluster size	MNI coordinates			T value
		X	Y	Z	
Controls					
0-back					
Cuneus L+R	192	0	-78	30	4.64
Posterior cingulate gyrus R		6	-57	21	4.63
Precuneus L		-15	-63	21	3.78
1-back					
Posterior cingulate gyrus R	417	6	-57	21	7.28
Precuneus L+R		0	-77	27	4.04
2-back					
Posterior cingulate gyrus L	562	-9	-57	18	10.95
MCI patients with CSVD					
0-back					
Posterior cingulate gyrus R	48	18	-60	15	5.53
1-back	-				
2-back	-				
MCI patients without CSVD					
0-back					
Posterior cingulate gyrus R	386	15	-57	15	6.37
Posterior cingulate gyrus L		-9	-54	6	4.55
Precuneus L		-9	-62	21	4.25
1-back					
Posterior cingulate gyrus L	141	-9	-54	18	4.73
Lingual gyrus R		12	-54	0	3.94
Medial frontal gyrus R	20	9	48	-6	4.31
2-back					
Medial frontal gyrus R	174	3	51	-6	5.68
Posterior cingulate gyrus R	435	6	-51	21	5.51
Posterior cingulate gyrus L		-12	-54	6	4.71
Precuneus R	28	6	-81	39	4.27

Results at p <0.001, not corrected for multiple comparisons.

Nordahl et al. studied MCI patients with either WMH or severe hippocampal atrophy, and found that while both MCI patient groups showed episodic memory impairment, MCI patients with severe WMH could be distinguished from MCI patients with hippocampal atrophy on the basis of frontal task performance. In the present study we could not distinguish between MCI patients with and without CSVD on the basis of neuropsychological profile, or hippocampal atrophy, which is supported by a study of Reed et al. in which the differentiation between AD cases and mixed pathology cases

on the basis of neuropsychological profiles was proven hard and inconclusive (Reed et al., 2007). This might be caused by the fact that it is not ruled out that Alzheimer and cerebrovascular pathology synergistically contribute to the clinical syndromes of MCI and dementia (Bennett et al., 2005; Zekry et al., 2002). In case of mixed pathology, the effects of CSVD on cognition were found to be most pronounced in the early stages of AD pathology (Esiri et al., 1999).

In the current study we found a reduction of precuneus/PCC deactivation in MCI patients with CSVD. A similar result has been reported within the ACC in an fMRI study in healthy elderly with high vascular burden (Mayda et al., 2011). This finding was related to diminished frontal functional connectivity. Our finding of reduced deactivation in the precuneus/PCC region supports a more widespread connectivity problem. Both the ACC and precuneus/PCC are regions known to be taking part in the DMN, a functional network of brain regions activated at rest, 'default', conditions and actively suppressed, i.e. deactivated, during various cognitive activities (Buckner et al., 2008). Deactivation failure or deteriorated functional connectivity in the DMN was found to be associated with cognitive task performance (Anticevic et al., 2010; Eichele et al., 2008; Kelly et al., 2008), and has been encountered in several neurodegenerative conditions (Seeley et al., 2009), among which MCI and AD (Greicius et al., 2004; Koch et al., 2012; Qi et al., 2010; Rombouts et al., 2005). It was recently suggested that deactivation is progressively disrupted along the continuum from normal aging to MCI and AD, with increased impairment in *APOE4* genotype carriers (Pihlajamaki and Sperling, 2009). While *APOE4* is known to be a vascular risk factor (Horsburgh et al., 2000), current DMN studies in AD and MCI do not take the effects of CSVD into account. Recent studies combining diffusion tensor imaging and fMRI though have provided evidence for a relationship between white matter integrity and functional connectivity within the DMN (Damoiseaux and Greicius, 2009; Teipel et al., 2010). In this view, CSVD, as well as other conditions influencing white matter integrity (Rocca et al., 2010), can affect cognition through interference with network functioning, resulting in diminished deactivation and cognitive failure (Anticevic et al., 2010; Eichele et al., 2008; Kelly et al., 2008).

Our observation of 'hyperactivation' during vigilance and less recruitment, 'hypoactivation', at high working memory load in MCI patients without CSVD, contrasted to the gradual increase in brain activation linear with increasing working memory in controls and MCI patients with CSVD. The latter pattern is in agreement with reports from the literature (Duncan and Owen, 2000; Owen et al., 2005). The different working memory load dependent activation pattern in MCI patients without CSVD was consistent with a study using the same fMRI paradigm in MCI (Kochan et al., 2010), and was claimed

to be the effect of compensatory mechanisms at low demanding tasks, and a failure of compensation at high demanding tasks. Gould et al. (2006) encountered a similar task difficulty dependent interaction effect between AD patients and controls. These results may clarify previous contradictory findings in fMRI studies in MCI or AD, hypoactivation vs. hyperactivation, (Bokde et al., 2010; Gigi et al., 2010; Johnson et al., 2006), which may be caused by differences in the difficulty of fMRI paradigms.

Our study has some potential limitations. First, we used a semi-quantitative rating scale in our definition of CSVD instead of a quantitative method. Although ratings based on automatic WMH segmentations are less susceptible to rater subjectivity, a classification based on advanced automated algorithms is highly dependent upon the cohort that is studied, making it difficult to translate findings to clinical practice or other studies. A second potential limitation is the modelling of fMRI BOLD response in participants with vascular risk factors known to affect cortical vasoreactivity (Glodzik et al., 2011). Some authors avoid this issue by excluding MCI patients with signs of CSVD from their fMRI study (Bokde et al., 2010; Gigi et al., 2010), and in other studies vascular risk factors in older participants are not assessed. We acknowledge that with our approach we are at risk of underestimating the BOLD-response in MCI patients with CSVD. However, in the present study we found no evidence for a reduction in BOLD-response in CSVD, as we found no differences in a direct comparison of brain activation between MCI patients with and without CSVD. A third drawback of this study is the use of a relatively lenient threshold not corrected for multiple comparisons when examining within group deactivation results. It is important to note that by thresholding statistical parametric maps at this more lenient threshold, false-positive findings increase. We would like to note though that our findings of deactivation in MCI patients were restricted to regions shown to deactivate in controls using FWE correction, and were reported in other studies as well (Lustig et al., 2003; Rombouts et al., 2005). A fourth limitation is the fact that even after stringent exclusion of participants on the basis of task performance, MCI patients still perform worse as compared with controls. While our results will have to be interpreted with some caution, we have to note that there were no differences between MCI patient groups in task performance. A final limitation is that in comparison with controls MCI patients in the current study were more frequently male, and in MCI patients without CSVD hypertension was less prevalent. This is the result of our inclusion method, as we included healthy controls based on age (aged 65 years or older) and cognitive functioning. Gender was found to have an effect on the lateralization of activation, females showing activation more predominantly in the left hemisphere (Speck et al., 2000). We acknowledge that this could influence our results, but we think that the underlying pathological changes in MCI will have a more profound effect on brain activation than gender.

In conclusion, MCI patients with CSVD have impaired deactivation in a region known to be involved in the DMN. MCI patients without CSVD show 'hyperactivation' during vigilance and 'hypoactivation' during high working memory load. These observed differences in brain activation and deactivation between MCI patients with and without CSVD, who had a similar 'clinical phenotype', supports the view that, in patients with MCI, different types of pathology can contribute to cognitive impairment through different pathways.

REFERENCES

Albert MS, DeKosky ST, Dickson D, Dubois B, Feldman HH, Fox NC*, et al.* The diagnosis

of mild cognitive impairment due to Alzheimer's disease: recommendations from the National Institute on Aging-Alzheimer's Association workgroups on diagnostic guidelines for Alzheimer's disease. Alzheimers Dement 2011; 7: 270-279.

Anticevic A, Repovs G, Shulman GL, Barch DM. When less is more: TPJ and default

network deactivation during encoding predicts working memory performance. Neuroimage 2010; 49: 2638-2648.

Ashburner J, Friston KJ. Unified segmentation. Neuroimage 2005; 26: 839-851.

Bennett DA, Schneider JA, Bienias JL, Evans DA, Wilson RS. Mild cognitive impairment is related to Alzheimer disease pathology and cerebral infarctions. Neurology 2005; 64: 834-841.

Bokde AL, Karmann M, Born C, Teipel SJ, Omerovic M, Ewers M*, et al.* Altered brain activation during a verbal working memory task in subjects with amnestic mild cognitive impairment. J Alzheimers Dis 2010; 21: 103-118.

Braver TS, Cohen JD, Nystrom LE, Jonides J, Smith EE, Noll DC. A parametric study of prefrontal cortex involvement in human working memory. Neuroimage 1997; 5: 49-62.

Buckner RL, Andrews-Hanna JR, Schacter DL. The brain's default network: anatomy, function, and relevance to disease. Ann N Y Acad Sci 2008; 1124: 1-38.

Cummings JL. Frontal-subcortical circuits and human behaviour. Arch Neurol 1993; 50: 873-880.

Damoiseaux JS, Greicius MD. Greater than the sum of its parts: a review of studies combining structural connectivity and resting-state functional connectivity. Brain Struct Funct 2009; 213: 525-533.

de Boer R, Vrooman HA, van der Lijn F, Vernooij MW, Ikram MA, van der Lugt A*, et al.* White matter lesion extension to automatic brain tissue segmentation on MRI. Neuroimage 2009; 45: 1151-1161.

DeCarli C. Mild cognitive impairment: prevalence, prognosis, aetiology, and treatment. Lancet Neurol 2003; 2: 15-21.

den Heijer T, van der Lijn F, Koudstaal PJ, Hofman A, van der Lugt A, Krestin GP*, et al.* A 10-year follow-up of hippocampal volume on magnetic resonance imaging in early dementia and cognitive decline. Brain 2010; 133: 1163-1172.

Duncan J, Owen AM. Common regions of the human frontal lobe recruited by diverse cognitive demands. Trends Neurosci 2000; 23: 475-483.

Eichele T, Debener S, Calhoun VD, Specht K, Engel AK, Hugdahl K*, et al.* Prediction of human errors by maladaptive changes in event-related brain networks. Proc Natl Acad Sci U S A 2008; 105: 6173-6178.

Esiri MM, Nagy Z, Smith MZ, Barnetson L, Smith AD. Cerebrovascular disease and threshold for dementia in the early stages of Alzheimer's disease. Lancet 1999; 354: 919-920.

Fazekas F, Barkhof F, Wahlund LO, Pantoni L, Erkinjuntti T, Scheltens P*, et al.* CT and MRI rating of white matter lesions. Cerebrovasc Dis 2002; 13 Suppl 2: 31-36.

Fisher CM. Lacunar strokes and infarcts: a review. Neurology 1982; 32: 871-876.

Frisoni GB, Galluzzi S, Bresciani L, Zanetti O, Geroldi C. Mild cognitive impairment with subcortical vascular features: clinical characteristics and outcome. J Neurol 2002; 249: 1423-1432.

Friston KJ. Testing for anatomically specified regional effects. Hum Brain Mapp 1997; 5: 133-136.

Galluzzi S, Sheu CF, Zanetti O, Frisoni GB. Distinctive clinical features of mild cognitive impairment with subcortical cerebrovascular disease. Dement Geriatr Cogn Disord 2005; 19: 196-203.

Gigi A, Babai R, Penker A, Hendler T, Korczyn AD. Prefrontal compensatory mechanism may enable normal semantic memory performance in mild cognitive impairment (MCI). J Neuroimaging 2010; 20: 163-168.

Glodzik L, Rusinek H, Brys M, Tsui WH, Switalski R, Mosconi L, *et al.* Framingham cardiovascular risk profile correlates with impaired hippocampal and cortical vasoreactivity to hypercapnia. J Cereb Blood Flow Metab 2011; 31: 671-679.

Gould RL, Arroyo B, Brown RG, Owen AM, Bullmore ET, Howard RJ (2006): Brain mechanisms of successful compensation during learning in Alzheimer disease. Neurology 67: 1011-1017.

Greicius MD, Krasnow B, Reiss AL, Menon V. Functional connectivity in the resting brain: a network analysis of the default mode hypothesis. Proc Natl Acad Sci U S A 2003; 100: 253-258.

Greicius MD, Srivastava G, Reiss AL, Menon V. Default-mode network activity distinguishes Alzheimer's disease from healthy aging: evidence from functional MRI. Proc Natl Acad Sci U S A 2004; 101: 4637-4642.

Horsburgh K, McCarron MO, White F, Nicoll JA. The role of apolipoprotein E in Alzheimer's disease, acute brain injury and cerebrovascular disease: evidence of common mechanisms and utility of animal models. Neurobiol Aging 2000; 21: 245-255.

Johnson SC, Schmitz TW, Moritz CH, Meyerand ME, Rowley HA, Alexander AL, *et al.* Activation of brain regions vulnerable to Alzheimer's disease: the effect of mild cognitive impairment. Neurobiol Aging 2006; 27: 1604-1612.

Kelly AM, Uddin LQ, Biswal BB, Castellanos FX, Milham MP. Competition between functional brain networks mediates behavioural variability. Neuroimage 2008; 39: 527-537.

Koch W, Teipel S, Mueller S, Benninghoff J, Wagner M, Bokde AL, *et al.* Diagnostic power of default mode network resting state fMRI in the detection of Alzheimer's disease. Neurobiol Aging 2012; 33: 466-478.

Kochan NA, Breakspear M, Slavin MJ, Valenzuela M, McCraw S, Brodaty H, *et al.* Functional alterations in brain activation and deactivation in mild cognitive impairment in response to a graded working memory challenge. Dement Geriatr Cogn Disord 2010; 30: 553-568.

Langeslag SJ, Morgan HM, Jackson MC, Linden DE, Van Strien JW. Electrophysiological correlates of improved short-term memory for emotional faces. Neuropsychologia 2009; 47: 887-896.

Luchsinger JA, Brickman AM, Reitz C, Cho SJ, Schupf N, Manly JJ, *et al.* Subclinical cerebrovascular disease in mild cognitive impairment. Neurology 2009; 73: 450-456.

Lustig C, Snyder AZ, Bhakta M, O'Brien KC, McAvoy M, Raichle ME, *et al.*Functional deactivations: chance with age and dementia of the Alzheimer type. Proc Natl Acad Sci USA 2003; 100: 14504-14509.

Mayda AB, Westphal A, Carter CS, DeCarli C. Late life cognitive control deficits are accentuated by white matter disease burden. Brain 2011; 134: 1673-1683.

Meyer JS, Xu G, Thornby J, Chowdhury MH, Quach M. Is mild cognitive impairment prodromal for vascular dementia like Alzheimer's disease? Stroke 2002; 33: 1981-1985.

Mitchell AJ, Shiri-Feshki M. Rate of progression of mild cognitive impairment to dementia--meta-analysis of 41 robust inception cohort studies. Acta Psychiatr Scand 2009; 119: 252-265.

Nordahl CW, Ranganath C, Yonelinas AP, DeCarli C, Reed BR, Jagust WJ. Different mechanisms of episodic memory failure in mild cognitive impairment. Neuropsychologia 2005; 43: 1688-1697.

Nordlund A, Rolstad S, Klang O, Lind K, Hansen S, Wallin A. Cognitive profiles of mild cognitive impairment with and without vascular disease. Neuropsychology 2007; 21: 706-712.

Owen AM, McMillan KM, Laird AR, Bullmore E. N-back working memory paradigm: a meta-analysis of normative functional neuroimaging studies. Hum Brain Mapp 2005; 25: 46-59.

Pantoni L. Cerebral small vessel disease: from pathogenesis and clinical characteristics to therapeutic challenges. Lancet Neurol 2010; 9: 689-701.

Petersen RC. Mild cognitive impairment as a diagnostic entity. J Intern Med 2004; 256: 183-194.

Petersen RC, Doody R, Kurz A, Mohs RC, Morris JC, Rabins PV, *et al.* Current concepts in mild cognitive impairment. Arch Neurol 2001; 58: 1985-1992.

Petersen RC, Morris JC. Mild cognitive impairment as a clinical entity and treatment target. Arch Neurol 2005; 62: 1160-1163; discussion 1167.

Pihlajamaki M, Sperling RA. Functional MRI assessment of task-induced deactivation of the default mode network in Alzheimer's disease and at-risk older individuals. Behav Neurol 2009; 21: 77-91.

Price CJ, Friston KJ. Scanning patients with tasks they can perform. Hum Brain Mapp 1999; 8: 102-108.

Prins ND, van Dijk EJ, den Heijer T, Vermeer SE, Jolles J, Koudstaal PJ, *et al.* Cerebral small-vessel disease and decline in information processing speed, executive function and memory. Brain 2005; 128: 2034-2041.

Pugh KG, Lipsitz LA. The microvascular frontal-subcortical syndrome of aging. Neurobiol Aging 2002; 23: 421-431.

Qi Z, Wu X, Wang Z, Zhang N, Dong H, Yao L, *et al.* Impairment and compensation coexist in amnestic MCI default mode network. Neuroimage 2010; 50: 48-55.

Raichle ME, MacLeod AM, Snyder AZ, Powers WJ, Gusnard DA, Shulman GL. A default mode of brain function. Proc Natl Acad Sci U S A 2001; 98: 676-682.

Reed BR, Mungas DM, Kramer JH, Ellis W, Vinters HV, Zarow C, *et al.* Profiles of neuropsychological impairment in autopsy-defined Alzheimer's disease and cerebrovascular disease. Brain 2007; 130: 731-739.

Rocca MA, Valsasina P, Absinta M, Riccitelli G, Rodegher ME, Misci P, *et al.* Default-mode network dysfunction and cognitive impairment in progressive MS. Neurology 2010; 74: 1252-1259.

Rombouts SA, Barkhof F, Goekoop R, Stam CJ, Scheltens P. Altered resting state networks in mild cognitive impairment and mild Alzheimer's disease: an fMRI study. Hum Brain Mapp 2005; 26: 231-239.

Seeley WW, Crawford RK, Zhou J, Miller BL, Greicius MD. Neurodegenerative diseases target large-scale human brain networks. Neuron 2009; 62: 42-52.

Smits M, Dippel DW, Houston GC, Wielopolski PA, Koudstaal PJ, Hunink MG, *et al.* Postconcussion syndrome after minor head injury: brain activation of working memory and attention. Hum Brain Mapp 2009; 30: 2789-2803.

Snodgrass JG, Corwin J. Pragmatics of measuring recognition memory: applications to dementia and amnesia. J Exp Psychol Gen 1988; 117: 34-50.

Speck O, Ernst T, Braun J, Koch C, Miller E, Chang L. Gender differences in the functional organization of the brain for working memory. Neuroreport 2000; 11: 2581-2585.

Teipel SJ, Bokde AL, Meindl T, Amaro E, Jr., Soldner J, Reiser MF, *et al.* White matter microstructure underlying default mode network connectivity in the human brain. Neuroimage 2010; 49: 2021-2032.

Tullberg M, Fletcher E, DeCarli C, Mungas D, Reed BR, Harvey DJ, *et al.* White matter lesions impair frontal lobe function regardless of their location. Neurology 2004; 63: 246-253.

van der Lijn F, den Heijer T, Breteler MM, Niessen WJ. Hippocampus segmentation in MR images using atlas registration, voxel classification, and graph cuts. Neuroimage 2008; 43: 708-720.

Verhage F. Intelligentie en leeftijd: onderzoek bij Nederlanders van twaalf tot zevenenzeventig jaar [Intelligence and age: Research on Dutch people aged twelve to seventy-seven years old]. Assen: Van Gorcum 1964.

Villeneuve S, Massoud F, Bocti C, Gauthier S, Belleville S. The nature of episodic memory deficits in MCI with and without vascular burden. Neuropsychologia 2011; 49: 3027-3035.

Vrooman HA, Cocosco CA, van der Lijn F, Stokking R, Ikram MA, Vernooij MW, *et al.* Multi-spectral brain tissue segmentation using automatically trained k-Nearest-Neighbor classification. Neuroimage 2007; 37: 71-81.

Worsley KJ, Marrett S, Neelin P, Vandal AC, Friston KJ, Evans A. A unified statistical approach for determining significant signals in images of cerebral activation. Hum Brain Mapp 1996; 4: 58-73.

Zekry D, Duyckaerts C, Moulias R, Belmin J, Geoffre C, Herrmann F, *et al.* Degenerative and vascular lesions of the brain have synergistic effects in dementia of the elderly. Acta Neuropathol 2002; 103: 481-487.

Chapter 2.4

Cerebral small vessel disease affects white matter microstructure in mild cognitive impairment

Janne M. Papma
Marius de Groot
Inge de Koning
Francesco U. Mattace Raso
Aad van der Lugt
Meike W. Vernooij
Wiro J. Niessen
John C. van Swieten
Peter J. Koudstaal
Niels D. Prins
Marion Smits

Human Brain Mapping; Major revision

ABSTRACT

Recent evidence suggests that impaired neural network functioning, in particular dysfunctioning of the default mode network, is an important factor in cognitive symptomatology in patients with mild cognitive impairment (MCI). Intact structural connectivity, represented by interconnecting white matter tracts, is a prerequisite for normal network functioning. Since microstructural white matter deterioration is a frequent finding in MCI, this could, at least partly, explain network dysfunctioning in this condition. Thus far, microstructural damage in MCI has been mostly attributed to Alzheimer's disease pathophysiology and the potential role of cerebrovascular pathology, in particular cerebral small vessel disease (CSVD), received less interest. In the present study we used diffusion tensor imaging (DTI) to examine the role of CSVD in microstructural deterioration within the normal appearing white matter (NAWM) in MCI patients. For this purpose we subdivided a cohort of MCI patients into those with (n = 20) and those without (n = 31) macrostructural evidence of CSVD on MRI. Using DTI TBSS analysis we compared the microstructural deterioration within whole brain NAWM between MCI patients with CSVD, MCI patients without CSVD and elderly controls (n = 23). Secondly, we segmented white matter tracts known to interconnect brain regions involved in the default mode network by means of automated tractography segmentation and used average DTI measures, including fractional anisotropy, mean, axial and perpendicular diffusivity, from the NAWM of these tracts as dependent variable in a stepwise linear regression analysis. Our results indicated widespread microstructural deterioration in MCI patients with CSVD, while MCI patients without CSVD showed microstructural damage restricted to a small portion of the temporal lobe white matter. Within the full cohort of MCI patients, microstructure within the NAWM of default mode network associated fiber tracts was found to be affected mainly by cerebrovascular pathology. These results indicate that the contribution of cerebrovascular pathology to the clinical and cognitive syndrome of MCI may be through network interference.

INTRODUCTION

Mild cognitive impairment (MCI) is a clinical construct that identifies individuals with cognitive impairment at high risk of dementia, in most cases Alzheimer's disease (AD) (Albert et al., 2011; DeCarli, 2003; Petersen, 2004). Within the past decades, structural MRI has been used extensively to study this prodromal dementia stage, as it offers the opportunity to identify early pathological brain changes in vivo. Numerous studies have identified MCI and ultimately AD related atrophy within the medial temporal lobe, temporal and parietal association regions, the cingulate gyrus and prefrontal cortex (Bozzali et al., 2006; Chetelat et al., 2005; Karas et al., 2004). Other commonly encountered MRI findings in MCI are white matter hyperintensities (WMH) and lacunar infarcts (Targosz-Gajniak et al., 2009; Yoshita et al., 2006), regarded as macrostructural MRI expressions of cerebral small vessel disease (CSVD), a condition that affects the microvessels supplying the white matter and subcortical brain regions (Pantoni, 2010). Interestingly, there is increasing evidence suggesting that CSVD and AD pathophysiological changes on MRI do not just coincide but may be interrelated (Bartzokis, 2004; Englund et al., 1988; Luchsinger et al., 2009; Nordahl et al., 2005; Targosz-Gajniak et al., 2009; Villeneuve et al., 2011; Yoshita et al., 2006).

While initially, MRI studies largely focused on region of interest analysis (Dickerson et al., 2001; Jack et al., 2000), the more current view is that widespread brain regions form interconnected neural networks. Research has therefore been more directed to networks and network connectivity lately (Bai et al., 2008; Greicius et al., 2004). A network often studied in MCI and AD is the default mode network (Buckner et al., 2008; Greicius et al., 2003; Raichle et al., 2001), known to be affected in several neurodegenerative conditions and thought to play a role in cognitive functioning (Greicius et al., 2004; Seeley et al., 2009). Within this network intact white matter, representing structural connectivity, is very important for normal network functioning (Damoiseaux and Greicius, 2009; Greicius et al., 2009), which subsequently implies that conditions affecting white matter structure can affect network functioning (Mayda et al., 2011; Rocca et al., 2010). While an assessment of macrostructural white matter deterioration can be obtained by means of T2 weighted Fluid Attenuated Inversion Recovery (T2-FLAIR) MRI, diffusion tensor imaging (DTI) can be used to non-invasively examine white matter damage on a microstructural level. DTI is an MRI technique based on the diffusion properties of unbound water molecules. In the presence of physical boundaries or restrictions diffusion becomes anisotropic, or directionally dependent, as water diffuses more rapidly in the direction aligned with an internal structure (axial diffusivity, $\lambda_{\parallel}$), instead of perpendicular to it (radial diffusivity, $\lambda_{\perp}$). DTI measures are considered sensitive markers for white matter microstructural damage,

as degradation of axons or demyelination will result in reduced restrictions, increased free diffusion of water, and consequently a decrease in anisotropy. Numerous previous studies have reported decreased fractional anisotropy (FA) and increased random or mean diffusivity (MD) in MCI and AD patients (Sexton et al., 2011), but the nature of these microstructural white matter changes is still a matter of debate. Some claim that microstructural deterioration is secondary to neuronal – grey matter – loss in AD, so-called Wallerian degeneration (Raff et al., 2002). However, the frequent co-occurrence of CSVD in AD patients also points towards a role of cerebrovascular pathology. Indeed, in MCI, microstructural white matter damage was found to correlate to macrostructural white matter changes such as WMH burden (Zhuang et al., 2010). This relationship however, was examined within the global white matter without controlling for WMH, like other DTI studies in MCI fail to control for the presence of WMH as well (Bai et al., 2009; Chua et al., 2009; Liu et al., 2011; Zhou et al., 2008; Zhuang et al., 2010). This is an important issue, as we already know that DTI measures differ within WMH regions (Horsfield and Jones, 2002). In the present study we aim to gain more insight into mechanisms affecting white matter microstructural integrity in MCI, in particular examining the role of CSVD. For this purpose we used DTI, and to avoid WMH influencing our results, we restricted our analyses specifically to the normal appearing white matter (NAWM). We compared NAWM DTI measures in MCI patients with and without CSVD and healthy controls globally, and furthermore examined the role of CSVD in specific white matter tracts known to be important in default mode network functioning (Bai et al., 2009; Damoiseaux and Greicius, 2009; Teipel et al., 2010; van den Heuvel et al., 2008; van den Heuvel et al., 2009).

METHODS

Participants

We recruited MCI patients, aged 65 years or older, from outpatient clinics of the Departments of Neurology and Geriatrics of the Erasmus MC – University Medical Center Rotterdam, and 7 surrounding hospitals, on the basis of criteria by Petersen et al. (2004). These criteria include: 1) presence of cognitive complaint by patient or relatives; 2) impairment in one or more cognitive domains as determined by neuropsychological assessment; 3) preserved overall general functioning, with possible increased difficulty in the performance of activities of daily living; and 4) absence of dementia according to the DSM-IV or NINCDS-ADRDA criteria for dementia. In total 57 MCI patients were screened for study eligibility. We excluded patients with a previous neurological or psychiatric diagnosis negatively affecting cognition (e.g. major stroke, cerebral tumor or depression) or contraindications for MRI (e.g. pacemaker or claustrophobia). After initial screening, 55 MCI patients underwent a structured interview, physical examination and brain MRI,

including 3D T1-weighted, T2-FLAIR MRI and DTI. After MRI examinations we excluded 4 patients, 2 due to physical inability or refusal to undergo MRI when confronted with the MRI scanner, 1 due to incomplete DTI data collection and 1 due to excessive head movement and consequently obvious blurring of the acquired data. Thus, for the present study, data of 51 MCI patients were available. Control subjects (n = 28), aged 65 years or older, were either relatives of MCI patients or were recruited by advertisement (e.g. posters and handouts) throughout the Erasmus MC. Controls did not meet any of the criteria for MCI, but were otherwise excluded on the basis of the same exclusion criteria as MCI patients. Controls underwent the exact same work up as MCI patients in this study. After MRI examinations we excluded 2 control participants on the basis of the quality of DTI imaging, caused by poor positioning of the head in the MRI head coil, and thus 26 participants were included in our study. All participants gave informed consent to the protocol of the study, which was approved by the medical ethics committee of the Erasmus MC.

Structured interview, physical examination and neuropsychological assessment

We collected data on demographics, medical history, and vascular risk factors during a structured interview. Level of education was assessed with a Dutch education scale, ranging from 1 (less than 6 years elementary school) to 7 (academic degree) (Verhage, 1964). As measured twice during physical examination, we defined hypertension as systolic blood pressure ≥ 160 mm Hg or diastolic blood pressure ≥ 90 mm Hg, or the use of antihypertensive medication. We determined *Apolipoprotein E* (*APOE*) genotype in all participants. The mini mental state examination (MMSE) was employed as a global cognitive screening method, and as an indicator for disease severity (Perneczky et al., 2006). Extensive neuropsychological assessment covered cognitive domains including episodic memory, processing speed, executive functioning, language, visuospatial and visuoconstructive ability, and was used both in the definition and diagnosis of MCI.

MRI acquisition

We performed MR imaging on a 3.0 T MRI scanner with an 8-channel head coil (HD platform, GE Healthcare, Milwaukee, WI, US). DTI data were acquired in the axial plane with a single shot T2* weighted echo-planar imaging (EPI) sequence with 25 non-collinear directions and the following parameters: repetition time (TR) = 14200 ms, echo time (TE) = 73.3 ms, acquisition matrix 64x128, field of view (FOV) = 220x220 mm^2, flip angle = 90°. Maximum b-value was 1000 s/mm^2 and three volumes were acquired without diffusion weighting (b-value = 0 s/mm^2). We acquired 70 contiguous slices with a slice thickness of 2.0 mm in a total acquisition time of 7:06 min. High resolution 3D T1-weighted structural

MRI was acquired in the axial plane with the following parameters: TR = 10.4 ms, TE = 2.1 ms, TI = 300 ms, flip angle = 18°, acquisition matrix = 416x256, FOV = 250x175 mm^2. In a total acquisition time of 4:57 min, we acquired 192 slices with a slice thickness of 1.6 mm and 0.8 mm overlap, resulting in an effective slice thickness of 0.8 mm. T2-FLAIR images were obtained with the following parameters: TR = 8000 ms, TE = 120 ms, TI = 2000 ms, acquisition matrix = 256x128, FOV = 210x210 mm^2. We acquired 64 contiguous slices with a slice thickness of 2.5 mm in a total acquisition time of 3:13 min.

Visual assessment of WMH and lacunar infarcts

Blinded for all clinical information, a neurologist (NDP), experienced in the assessment of CSVD on MRI, examined 3D T1-weighted and T2-FLAIR MRI images for the presence of lacunar infarcts and WMH. The extent of WMH was assessed using the semi-quantitative rating scale of Fazekas (Fazekas et al., 2002). In line with the definition of CSVD on MRI used in previous studies (Frisoni et al., 2002), we defined the presence of CSVD as the presence of substantial WMH (Fazekas score 2 or higher) affecting both the posterior and anterior white matter regions and/or the presence of two or more lacunar infarcts. Based on these ratings we classified MCI patients as MCI patients with CSVD (n = 20) and MCI patients without CSVD (n = 31). In addition, we excluded three control subjects, as they met the criteria for CSVD on MRI, eventually including 23 controls without CSVD on MRI in our analyses. Although available (see below), we did not make use of automated brain tissue segmentation and volumetric analysis of WMH for this subdivision, as these ratings are highly dependent upon the studied cohort and therefore difficult to translate to clinical practice or compare with previous studies.

Automated MRI tissue segmentation and volumetric analysis of WMH and hippocampi

Based on the intensities of the 3D T1-weighted and T2-FLAIR MRI scans we used a validated k-nearest neighbour classifier to automatically segment brain tissue into cerebrospinal fluid, grey matter, normal appearing white matter and WMH (de Boer et al., 2009; Vrooman et al., 2007). We refer to Figure 1 for the distribution of WMH in all participants. We segmented hippocampi on the basis of the 3D T1-weighted images by means of an automated method as described previously (den Heijer et al., 2010; van der Lijn et al., 2008). Blinded for clinical information, all automated segmentations were visually inspected and if necessary, we manually corrected the segmentations using FSLview, part of FSL (Woolrich et al., 2009). Subsequently, we assessed total intracranial volume (TIV).

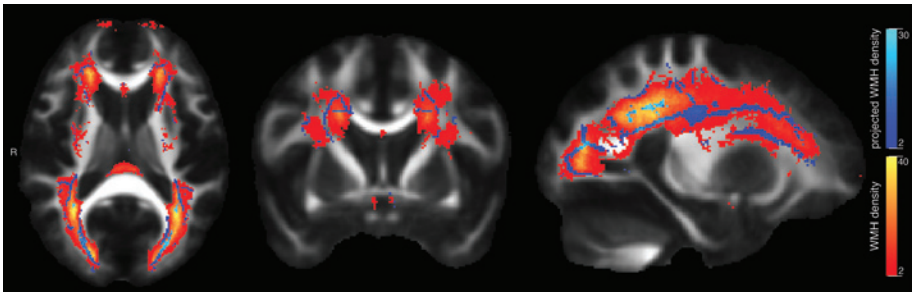

Figure 1 TBSS skeleton projections on white mater hyperintensity map in axial, coronal and sagittal planes. White matter hyperintensities range from red to yellow, indicating respectively voxelwise low to high prevalence of white matter hyperintensity. TBSS skeleton projections depicted in a range from dark blue to light blue, indicating respectively low to high prevalence of affected TBSS skeleton voxels.

DTI data processing

As a first step in DTI processing, we corrected diffusion data for motion and Eddy currents by affine co-registration of the diffusion weighted volumes to the average b=0 s/mm^2 volume. These registrations were performed using Elastix, an open source ITK based registration package (Klein et al., 2010). The rotation component of each transformation was used to realign the gradient vector for each diffusion-weighted volume to compensate for motion during the acquisition (Leemans and Jones, 2009). Then, resampling of the transformed diffusion weighted images was performed at an isotropic resolution of 1.0 mm for the tensor fit, and 2.0 mm for the probabilistic tractography. We used the Brain Extraction Tool (BET) (Smith, 2002) from FSL 4.1.9, to identify brain tissue in three random subjects, and subsequently manually corrected the resulting masks using FSLview. The corrected masks were then transformed to individual subject space using a nonlinear co-registration of the b=0 s/mm^2 volumes obtained with Elastix (three registrations per subject). Subsequently, majority voting on the three transformed brain masks was used to obtain a brain mask for all individual subjects, which was then used to mask the diffusion data. We fitted diffusion tensors with a Levenberg-Marquard non-linear least squares optimization algorithm, available in ExploreDTI, on the 1.0 mm data. The 2.0 mm data were used to fit a probabilistic model of fiber orientations for each voxel by means of Bedpostx (Behrens et al., 2007). Afterwards, data quality was examined through visual inspection of axial FA slices 4 mm apart, combined with two coronal and two sagittal slices around the center of the brain.

DTI data analysis

To examine the role of CSVD in white matter microstructural damage in MCI, we used several DTI analysis techniques. All analyses were restricted to the NAWM by mapping the individual WMH segmentation masks, as obtained from automated tissue segmentation,

to the DTI data and thus excluding voxels originating from WMH (Vernooij et al., 2008). In a first analysis, we examined DTI measures within the global NAWM. Second, we used the whole brain explorative framework of tract based spatial statistics (TBSS), to gain insight into the spatial distribution of white matter microstructural abnormalities related to CSVD in MCI patients. We compared DTI measures in this patient group with those in MCI patients without CSVD and those in controls. Third, considering specific white matter tracts as important connections subserving normal default mode network functioning, we investigated specific white matter tracts, the cingulum in the cingulate cortex (CGC), the cingulum along the hippocampal cortex (CGH) and the superior longitudinal fasciculus (SLF), by means of probabilistic tractography (Damoiseaux and Greicius, 2009; Teipel et al., 2010; van den Heuvel et al., 2008; van den Heuvel et al., 2009). In addition, we included tracts that were found to be significantly affected in the whole brain TBSS analysis. Control tracts were tracts known to be unaffected by AD disease mechanisms, and included the corticospinal tract (CST) and middle cerebellar peduncle (MCP) (Kiuchi et al., 2009). We extracted the tracts of interest and control tracts for every individual, and performed between group comparisons of DTI measures as well as regression analysis with -DTI measurements within the NAWM of tracts- as dependent variable. All of the mentioned between group analyses were corrected for the effects of age and sex.

DTI data analysis: global NAWM measurements

T1-weighted images were co-registered to the individuals' FA images using an affine registration with mutual information as similarity metric by means of FLIRT (Jenkinson and Smith, 2001). We averaged DTI measures, FA, MD, λ_{II} and $\lambda_{\perp}$ within the whole brain NAWM, using the tissue segmentation masks created in the automated MRI brain tissue segmentation, in diffusion space. We compared these measures between groups.

DTI data analysis: Tract Based Spatial Statistics

For the TBSS analysis (Smith et al., 2006), we followed the default pipeline. In short, individual subjects' FA images were co-registered to a FA template in standard MNI space. Next, a mean FA image was created and thinned to obtain a mean FA skeleton which represented the centers of all tracts common to the entire group. We thresholded the white matter skeleton image at an FA value of 0.2 to constrain the analyses to those tracts that could reliably be identified. FA measurements were projected onto the white matter skeleton by searching the maximum FA value in a region perpendicular to the skeleton. This projection was performed in every skeleton voxel. MD, $\lambda_{\perp}$ and λ_{II} values and WMH status were then projected onto the white matter skeleton, using the same projection as for the FA. Hereafter, we performed voxelwise group comparions while regressing out the linear effects of age and sex. All statistical analyses were corrected for multiple

comparisons using 5000 permutations in Randomise as available in FSL. We implemented the WMH exclusion by supplying voxelwise NAWM status masks per group to Randomise. Spatial clustering of results was performed with TCFE (Smith and Nichols, 2009).

DTI data analysis: Tractography measurements

We performed automated probablistic tractography in subject native space by means of Probtrackx, available in FSL. For these analyses we used standard space seed, target, stop and exclusion masks, which were based on protocols described by Mori et al., 2002; Stieltjes et al., 2001; Wakana et al., 2007 and Wakana et al., 2004. The masks were transferred to subject-native space using a nonlinear registration obtained with default settings for FA images in FNIRT. As mentioned before, tractography was performed for the CGC, CGH, SLF, CST and MCP. As the TBSS group statistics indicated that the genu of the corpus callosum (CC) was particularly affected in MCI patients with CSVD, we also extracted the forceps minor (FMI), the most prominent white matter tract within the genu of the CC, as an additional tract of interest. The tract density image for each tract was normalized by division with the total number of fiber paths recorded in the tract density image. These images were then thresholded at 0.005 to yield binary segmentations. Tracts that could not be identified using the automated protocols were treated as missing values. Individual diffusion measurements were averaged within the NAWM, i.e. excluding voxels that were classified as WMH. Mean FA, MD, $\lambda_{\perp}$ and $\lambda_{||}$, resulting from the tractography-based segmentations were compared between groups.

Statistical analysis

We compared demographics, neuropsychological data and imaging measures between groups using the statistical package SPSS (version 17.0 for Windows, Chicago, IL, US). Imaging and neuropsychological data comparisons were corrected for age, sex, and in case of neuropsychological data, education. Differences between groups on continuous variables were assessed with ANOVA or ANCOVA and post hoc two sample t-tests. We compared non-parametric data using Kruskal-Wallis, followed by Mann-Whitney *U* tests. Between group analyses of nominal variables were performed by means of Pearson Chi-square tests. To disentangle the role of CSVD in microstructural white matter damage in MCI, we performed a stepwise linear regression analysis within the full cohort of MCI patients with -DTI measures within the NAWM of tracts of interest- as dependent variables. We examined which of the following determinants resulted in the best model fit: WMH volume in ml, presence of lacunar infarcts, TIV in ml, grey matter volume in ml, white matter volume in ml, left and right hippocampal volume in ml, age, sex, education and the MMSE score as a measure of disease severity. We considered the model that predicted the most variance in the dependent variable. In all of the analyses a p value <0.05 was considered statistically significant.

RESULTS

Participant characteristics

Characteristics of MCI patients and controls are presented in Table 1. Briefly, in comparison with controls, MCI patients with CSVD were on average 4.8 years older and showed a higher prevalence of apolipoprotein E (*APOE*)-E4 genotyping (prevalence in 72% of MCI with CSVD cases, and in 25% of control cases). MCI patients with CSVD more often had hypertension compared with MCI patients without CSVD (prevalence in 85% and 42 %, respectively).

Table 1 Characteristics of controls and MCI patients with and without cerebral small vessel disease

	Controls (n = 23)	Total MCI group (n = 51)	MCI without CSVD (n = 31)	MCI with CSVD (n = 20)
Age, years	70.9 (5.0)	74.1 (4.9)[a]	73.1 (4.3)	75.7 (5.4)[a]
Sex, women (%)	10 (0.43)	14 (0.27)	7 (0.23)	7 (0.35)
Education	5.4 (1.2)	5.2 (1.3)	5.0 (1.4)	5.4 (1.2)
MMSE	28.9 (1.1)	27.2 (1.9)[a]	27.0 (2.0)[a]	27.4 (1.8)[a]
Hypertension, prevalence (%)	15 (0.65)	30 (0.58)	13 (0.42)	17 (0.85)[b]
Smoking, prevalence (%)*	13 (0.57)	34 (0.67)	19 (0.61)	15 (0.75)
APOE -/ε4, prevalence (%)†	5 (0.25)	27 (0.56)[a]	14 (0.47)	13 (0.72)[a]
APOE ε4/ε4, prevalence (%)†	0 (0.00)	5 (0.10)	2 (0.07)	3 (0.17)

Values are unadjusted means (standard deviation) or number of participants (percentages). MCI: mild cognitive impairment. CSVD: cerebral small vessel disease. MMSE: mini mental state examination. *APOE*: apolipoprotein E * Prevalence current and former smoking. † missing data for 2 MCI patients with CSVD, 1 MCI patient without CSVD and 3 healthy controls. Differences between groups analyzed by means of independent sample t-test or Chi-Square test: [a] $p < 0.05$ compared with controls. [b] $p < 0.05$ compared with MCI patients without CSVD.

MRI characteristics

After correction for age and sex, by definition MCI patients with CSVD more often showed lacunar infarcts and more severe WMH burden, i.e. higher Fazekas scores and greater WMH volume, than controls or MCI patients without CSVD (Table 2). MCI patients with CSVD showed significantly lower FA of the global NAWM relative to controls and MCI patients without CSVD. Relative to controls, both MCI patient groups showed significant lower hippocampal volumes, with no differences between MCI patients with and without CSVD (Table 2).

Table 2 MRI characteristics for controls and MCI patients with and without cerebral small vessel disease

	Controls (n = 23)	Total MCI group (n = 51)	MCI without CSVD (n = 31)	MCI with CSVD (n = 20)
WMH, Fazekas score*	1 (0; 1)	1 (1; 2)[a]	1 (0; 1)	2 (2; 2)[a,b]
Lacunar infarcts, presence (%)	2 (7.7)	12 (23.5)	3 (9.7)	9 (45.0)[a,b]
TIV in ml	1085.6 (88.4)	1123.7 (134.3)	1131.7 (122.2)	1111.3 (153.7)
Grey matter in ml	445.9 (56.9)	453.8 (69.2)	462.7 (60.8)	439.9 (80.5)
White matter in ml	415.9 (38.2)	402.8 (51.4)[a]	412.3 (49.2)	387.9 (52.4)[a]
WMH in ml*	13.1 (10.6; 21.4)	19.9 (14.1; 30.7)[a]	16.0 (10.5; 19.9)	33.8 (25.7; 50.4)[a,b]
Left hippocampus in ml	3.13 (0.40)	2.78 (0.53)[a]	2.76 (0.51)[a]	2.80 (0.57)
Right hippocampus in ml	3.05 (0.41)	2.80 (0.42)[a]	2.80 (0.43)[a]	2.81 (0.42)[a]
NAWM whole brain FA	0.391 (0.018)	0.375 (0.021)	0.381 (0.020)	0.366 (0.021)[a,b]
NAWM whole brain MD	0.954 (0.033)	0.993 (0.103)	0.997 (0.118)	0.986 (0.079)
NAWM whole brain λ_{II}	1.373 (0.028)	1.411 (0.160)	1.423 (0.191)	1.384 (0.095)
NAWM whole brain $\lambda_{\perp}$	0.744 (0.037)	0.786 (0.080)	0.784 (0.086)	0.788 (0.073)

Values are unadjusted means (standard deviation); or number of participants (percentages). * median (interquartile range). MCI: mild cognitive impairment. CSVD: cerebral small vessel disease. TIV: total intracranial volume. WMH: white matter hyperintensities. NAWM: normal appearing white matter. NAWM whole brain measurements within the cerebral NAWM mask. WMH whole brain measurements within the cerebral WMH mask. MD, λ_{II}, $\lambda_{\perp}$ measures are shown as 10^{-3}. Differences between groups analyzed by means of ANCOVA corrected for age and sex, Mann-Whitney *U* test or Chi Square tests: [a] p <0.05 compared with controls. [b] p <0.05 compared with MCI patients without CSVD.

Tract based spatial statistics

After correction for age and sex, analyses within the NAWM-skeleton showed no differences for MD, λ_{II} or $\lambda_{\perp}$ in MCI patients relative to controls, but decreased FA in the right perforant path, in the temporal lobe. This difference was driven by MCI patients without CSVD, as they showed a significant FA decrease in the same region in comparison with controls (Figure 2 A). Relative to controls, MCI patients with CSVD showed decreased FA and increased $\lambda_{\perp}$ in the genu of the corpus callosum (CC), the bilateral internal and external capsule as well as periventricular white matter regions (Figure 2 B). Compared with MCI patients without CSVD, MCI patients with CSVD showed even more pronounced decreased FA (Figure 2 C) and increased $\lambda_{\perp}$ (Figure 2 D) in these same regions.

Automated tractography segmentation

Not all selected white matter tracts could be identified with the automated probabilistic tractography approach. The left and right CGC were identified in 60 out of 74 participants, the left CST in 72 of 74 participants and the right CST was found in 73 of 74 participants. All other tracts were identified in all subjects, as illustrated in Figure 3 A and B.

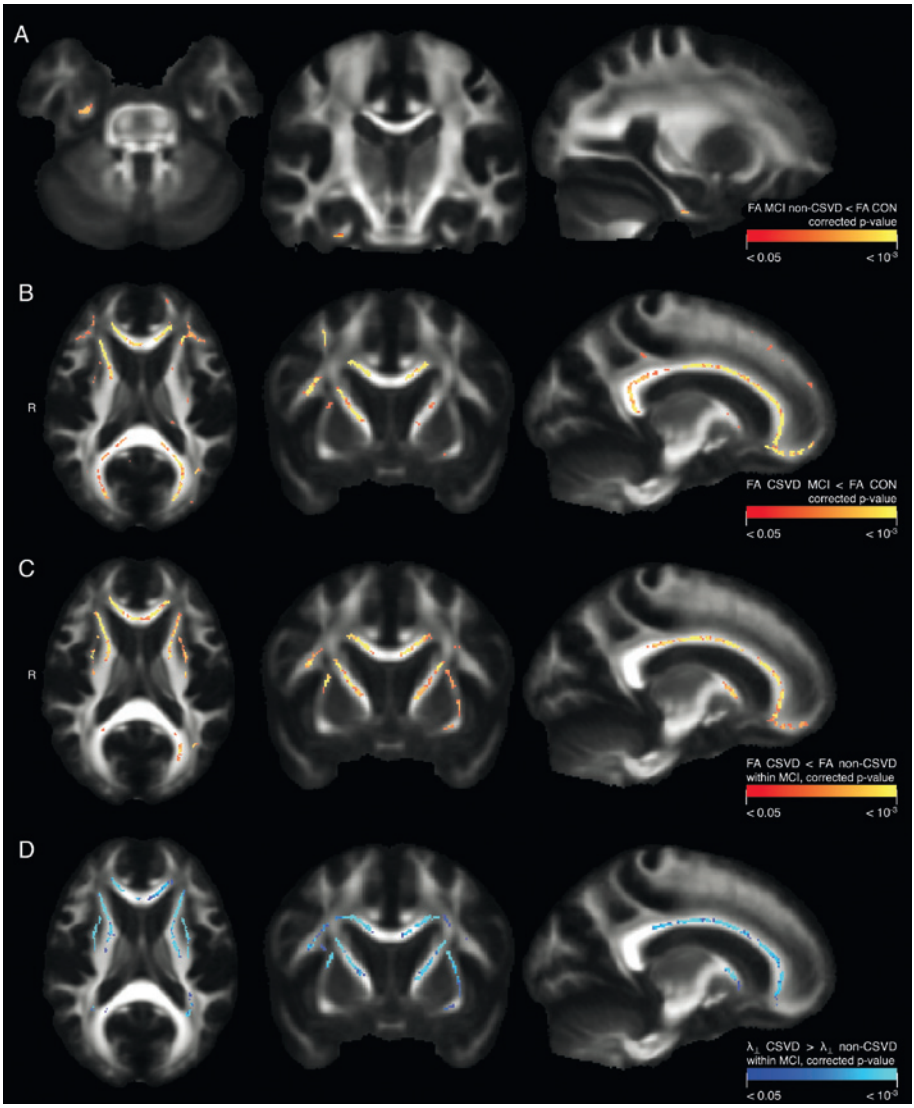

Figure 2 A) Significantly decreased FA in MCI patients without CSVD relative to controls. B) Significantly decreased FA in MCI patients with CSVD relative to controls. C) Significantly decreased FA in MCI patients with CSVD relative to MCI patients without CSVD. D) Significantly increased perpendicular diffusivity in MCI patients with CSVD relative to MCI patients without CSVD.

Subtracting the a priori defined white matter tracts, we found that relative to controls, MCI patients showed significant differences in DTI measures in the left and right CGH, and the FMI (Table 3). When subdividing MCI patients into those with and without CSVD, MCI patients with CSVD differed in DTI measures in the left and right CGH and right SLF relative to controls; and the left CGC, left and right CST, FMI and the left SLF in comparison to both controls as well as MCI patients without CSVD (Table 3), whereas MCI patients

without CSVD showed lower FA and higher MD and $\lambda_{\perp}$ only within the left and right CGH relative to controls (Table 3). It is important to note that the CST was included in our analysis as control tract in first instance.

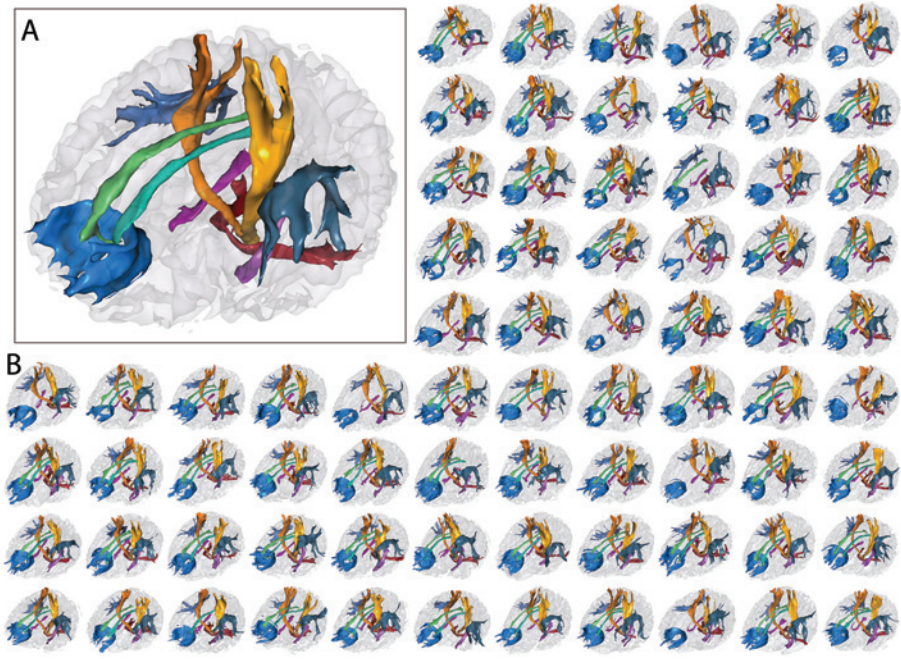

Figure 3 A) Probablistic tractography of tracts of interest and control tracts in a single subject, blue: forceps minor; light and dark green: left and right cingulum cingulate part; orange and yellow: left and right corticospinal tract; light and dark purple: left and right cingulum hippocampus part; light and dark grey: left and right superior longitudinal fasciculus; red: middle cerebellar peduncle. B) Probablistic tractography of tracts of interest in all participants, controls and MCI patients in native space.

Regression analyses of tracts of interest

We analyzed the predictive value of several determinants on white matter microstructure within the full cohort of MCI patients. The analyses were restricted to tracts and DTI measures that differed ($p < 0.10$) between the full cohort of MCI patients and controls (bold and italic figures in Table 3). For the left and right CGH, the left and right hippocampal volume respectively were the most important determinants for FA and $\lambda_{\perp}$, with WMH volume as second most important determinant in left CGH FA and $\lambda_{\perp}$ (Table 4). In these tracts lower hippocampal volumes and higher WMH volume were associated with lower FA and higher $\lambda_{\perp}$ values (Table 4). Within the FMI and right CST, WMH volume was the most important determinant for FA, followed by age. In these tracts, higher WMH volume and higher age were associated with lower FA values.

Table 3 DTI measures within tracts of interest as extracted by means of probabilistic tractography

	FA				MD				$\lambda_{\parallel}$				$\lambda_{\perp}$			
Tracts	Controls	Total MCI	MCI without CSVD	MCI CSVD	Controls	Total MCI	MCI without CSVD	MCI CSVD	Controls	Total MCI	MCI without CSVD	MCI CSVD	Controls	Total MCI	MCI without CSVD	MCI CSVD
CGC l	0.51	0.50	0.51	0.48	0.92	0.95	0.94	0.95	1.53	1.54	1.55	1.52	0.63	0.65	0.64	0.67
	(0.03)	(0.04)	(0.04)	(0.03)[a,b]	(0.03)	(0.06)	(0.06)	(0.06)	(0.06)	(0.10)	(0.09)	(0.13)	(0.04)	(0.06)	(0.05)	(0.05)[a]
CGC r	0.48	***0.47***	0.48	0.46	0.94	0.95	0.96	0.95	1.51	1.49	1.51	1.46	0.66	0.68	0.68	0.69
	(0.04)	***(0.04)****	(0.04)	(0.04)	(0.03)	(0.07)	(0.06)	(0.09)	(0.07)	(0.11)	(0.09)	(0.13)	(0.05)	(0.06)	(0.06)	(0.07)
CGH l	0.38	***0.36***	0.37	0.35	1.01	***1.06***	1.06	1.07	1.44	1.49	1.49	1.48	0.79	***0.85***	0.84	0.86
	(0.03)	***(0.03)****	(0.03)	(0.03)[a]	(0.06)	***(0.08)[a]***	(0.09)[a]	(0.06)	(0.06)	(0.11)	(0.12)	(0.10)	(0.06)	***(0.08)[a]***	(0.08)[a]	(0.06)[a]
CGH r	0.40	***0.38***	0.38	0.38	1.00	***1.06***	1.05	1.08	1.46	1.51	1.50	1.53	0.77	***0.83***	0.82	0.85
	(0.03)	***(0.03)****	(0.03)[a]	(0.04)	(0.05)	***(0.08)[a]***	(0.08)[a]	(0.09)[a]	(0.06)	(0.11)	(0.11)	(0.10)	(0.06)	***(0.08)[a]***	(0.07)[a]	(0.09)[a]
SLF l	0.49	0.48	0.49	0.47	0.90	0.92	0.90	0.95	1.43	1.44	1.43	1.46	0.64	0.66	0.64	0.69
	(0.02)	(0.03)	(0.03)	(0.04)[a,b]	(0.03)	(0.06)	(0.06)	(0.07)[b]	(0.05)	(0.09)	(0.08)	(0.10)	(0.03)	(0.06)	(0.05)	(0.06)[a,b]
SLF r	0.48	0.47	0.48	0.46	0.92	0.93	0.92	0.95	1.44	1.45	1.44	1.47	0.65	0.68	0.66	0.70
	(0.03)	(0.03)	(0.03)	(0.03)[a]	(0.04)	(0.07)	(0.06)	(0.07)	(0.05)	(0.10)	(0.09)	(0.11)	(0.04)	(0.06)	(0.06)	(0.05)
FMI	0.55	***0.51***	0.53	0.49	0.97	1.01	0.99	1.02	1.65	1.66	1.66	1.65	0.63	0.68	0.66	0.71
	(0.03)	***(0.04)[a]***	(0.03)	(0.04)[a,b]	(0.05)	(0.07)	(0.07)	(0.08)	(0.05)	(0.10)	(0.10)	(0.11)	(0.05)	(0.07)	(0.06)	(0.08)[a,b]
CST l	0.53	0.52	0.53	0.52	0.91	0.92	0.90	0.94	1.49	1.50	1.49	1.53	0.62	0.62	0.61	0.65
	(0.02)	(0.03)	(0.02)	(0.03)[b]	(0.04)	(0.05)	(0.04)	(0.05)[a,b]	(0.06)	(0.08)	(0.07)	(0.09)	(0.03)	(0.05)	(0.04)	(0.05)[a,b]
CST r	0.52	0.52	0.52	0.51	0.92	0.93	0.92	0.95	1.51	1.52	1.51	1.53	0.62	***0.64***	0.63	0.65
	(0.02)	(0.03)	(0.02)	(0.03)[a]	(0.03)	(0.05)	(0.05)	(0.05)[a]	(0.06)	(0.09)	(0.08)	(0.09)	(0.03)	***(0.04)****	(0.04)	(0.04)[a,b]
MCP	0.52	0.53	0.52	0.54	0.98	1.00	1.01	0.98	1.59	1.63	1.64	1.61	0.68	0.69	0.70	0.66
	(0.04)	(0.04)	(0.05)	(0.04)	(0.08)	(0.12)	(0.13)	(0.09)	(0.11)	(0.15)	(0.15)	(0.13)	(0.07)	(0.12)	(0.13)	(0.08)

Values are unadjusted means (standard deviation). MD, $\lambda_{\parallel}$, $\lambda_{\perp}$ shown as 10^{-3}. Differences between groups analyzed by means of ANCOVA corrected for age and sex: [a] $p < 0.05$ in comparison with controls. [b] $p < 0.05$ in comparison with MCI without CSVD. * $p < 0.10$ in comparison with controls.

Table 4. Results of the stepwise regression model in tracts of interest

Dependent variable	Predictors WMH corrected tract	Beta value	Significance
FA CGC r	1. White matter volume	0.638	<0.001
FA CGH l	1. Left hippocampal volume	0.530	<0.001
	2. WMH volume	-0.327	0.012
FA CGH r	1. Right hippocampal volume	0.392	0.005
FA FMI	1. WMH volume	-0.492	<0.001
	2. Age at scan	-0.343	0.004
MD CGH l	1. Age at scan	0.385	0.006
MD CGH r	-		
$\lambda_{\perp}$ CGH l	1. Left hippocampal volume	-0.521	<0.001
	2. WMH volume	0.383	0.003
$\lambda_{\perp}$ CGH r	1. White matter volume	-0.810	0.003
	2. TIV volume	0.597	0.035
$\lambda_{\perp}$ CST r	1. WMH volume	0.329	0.021

Significant predictors in a stepwise regression model. WMH: white matter hyperintensity. TIV: total intracranial volume. Volumes in ml. Beta values are standardized coefficients.

DISCUSSION

In the present study our aim was to examine the role of CSVD, represented by the extent of WMH and the presence of lacunar infarcts, in white matter microstructure deterioration in MCI patients. We found widespread microstructural changes in the brain's NAWM in MCI patients with CSVD as compared with controls and MCI patients without CSVD. Moreover, the presence of macrostructural manifestations of CSVD on MRI in patients with MCI was found to be one of the most important determinants of the NAWM microstructural deterioration of fiber tracts interconnecting several brain regions involved in the default mode network.

A first strength of the present study is the fact that all our analyses were restricted to the NAWM. It is known that the white matter microstructure is affected in WMH regions (Horsfield and Jones, 2002), and therefore global white matter analyses would be biased by WMH load. Second, we based the subdivision of MCI patients with and without CSVD on a semiquantitative rating scale often used in clinical practice (Fazekas et al., 2002). Using such a scale, our results can easily be translated to common clinical practice and other studies. Finally, we used several advanced DTI post processing techniques as well as automated MRI tissue segmentation. By using an automated tractography procedure based on standard masks, we avoided the subjectivity and reproducibility issues of manually drawing and placing ROIs as a starting point for tractography. A limitation of

our study may be the relatively small sample size of our patient cohort, which limits the generalizability of our findings to the MCI population at large. Another limitation is the age difference between controls and MCI patients as a result of our inclusion method. In this study control subjects had to be at least 65 years of age, but were not specifically age or sex matched with MCI patients. We expect however, that we dealt with this potential problem by regressing out the effects of age and sex in all between group analyses.

In line with other studies we included the CST as a control tract (Kiuchi et al., 2009). A control tract is a tract that remains unaffected by the disease process, like the CST is thought to remain unaffected in AD for a long time (Kiuchi et al., 2009; Rose et al., 2000). Our results however, point out that the CST was affected in MCI patients with CSVD as compared to those without CSVD, suggesting vascular related damage. Interestingly, CST damage was associated with gait problems and other corticospinal signs in patients with Binswanger's disease, a subcortical white matter disorder, as well as in stroke patients (Thomson et al., 1987, Jang, 2011). Probably dependent upon its localization, the CST is affected in MCI patients with CSVD, which could be related to findings in the literature (Frisoni et al., 2002). In the present study we therefore selected the MCP as a second control tract.

In MCI patients with CSVD we found widespread damage of the NAWM microstructure, within the genu of the CC, the internal and external capsule bilaterally and periventricular white matter regions. These findings are in line with a recent DTI study in patients with subcortical ischemic vascular dementia, in which similar fiber tracts were found to be affected (Chen et al., 2009). A study in healthy elderly subjects reported NAWM microstructural deterioration to be greater in subjects with macrostructural findings of CSVD on MRI than in those without (O'Sullivan et al., 2001; Vernooij et al., 2008). Although we already know that microstructure is affected within WMH regions (Horsfield and Jones, 2002), our findings suggest that also widespread NAWM microstructural changes are associated with the presence of CSVD in MCI. Most previous DTI studies in MCI failed to control for WMH load or any other expression of CSVD on MRI (Bai et al., 2009; Chua et al., 2009; Liu et al., 2011; Zhou et al., 2008; Zhuang et al., 2010), and attribute findings of widespread microstructural damage to AD-related neurodegeneration (Bai et al., 2009; Sexton et al., 2011; Zhuang et al., 2010), even though it was shown that the widespread pattern of white matter deterioration cannot be explained solely by grey matter atrophy (Xie et al., 2006). Based on our results, we would suggest that the widespread changes in the NAWM microstructure specifically encountered in MCI patients with CSVD and not in those without CSVD, represent an early stage of cerebrovascular damage preceding the development of macrostructural lesions in the NAWM (O'Sullivan et al., 2001; Schmidtke and Hull, 2005; Maillard et al., 2012).

Relative to controls, MCI patients without CSVD showed microstructural deterioration within the right perforant path, a fiber tract connecting the entorhinal cortex and the hippocampus (Witter et al., 2000) thought to play an important role in the limbic system (Thal et al., 2000). This finding within a group of MCI patients with a clinical, cognitive and pathophysiological profile of early AD without any macrostructural and clinical signs of cerebrovascular interference is in line with other DTI studies in MCI and AD, that reported either anterior temporal lobe microstructural damage, or specific perforant path deterioration (Damoiseaux et al., 2009; Kalus et al., 2006; Rogalski et al., 2009). Moreover, Damoiseaux et al. (2009) found DTI changes in AD confined to the anterior temporal lobe in a whole brain TBSS analysis, when explicitly excluding subjects with macrostructural white matter abnormalities on MRI. Our results are furthermore consistent with current knowledge of neuropathological processes in AD (Braak and Braak, 1991), in which specifically the entorhinal cortex, hippocampus and other regions in the medial temporal lobe are known to be affected early in the disease process.

When we focused on specific tracts interconnecting brain regions involved in the default mode network, we found that the CGH, a fiber tract connecting the hippocampus, parahippocampal cortex and the posterior cingulate cortex, consistently showed microstructural damage in MCI patients with and without CSVD compared with controls. Other tracts important in default mode network functioning like the left CGC and bilateral SLF were primarily affected in MCI patients with CSVD. The finding of loss of CGH microstructural integrity is consistent with the current literature on MCI (Clerx et al., 2012), and was previously found to be related to atrophy of the hippocampal formation (Sydykova et al., 2007; Villain et al., 2008). There is much debate concerning the pathophysiology underlying white matter abnormalities in MCI. One theory states that microstructural changes occur as a process secondary to grey matter atrophy, so-called Wallerian degeneration (Raff et al., 2002; Sexton et al., 2011). Another theory focuses on the role of microvascular changes in white matter pathology, i.e. a process directly affecting the white matter (Sexton et al., 2011). Within the full cohort of MCI patients we found a relationship between CGH microstructure and ipsilateral hippocampal volume as well as the presence and extent of macrostructural manifestations of CSVD, in terms of WMH volume and lacunar infarcts. These results suggest that - default mode network associated fiber tracts - may be damaged in MCI as the consequence of both Wallerian neurodegenerative as well as vascular effects. In the present study though, other fiber tracts thought to be important in default mode network functioning were found only to be affected in MCI patients with CSVD, even when compared with MCI patients without CSVD. Thus, although we did find evidence for Wallerian related microstructure deterioration in default mode network associated white matter tracts in MCI, the vascular

effects seemed to be most prominent in MCI patients with CSVD. The localization of a tract might be decisive here, as tracts nearby the ventricles are shown to be susceptible to cerebrovascular damage (the FMI and CST) (De Reuck, 1971; Longstreth et al., 1996), while tracts connecting degenerating grey matter regions show influence of atrophy, i.e. Wallerian influence (the CGH, the perforant path), and furthermore white matter near the brain stem was not affected (the MCP).

We measured white matter microstructure not only in terms of FA and MD, but also with respect to the directional properties of diffusion, i.e. axial and perpendicular diffusivity. Studies in mice suggest that a difference in the pathophysiology underlies axial and perpendicular diffusivity, as axial diffusivity was found to relate to axonal injury while perpendicular diffusivity was linked to myelin damage (Song et al., 2005; Sun et al., 2006). In the current study we found that axial diffusivity was less sensitive in distinguishing MCI patients from controls compared with the other DTI measures, suggesting little axonal injury in our MCI cohort. Perpendicular diffusivity increase was found primarily in MCI patients with CSVD compared to either controls or MCI patients without CSVD. This indicates that the underlying pathophysiology in our cohort of MCI patients with CSVD would primarily be myelin loss. Interestingly, myelin damage was found to be associated with transmission velocity reduction (Bartzokis, 2004), which might be the link between changes in myelin basic protein and the typical cognitive profile of decreased psychomotor speed in elderly with CSVD (Prins et al., 2005; Wang et al., 2004).

The pathological mechanisms of Alzheimer's disease and cerebrovascular damage have traditionally been considered separate, sometimes even mutually exclusive (Erkinjuntti and Gauthier, 2009; Frisoni et al., 2002). The fact that in a large proportion of dementia cases underlying pathology was mixed, i.e. combined vascular and degenerative pathology at autopsy, as well as on MRI (Englund et al., 1988; Reed et al., 2007; Targosz-Gajniak et al., 2009), contradicts this view. In the present study we show that atrophy related to AD and cerebrovascular damage both affect the white matter. Whether the different pathological processes influence each other, as suggested by studies reporting a reciprocal effect of cerebrovascular insufficiency promoting neurodegenerative changes and vice versa (Iadecola, 2010), are synergistic or additive to the clinical and cognitive syndrome has yet to be further elucidated. We however think that where AD pathology affects mainly the grey matter, CSVD is responsible for the majority of white matter damage in MCI, thereby affecting the white matter interconnecting important grey matter regions, and interfering with neuronal network functioning.

This study indicates that in patients with MCI, CSVD affects the brain's white matter more extensively than the macrostructural findings visible on T2-FLAIR imaging. We found evidence of cerebrovascular disease related microstructural damage in important fiber tracts that subserve the default mode network. We postulate that such damage interferes with the normal functioning of the default mode network and consequently cognitive functioning. Our results also highlight a role for atrophy driven degeneration of white matter microstructure and therefore point towards a neuropathological white matter substrate in MCI in which both direct cerebrovascular damage and Wallerian degeneration play a role.

REFERENCES

Albert MS, DeKosky ST, Dickson D, Dubois B, Feldman HH, Fox NC, *et al.* The diagnosis of mild cognitive impairment due to Alzheimer's disease: recommendations from the National Institute on Aging-Alzheimer's Association workgroups on diagnostic guidelines for Alzheimer's disease. Alzheimers Dement 2011; 7: 270-279.

Bai F, Zhang Z, Watson DR, Yu H, Shi Y, Yuan Y, *et al.* Abnormal integrity of association fiber tracts in amnestic mild cognitive impairment. J Neurol Sci 2009; 278: 102-106.

Bai F, Zhang Z, Yu H, Shi Y, Yuan Y, Zhu W, *et al.* Default-mode network activity distinguishes amnestic type mild cognitive impairment from healthy aging: a combined structural and resting-state functional MRI study. Neurosci Lett 2008; 438: 111-115.

Bartzokis G. Age-related myelin breakdown: a developmental model of cognitive decline and Alzheimer's disease. Neurobiol Aging 2004; 25: 5-18; author reply 49-62.

Behrens TE, Berg HJ, Jbabdi S, Rushworth MF, Woolrich MW. Probabilistic diffusion tractography with multiple fibre orientations: What can we gain? Neuroimage 2007; 34: 144-155.

Bozzali M, Filippi M, Magnani G, Cercignani M, Franceschi M, Schiatti E, *et al.* The contribution of voxel-based morphometry in staging patients with mild cognitive impairment. Neurology 2006; 67: 453-460.

Braak H, Braak E. Neuropathological stageing of Alzheimer-related changes. Acta Neuropathol 1991; 82: 239-259.

Buckner RL, Andrews-Hanna JR, Schacter DL. The brain's default network: anatomy, function, and relevance to disease. Ann N Y Acad Sci 2008; 1124: 1-38.

Chen TF, Lin CC, Chen YF, Liu HM, Hua MS, Huang YC, *et al.* Diffusion tensor changes in patients with amnesic mild cognitive impairment and various dementias. Psychiatry Res 2009; 173: 15-21.

Chetelat G, Landeau B, Eustache F, Mezenge F, Viader F, de la Sayette V, *et al.* Using voxel-based morphometry to map the structural changes associated with rapid conversion in MCI: a longitudinal MRI study. Neuroimage 2005; 27: 934-946.

Chua TC, Wen W, Chen X, Kochan N, Slavin MJ, Trollor JN, *et al.* Diffusion tensor imaging of the posterior cingulate is a useful biomarker of mild cognitive impairment. Am J Geriatr Psychiatry 2009; 17: 602-613.

Clerx L, Visser PJ, Verhey F, Aalten P. New MRI markers for Alzheimer's disease: a meta-analysis of diffusion tensor imaging and a comparison with medial temporal lobe measurements. J Alzheimers Dis 2012; 29: 405-429.

Damoiseaux JS, Greicius MD. Greater than the sum of its parts: a review of studies combining structural connectivity and resting-state functional connectivity. Brain Struct Funct 2009; 213: 525-533.

Damoiseaux JS, Smith SM, Witter MP, Sanz-Arigita EJ, Barkhof F, Scheltens P, *et al.* White matter tract integrity in aging and Alzheimer's disease. Hum Brain Mapp 2009; 30: 1051-1059.

de Boer R, Vrooman HA, van der Lijn F, Vernooij MW, Ikram MA, van der Lugt A, *et al.* White matter lesion extension to automatic brain tissue segmentation on MRI. Neuroimage 2009; 45: 1151-1161.

De Reuck J. The human periventricular arterial blood supply and the anatomy of cerebral infarctions. Eur Neurol 1971; 5: 321-334.

DeCarli C. Mild cognitive impairment: prevalence, prognosis, aetiology, and treatment. Lancet Neurol 2003; 2: 15-21.

den Heijer T, van der Lijn F, Koudstaal PJ, Hofman A, van der Lugt A, Krestin GP, *et al.* A 10-year follow-up of hippocampal volume on magnetic resonance imaging in early dementia and cognitive decline. Brain 2010; 133: 1163-1172.

Dickerson BC, Goncharova I, Sullivan MP, Forchetti C, Wilson RS, Bennett DA, *et al.* MRI-derived entorhinal and hippocampal atrophy in incipient and very mild Alzheimer's disease. Neurobiol Aging 2001; 22: 747-754.

Englund E, Brun A, Alling C. White matter changes in dementia of Alzheimer's type. Biochemical and neuropathological correlates. Brain 1988; 111 (Pt 6): 1425-1439.

Erkinjuntti T, Gauthier S. The concept of vascular cognitive impairment. Front Neurol Neurosci 2009; 24: 79-85.

Fazekas F, Barkhof F, Wahlund LO, Pantoni L, Erkinjuntti T, Scheltens P, *et al.* CT and MRI rating of white matter lesions. Cerebrovasc Dis 2002; 13 Suppl 2: 31-36.

Frisoni GB, Galluzzi S, Bresciani L, Zanetti O, Geroldi C. Mild cognitive impairment with subcortical vascular features: clinical characteristics and outcome. J Neurol 2002; 249: 1423-1432.

Greicius MD, Krasnow B, Reiss AL, Menon V. Functional connectivity in the resting brain: a network analysis of the default mode hypothesis. Proc Natl Acad Sci U S A 2003; 100: 253-258.

Greicius MD, Srivastava G, Reiss AL, Menon V. Default-mode network activity distinguishes Alzheimer's disease from healthy aging: evidence from functional MRI. Proc Natl Acad Sci U S A 2004; 101: 4637-4642.

Greicius MD, Supekar K, Menon V, Dougherty RF. Resting-state functional connectivity reflects structural connectivity in the default mode network. Cereb Cortex 2009; 19: 72-78.

Horsfield MA, Jones DK. Applications of diffusion-weighted and diffusion tensor MRI to white matter diseases - a review. NMR Biomed 2002; 15: 570-577.

Iadecola C. The overlap between neurodegenerative and vascular factors in the pathogenesis of dementia. Acta Neuropathol 2010; 120: 287-296.

Jack CR, Jr., Petersen RC, Xu Y, O'Brien PC, Smith GE, Ivnik RJ, *et al.* Rates of hippocampal atrophy correlate with change in clinical status in aging and AD. Neurology 2000; 55: 484-489.

Jang SH. Diffusion tensor imaging studies on corticospinal tract injury following traumatic brain injury: a review. NeuroRehabilitation 2011; 29: 339-345.

Jenkinson M, Smith S. A global optimisation method for robust affine registration of brain images. Med Image Anal 2001; 5: 143-156.

Kalus P, Slotboom J, Gallinat J, Mahlberg R, Cattapan-Ludewig K, Wiest R, *et al.* Examining the gateway to the limbic system with diffusion tensor imaging: the perforant pathway in dementia. Neuroimage 2006; 30: 713-720.

Karas GB, Scheltens P, Rombouts SA, Visser PJ, van Schijndel RA, Fox NC, *et al.* Global and local gray matter loss in mild cognitive impairment and Alzheimer's disease. Neuroimage 2004; 23: 708-716.

Kiuchi K, Morikawa M, Taoka T, Nagashima T, Yamauchi T, Makinodan M, *et al.* Abnormalities of the uncinate fasciculus and posterior cingulate fasciculus in mild cognitive impairment and early Alzheimer's disease: a diffusion tensor tractography study. Brain Res 2009; 1287: 184-191.

Klein S, Staring M, Murphy K, Viergever MA, Pluim JP. elastix: a toolbox for intensity-based medical image registration. IEEE Trans Med Imaging 2010; 29: 196-205.

Leemans A, Jones DK. The B-matrix must be rotated when correcting for subject motion in DTI data. Magn Res in Medicine 2009; 62(1): 1336-1349.

Liu Y, Spulber G, Lehtimaki KK, Kononen M, Hallikainen I, Grohn H, *et al.* Diffusion tensor imaging and tract-based spatial statistics in Alzheimer's disease and mild cognitive impairment. Neurobiol Aging 2011; 32: 1558-1571.

Longstreth WT, Jr., Manolio TA, Arnold A, Burke GL, Bryan N, Jungreis CA, *et al.* Clinical correlates of white matter findings on cranial magnetic resonance imaging of 3301 elderly people. The Cardiovascular Health Study. Stroke 1996; 27: 1274-1282.

Luchsinger JA, Brickman AM, Reitz C, Cho SJ, Schupf N, Manly JJ, *et al.* Subclinical cerebrovascular disease in mild cognitive impairment. Neurology 2009; 73: 450-456.

Maillard P, Carmichael O, Harvey D, Fletcher E, Reed B, Mungas D, DeCarli C. FLAIR and diffusion MRI signals are independent predictors of white matter hyperintensities. AJNR 2012; Epub.

Mayda AB, Westphal A, Carter CS, DeCarli C. Late life cognitive control deficits are accentuated by white matter disease burden. Brain 2011; 134: 1673-1683.

Mori S, Kaufmann WE, Davatzikos C, Stieltjes B, Amodei L, Fredericksen K, *et al.* Imaging cortical association tracts in the human brain using diffusion-tensor-based axonal tracking. Magn Reson Med 2002; 47: 215-223.

Nordahl CW, Ranganath C, Yonelinas AP, DeCarli C, Reed BR, Jagust WJ. Different mechanisms of episodic memory failure in mild cognitive impairment. Neuropsychologia 2005; 43: 1688-1697.

O'Sullivan M, Summers PE, Jones DK, Jarosz JM, Williams SC, Markus HS. Normal-appearing white matter in ischemic leukoaraiosis: a diffusion tensor MRI study. Neurology 2001; 57: 2307-2310.

Pantoni L. Cerebral small vessel disease: from pathogenesis and clinical characteristics to therapeutic challenges. Lancet Neurol 2010; 9: 689-701.

Perneczky R, Wagenpfeil S, Komossa K, Grimmer T, Diehl J, Kurz A. Mapping scores onto stages: mini-mental state examination and clinical dementia rating. Am J Geriatr Psychiatry 2006; 14: 139-144.

Petersen RC. Mild cognitive impairment as a diagnostic entity. J Intern Med 2004; 256: 183-194.

Prins ND, van Dijk EJ, den Heijer T, Vermeer SE, Jolles J, Koudstaal PJ, *et al.* Cerebral small-vessel disease and decline in information processing speed, executive function and memory. Brain 2005; 128: 2034-2041.

Raff MC, Whitmore AV, Finn JT. Axonal self-destruction and neurodegeneration. Science 2002; 296: 868-871.

Raichle ME, MacLeod AM, Snyder AZ, Powers WJ, Gusnard DA, Shulman GL. A default mode of brain function. Proc Natl Acad Sci U S A 2001; 98: 676-682.

Reed BR, Mungas DM, Kramer JH, Ellis W, Vinters HV, Zarow C, *et al.* Profiles of neuropsychological impairment in autopsy-defined Alzheimer's disease and cerebrovascular disease. Brain 2007; 130: 731-739.

Rocca MA, Valsasina P, Absinta M, Riccitelli G, Rodegher ME, Misci P, *et al.* Default-mode network dysfunction and cognitive impairment in progressive MS. Neurology 2010; 74: 1252-1259.

Rogalski EJ, Murphy CM, deToledo-Morrell L, Shah RC, Moseley ME, Bammer R, *et al.* Changes in parahippocampal white matter integrity in amnestic mild cognitive impairment: a diffusion tensor imaging study. Behav Neurol 2009; 21: 51-61.

Rose SE, Chen F, Chalk JB, Zelaya FO, Strugnell WE, Benson M, *et al.* Loss of connectivity in Alzheimer's disease: an evaluation of white matter tract integrity with colour coded MR diffusion tensor imaging. J Neurol Neurosurg Psychiatry 2000; 69: 528-530.

Schmidtke K, Hull M. Cerebral small vessel disease: how does it progress? J Neurol Sci 2005; 229-230: 13-20.

Seeley WW, Crawford RK, Zhou J, Miller BL, Greicius MD. Neurodegenerative diseases target large-scale human brain networks. Neuron 2009; 62: 42-52.

Sexton CE, Kalu UG, Filippini N, Mackay CE, Ebmeier KP. A meta-analysis of diffusion tensor imaging in mild cognitive impairment and Alzheimer's disease. Neurobiol Aging 2011; 32: 2322 e2325-2318.

Smith SM. Fast robust automated brain extraction. Hum Brain Mapp 2002; 17: 143-155.

Smith SM, Jenkinson M, Johansen-Berg H, Rueckert D, Nichols TE, Mackay CE, *et al.* Tract-based spatial statistics: voxelwise analysis of multi-subject diffusion data. Neuroimage 2006; 31: 1487-1505.

Smith SM, Nichols TE. Threshold-free cluster enhancement: addressing problems of smoothing, threshold dependence and localisation in cluster inference. Neuroimage 2009; 44: 83-98.

Song SK, Yoshino J, Le TQ, Lin SJ, Sun SW, Cross AH, *et al.* Demyelination increases radial diffusivity in corpus callosum of mouse brain. Neuroimage 2005; 26: 132-140.

Stieltjes B, Kaufmann WE, van Zijl PC, Fredericksen K, Pearlson GD, Solaiyappan M, *et al.* Diffusion tensor imaging and axonal tracking in the human brainstem. Neuroimage 2001; 14: 723-735.

Sun SW, Liang HF, Le TQ, Armstrong RC, Cross AH, Song SK. Differential sensitivity of in vivo and ex vivo diffusion tensor imaging to evolving optic nerve injury in mice with retinal ischemia. Neuroimage 2006; 32: 1195-1204.

Sydykova D, Stahl R, Dietrich O, Ewers M, Reiser MF, Schoenberg SO, *et al.* Fiber connections between the cerebral cortex and the corpus callosum in Alzheimer's disease: a diffusion tensor imaging and voxel-based morphometry study. Cereb Cortex 2007; 17: 2276-2282.

Targosz-Gajniak M, Siuda J, Ochudlo S, Opala G. Cerebral white matter lesions in patients with dementia - from MCI to severe Alzheimer's disease. J Neurol Sci 2009; 283: 79-82.

Teipel SJ, Bokde AL, Meindl T, Amaro E, Jr., Soldner J, Reiser MF, *et al.* White matter microstructure underlying default mode network connectivity in the human brain. Neuroimage 2010; 49: 2021-2032.

Thal DR, Holzer M, Rub U, Waldmann G, Gunzel S, Zedlick D, Schober R. Alzheimer-related tau-pathology in the perforant path target zone and in hippocampal stratum oriens and radiatum correlates with onset and degree of dementia. Exp Neurol 2000; 163: 98-110.

Thompson PD, Marsden CD. Gait disorder of subcortical arteriosclerotic encephalopathy: Binswanger's disease. Movement disorders 1987; 2 (1): 1-8.

van den Heuvel M, Mandl R, Luigjes J, Hulshoff Pol H. Microstructural organization of the cingulum tract and the level of default mode functional connectivity. J Neurosci 2008; 28: 10844-10851.

van den Heuvel MP, Mandl RC, Kahn RS, Hulshoff Pol HE. Functionally linked resting-state networks reflect the underlying structural connectivity architecture of the human brain. Hum Brain Mapp 2009; 30: 3127-3141.

van der Lijn F, den Heijer T, Breteler MM, Niessen WJ. Hippocampus segmentation in MR images using atlas registration, voxel classification, and graph cuts. Neuroimage 2008; 43: 708-720.

Verhage F. Intelligentie en leeftijd: onderzoek bij Nederlanders van twaalf tot zevenenzeventig jaar [Intelligence and age: Research on Dutch people aged twelve to seventy-seven years old]. Assen: Van Gorcum 1964.

Vernooij MW, de Groot M, van der Lugt A, Ikram MA, Krestin GP, Hofman A, *et al.* White matter atrophy and lesion formation explain the loss of structural integrity of white matter in aging. Neuroimage 2008; 43: 470-477.

Villain N, Desgranges B, Viader F, de la Sayette V, Mezenge F, Landeau B, *et al.* Relationships between hippocampal atrophy, white matter disruption, and gray matter hypometabolism in Alzheimer's disease. J Neurosci 2008; 28: 6174-6181.

Villeneuve S, Massoud F, Bocti C, Gauthier S, Belleville S. The nature of episodic memory deficits in MCI with and without vascular burden. Neuropsychologia 2011; 49: 3027-3035.

Vrooman HA, Cocosco CA, van der Lijn F, Stokking R, Ikram MA, Vernooij MW, *et al.* Multi-spectral brain tissue segmentation using automatically trained k-Nearest-Neighbor classification. Neuroimage 2007; 37: 71-81.

Wakana S, Caprihan A, Panzenboeck MM, Fallon JH, Perry M, Gollub RL, *et al.* Reproducibility of quantitative tractography methods applied to cerebral white matter. Neuroimage 2007; 36: 630-644.

Wakana S, Jiang H, Nagae-Poetscher LM, van Zijl PC, Mori S. Fiber tract-based atlas of human white matter anatomy. Radiology 2004; 230: 77-87.

Wang DS, Bennett DA, Mufson EJ, Mattila P, Cochran E, Dickson DW. Contribution of changes in ubiquitin and myelin basic protein to age-related cognitive decline. Neurosci Res 2004; 48: 93-100.

Witter MP, Wouterlood FG, Naber PA, Van Haeften T. Anatomical organization of the parahippocampal-hippocampal network. Ann N Y Acad Sci 2000; 911: 1-24.

Woolrich MW, Jbabdi S, Patenaude B, Chappell M, Makni S, Behrens T, *et al.* Bayesian analysis of neuroimaging data in FSL. Neuroimage 2009; 45: S173-186.

Xie S, Xiao JX, Gong GL, Zang YF, Wang YH, Wu HK, *et al.* Voxel-based detection of white matter abnormalities in mild Alzheimer disease. Neurology 2006; 66: 1845-1849.

Yoshita M, Fletcher E, Harvey D, Ortega M, Martinez O, Mungas DM, *et al.* Extent and distribution of white matter hyperintensities in normal aging, MCI, and AD. Neurology 2006; 67: 2192-2198.

Zhou Y, Dougherty JH, Jr., Hubner KF, Bai B, Cannon RL, Hutson RK. Abnormal connectivity in the posterior cingulate and hippocampus in early Alzheimer's disease and mild cognitive impairment. Alzheimers Dement 2008; 4: 265-270.

Zhuang L, Wen W, Zhu W, Trollor J, Kochan N, Crawford J, *et al.* White matter integrity in mild cognitive impairment: a tract-based spatial statistics study. Neuroimage 2010; 53: 16-25.

Chapter 3

Functional neuroimaging in neurodegenerative disorders

Chapter 3.1

Episodic memory impairment in frontotemporal dementia: a ^{99m}TC HMPAO SPECT study

Janne M. Papma
Harro Seelaar
Inge de Koning
Djo Hasan
Ambroos E.M. Reijs
Roelf Valkema
Niels D. Prins
John C. van Swieten

Current Alzheimer Research 2012; Published online 2012 Sep 25.

ABSTRACT

Alzheimer's disease (AD) and frontotemporal dementia (FTD) are the most common types of dementia in the presenile population. Episodic memory impairment, the clinical hallmark of AD, can also be encountered in patients with FTD, complicating accurate diagnosis. Several studies in FTD have correlated memory deficits with neuroimaging findings in FTD, but lacked to compare neuroimaging results in FTD patients with and without memory impairment. This latter analysis may give us insight into the underlying mechanisms of memory impairment in FTD. The aim of the present study was to compare the ^{99m}Tc-HMPAO SPECT hypoperfusion patterns between FTD with episodic memory impairment (n = 13), FTD patients without episodic memory impairment (n = 10) as well as early onset (< 70 yrs) AD patients (n = 13) and controls (n = 15). We performed group analyses by means of Statistical Parametric Mapping software (SPM5), and show that FTD patients with episodic memory impairment had lower perfusion in the right temporal lobe compared with FTD patients without memory impairment. Lower perfusion in this region correlated with worse memory performance on the Clinical Dementia Rating scale in FTD patients. With equal performances on memory tests, patients with early onset AD showed posterior temporal and parietal hypoperfusion in comparison with patients with FTD and memory impairment, while vice versa hypoperfusion in the anterior frontotemporal regions was found in FTD patients with memory impairment in comparison with AD.

INTRODUCTION

Alzheimer's disease (AD) and frontotemporal dementia (FTD) are the most common types of dementia in the presenile population. The clinical hallmark of AD is progressive episodic memory impairment associated with neuropathological processes affecting initially the medial temporal lobes (MTL) (Braak and Braak, 1991b; McKhann et al., 1984), i.e. intraneuronal phosphorylated tau protein and extracellular accumulation of amyloid beta protein (Braak and Braak, 1991a). The clinical characteristics of the most common subtype of FTD, behavioral variant FTD (bvFTD), are behavioral changes and language disorders associated with prominent frontal and anterior temporal lobe deterioration. Neuropathological findings in these regions include tau-positive inclusions (frontotemporal lobar degeneration-tau, FTLD-tau) or ubiquitin-positive and TDP-43 positive inclusions (FTLD-TDP), for an overview see Seelaar et al. (2011). Despite clear post-mortem differentiation between the two neurodegenerative disorders, an early and accurate discrimination during life is hampered by the fact that clinically a number of bvFTD patients show episodic memory impairment (Hornberger et al., 2010; Pasquier et al., 2001), even as presenting symptom in 10 percent of pathological proven cases (Graham et al., 2005; Hodges et al., 2004). Furthermore, while neuroimaging studies show that medial temporal lobe involvement can initially be absent in early onset AD patients (Frisoni et al., 2005; Karas et al., 2007), hippocampal atrophy was found to be present in a subset of FTD patients (Broe et al., 2003; Hodges, 2001; Laakso et al., 2000; van de Pol et al., 2006). The specific contribution of the medial temporal lobe atrophy to memory disorders in FTD remains controversial, as conflicting results were found in the few studies that related memory functioning to neuroimaging findings (Bastin et al., 2012; Lavenu et al., 1998; Pennington et al., 2011; Soderlund et al., 2008). Quantitative studies examining neuroimaging differences in bvFTD patients with and without episodic memory impairment are lacking, but would contribute to our understanding of the underlying mechanisms of memory impairment in bvFTD. The aim of this study was to quantitatively determine differences of ^{99m}Tc-HMPAO single photon emission computed tomography (SPECT) perfusion patterns in bvFTD patients with and without episodic memory impairment, early onset AD patients and controls, using Statistical Parametric Mapping software (SPM5).

METHODS

Participants

We included 23 FTD patients of the behavioral variant type and 13 early onset AD patients in this retrospective study, hereafter referred to as FTD and AD. Patients were selected from a patient cohort attending the outpatient clinics of the Neurology department of the Erasmus MC – University Medical Center Rotterdam, the Netherlands, from 1994 till present. The selection of patients was based upon: a) clinical diagnosis of bvFTD according to the criteria of McKhann et al. (2001), or clinical diagnosis of AD according to the criteria of the NINCDS-ADRDA for clinical probable Alzheimer's dementia (McKhann et al., 1984). The clinical diagnosis of FTD was further supported by a neuropathological diagnosis, the presence of familial FTD, the presence of a *MAPT* or *Progranulin* gene mutation (Seelaar et al., 2008; Seelaar et al., 2010), and normal phospho-tau en beta-amyloid levels in CSF (Grossman et al., 2005); b) age at onset younger than 70 years, defined as the age at which the first symptoms related to the diagnosis were observed by relatives or caretakers; c) the presence of ^{99m}Tc-HMPAO SPECT and neuropsychological assessment data; d) MMSE score of at least 16 out of 30 at ascertainment; e) no diagnosis of primary progressive aphasia assessed by an experienced neuropsychologist (IdK). FTD patients in whom the clinical diagnosis was not supported by a neuropathological diagnosis or proven gene mutation were included in the study only if they showed progression over time in terms of disease severity. This way we excluded the 'non-progressive' form of FTD (Pennington et al., 2011). Average follow up in the FTD patient group was 21.5 months. Age matched controls (n = 15) were selected from the Rotterdam Elderly Study (n = 5) (Claus et al., 1994) or were selected from a ^{99m}Tc-HMPAO SPECT Erasmus MC database of subjects in stable health without abnormalities at neuropsychological and neurological examination (n = 10). These participants visited the outpatient clinics with subjective complaints, but showed normal examinations. Participants gave written informed consent to our protocol which was approved by the medical ethics committee of the Erasmus MC. Neuropsychological examinations and ^{99m}Tc-HMPAO SPECT scanning were part of the diagnostic work up in all patients and controls, with the exception of the five controls from the Rotterdam Elderly Study.

Neuropsychological assessment

All patients and controls underwent neuropsychological assessment. The neuropsychological battery included the MMSE as a cognitive screening method; Trail Making Test (TMT) part A and Stroop I as measures of cognitive processing speed; TMT B, Stroop III, Wisconsin Card Sorting Test (WCST), semantic fluency and a phonological letter fluency task (DAT) to assess executive functioning, and the 15-WVLT or WLM to

assess memory functioning as described into more detail below. Furthermore the Clinical Dementia Rating scale (CDR) was assessed in FTD and AD patients, the global CDR score was based on the CDR box scores. Average t-scores, corrected for age, gender and education were calculated for every test based on Dutch norms. As the neuropsychological test battery underwent some changes over a time period of 15 years, some tests showed missing data (Table 2). Furthermore, FTD patients were subdivided into apathetic, disinhibited and a stereotyped-compulsive syndrome upon presentation. In some cases the symptoms co-occurred and a specific syndrome could not be defined; for an overview see Seelaar et al. (2011).

Memory assessment

We assessed episodic memory either by means of the Dutch CERAD Word List Memory test (WLM; used between 1994-1998) (Morris et al., 1989), or by means of the Dutch 15 Word Verbal Learning Test (15-WVLT; used after 1998) (Brand and Jolles, 1985). The 15-WVLT consists of 15 monosyllabic words auditory presented in five subsequent trials with an immediate free recall following each presentation. This is followed by a delayed free recall and a forced choice recognition trial after approximately 20 minutes. The WLM consists of 10 monosyllabic words auditory presented in three trials. Similar to the 15-WVLT an immediate free recall follows every presentation and after 20 minutes delayed free recall and forced choice recognition memory are tested. We calculated t-scores for the 15-WVLT immediate recall (sum of 5 trials) and delayed recall based on normative data of 262 healthy Dutch participants aged 15 till 87 years. WLM immediate recall (sum of 3 trials) and delayed recall t-scores were based on normative data of 278 healthy people in the age range of 51 to 88 years (Andel et al., 2003; Morris et al., 1989). For the immediate or delayed recall of both tests we took two standard deviations below the mean as a cut-off value for memory impairment (t = 30). If at least one of the t-scores fell above this cut-off we considered this normal memory performance and subsequently divided FTD patients into FTD with episodic memory impairment, amnestic FTD (n = 13; A-FTD) and without episodic memory impairment, non-amnestic FTD (n = 10; NA-FTD). Recognition memory was not taken into account in the subdivision of memory impairment. The 15-WVLT was used to assess memory in 60 percent of control cases, in 61.5 percent of FTD cases with episodic memory impairment, in 70 percent of FTD cases without episodic memory impairment and in all cases of AD.

Cerebrospinal fluid markers

We obtained cerebrospinal fluid (CSF) during diagnostic lumbar punction as part of the clinical diagnostic process. Lumbar punction is not standard in our diagnostic process, which is why CSF samples were missing in a large proportion of patients. The handling of

CSF and the analysis of total tau levels and $A\beta_{42}$ are described elsewhere (Bian et al., 2008; Grossman et al., 2005). In line with Bian et al. we created a ratio of tau/ $A\beta_{42}$ which we compared between groups.

^{99m}Tc-HMPAO SPECT scanning and image processing

Patients and controls underwent brain perfusion SPECT imaging with 740 MBq ^{99m}Tc-hexamethyl propylene amine oxime (^{99m}Tc-HMPAO). We injected participants intravenously on average 20 minutes before imaging while seated in a quit room. A difference in time could occur due to the clinical setting, where sometimes two patients were injected at the same time. Images were acquired with a Prism 3000XP Philips (Picker) three-headed system, with a fan-beam collimator and 120 projections (3 x 40 steps of 3°, and 20 seconds per step). This SPECT imaging protocol did not change over the years. Image reconstruction was performed by a ramp-filtered back projection and three-dimensionally smoothed with a Metz Filter. After gross manual image reorientation and approximated definition of the image center point, SPECT scans were spatially processed by means of SPM5 (Wellcome department of Cognitive Neurology, London, UK) implemented in Matlab 7.9 (Mathworks, Natick, MA, USA). The effect of differences in spatial resolution was minimized by masking the images. SPECT images were resliced into similar orientations and spatially normalized onto the SPM5 MNI SPECT brain template with a 12-parameter affine transformation followed by non-linear transformations (Ashburner and Friston, 1999). Normalized images were represented on a 128 x 128 pixel matrix with a voxel size of 3 x 3 x 3 mm, and checked visually to ensure that no cerebral regions were incorrectly normalized into MNI space. During normalization, estimation of individual parameters was constrained by a source weighting image, a method used to correct for the registering of 'abnormal' or lesioned brains. Afterwards, normalized images were smoothed using a 16 mm full width at half maximum (FWHM) kernel, limited to measured brain tissue. For SPECT data, smoothing with at least twice the FWHM of the imaging system was shown to provide optimal detection sensitivity (Van Laere et al., 2002), and is used in studies in neurodegenerative conditions with SPECT or PET (Kim et al., 2005; Nishimiya et al., 2008). A proportional scaling route to the individual mean intensity was used to achieve global normalization of voxel values between images and subsequently correct for a possible difference in individual uptake of ^{99m}Tc-HMPAO. The use of a regional reference area was not suitable for our data since we were unable to obtain a reference area where perfusion was relatively preserved in all patient groups and controls (Soonawala et al., 2002; Yakushev et al., 2008). We conducted voxel based group analyses within the framework of the general linear model (Friston et al., 1995), using a full factorial design in SPM5 in which we included A-FTD patients, NA-FTD patients, AD patients and controls in a design matrix with age and gender as nuisance variables. We assessed hypoperfusion patterns

for significance at a relatively lenient threshold of $p < 0.001$ not corrected for multiple comparisons, with a minimum cluster size of 20 contiguous voxels, or in case of the between group comparisons of NA-FTD and A-FTD at an even more lenient threshold of $p < 0.005$ not corrected for multiple comparisons. The latter threshold was used to obtain regions with subtle perfusion differences between these two groups, which we used as a starting point for our ROI analysis. Post hoc, we created a mask image for the significant difference in right temporal lobe perfusion between NA-FTD and A-FTD, and extracted individual mean perfusion for all FTD patients using the Matlab toolbox MarsBaR 0.41 (Marseille Boîte À Région d'Intérêt), subsequently exporting these perfusion measures to SPSS (version 17.0 for Windows, Chicago, Ill. U.S.A.) for further analyses.

Statistical analysis

We evaluated demographic and neuropsychological characteristics and perfusion measures using SPSS. Differences between patient and control groups were tested for significance using one-way ANOVA and independent sample t-test (continuous variables), chi-square test (nominal variables), Kruskall-Wallis test and Mann Whitney U test (ordinal variables). We calculated the correlation between perfusion measures and cognitive functioning (15-WVLT immediate recall, delayed recall and recognition; WLM immediate recall, delayed recall and recognition; Trail making A and B; Stroop I and III, WCST concepts and letter fluency, MMSE) or CDR domains. For this purpose we used either Pearson's r for a correlation with continuous variables or Spearman's rho for a correlation with ordinal variables. A p value <0.05 was considered statistically significant.

RESULTS

Characteristics and neuropsychological data

Characteristics of patient groups and controls are summarized in Table 1. Patients with A-FTD were older at time of SPECT relative to NA-FTD patients, but in a similar disease stage as indicated by global CDR scores. A-FTD patients showed a significant lower CSF ratio of tau/$A\beta_{42}$ compared with AD patients.

Table 1 Characteristics of patient groups and controls

	Controls (n = 15)	NA-FTD (n = 10)	A-FTD (n = 13)	AD (n = 13)	P value
Mean age at onset, yrs	-	53.6 (8.2)	59.5 (7.0)	56.7 (6.6)	0.165
Mean age at SPECT, yrs	59.0 (8.4)	55.8 (9.1)	62.6 (7.1)[b]	60.6 (5.4)	0.187
Disease duration, yrs	-	2.2 (1.9)	3.2 (1.7)	3.8 (2.5)	0.217
Women, prevalence (%)	8 (0.53)	4 (0.40)	9 (0.69)	5 (0.38)	0.391
Education	4.3 (1.3)	4.4 (1.2)	4.2 (1.8)	4.9 (1.3)	0.586
MMSE	28.3 (1.6)	23.9 (2.7)[a]	22.3 (3.6)[a]	23.2 (3.7)[a]	**<0.001**
Global CDR scores	-	0.7 (0.3)	0.7 (0.4)	0.7 (0.3)	0.938
Apathy*	-	5 (50.0)	6 (46.2)	-	0.855
Disinhibition*	-	1 (10.0)	4 (30.8)	-	0.231
Obsessive-compulsive*	-	2 (20.0)	0 (0.0)	-	0.092
Undefined presentation*	-	2 (20.0)	3 (23.1)	-	0.859
CSF ratio total tau/$A\beta_{42}$†	-	-	0.3 (0.2)	1.6 (0.7)[c]	**0.019**
FTLD-TDP/FTLD-TAU*	-	1/2	3/2	-	0.714
*Progranulin/MAPT**	-	2/2	2/-	-	0.405

Values are unadjusted means or percentages (standard deviations). * Prevalence (percentage). NA-FTD: non amnestic FTD. A-FTD: amnestic FTD. AD: early onset AD. MMSE = mini mental state examination. CDR: clinical dementia rating. CSF: cerebrospinal fluid. FTLD: frontotemporal lobar degeneration. † CSF samples available in 3 A-FTD patients and 6 AD patients. Education according to (Verhage, 1964) range from 1 (less than elementary school) – 7 (academic degree). Between group comparisons by means of independent sample t-test or Chi-square test. [a] $p < 0.05$ compared with controls. [b] $p < 0.05$ compared with NA-FTD. [c] $p < 0.05$ compared with A-FTD.

Perfusion SPECT analyses

The 3-dimensional renderings in Figure 1 show hypoperfusion patterns in patient groups relative to controls (Figure 1, threshold $p < 0.001$ not corrected for multiple comparisons). Cerebral hypoperfusion patterns in NA-FTD and A-FTD groups were both evocative of bvFTD with predominant frontal and temporal lobe involvement, although hypoperfusion in NA-FTD was somewhat less extensive (Figure 1, Table 3). AD patients showed hypoperfusion in posterior cortical regions, including the bilateral posterior temporal lobe, inferior parietal lobe, left precuneus and thalamus (Table 3). The differences in hypoperfusion patterns in bvFTD and AD were confirmed in between patient group comparisons showing significant anterior cortical hypoperfusion in both bvFTD groups relative to AD and posterior cortical hypoperfusion in AD relative to both bvFTD groups (Table 3).

Table 2 shows t-scores of neuropsychological tests for patient groups and controls. AD and A-FTD were impaired on the immediate recall, delayed recall and the forced choice format recognition memory task relative to controls. In general both NA-FTD and A-FTD patients performed worse than controls on both processing speed and executive functioning, whereas AD patients performed worse than controls on the executive domain only (Table 2).

Table 2 Neuropsychological performance on tasks for memory, attention and executive functioning

	N	Controls (n = 15)	N	NA-FTD (n = 10)	N	A-FTD (n = 13)	N	AD (n = 13)	P value
Memory									
Immediate Recall	15	45 (10)	10	37 (8)	13	17 (11)	13	19 (5)	**<0.001**
Delayed Recall	15	47 (12)	10	33 (8)	13	14 (5)	13	14 (9)	**<0.001**
Recognition memory (%)	9	0.93 (0.10)	8	0.80 (0.19)	11	0.64 (0.17)[a]	13	0.74 (0.13)[a]	**<0.001**
Processing speed									
Trail Making A	14	48 (17)	10	35 (15)	13	34 (16)	13	36 (27)	0.193
Stroop I	13	41 (14)	9	28 (16)[a]	11	20 (13)[a, c]	12	33 (15)	**0.009**
Executive functioning									
Trail Making B	14	46 (16)	10	32 (13)[a]	13	25 (10)[a]	13	26 (17)[a]	**0.001**
Stroop III	13	52 (19)	9	40 (21)	11	35 (26)[a]	12	34 (19)[a]	0.133
Letter fluency	14	46 (10)	10	29 (14)[a, c]	10	25 (8)[a, c]	12	45 (10)	**<0.001**
WCST Concepts	11	43 (14)	10	25 (17)[a]	11	22 (12)[a]	10	28 (14)[a]	**0.006**

Values are mean t-scores (standard deviations). NA-FTD: non amnestic bvFTD. A-FTD: amnestic bvFTD. AD: early onset AD. WVLT: word verbal learning test. WLM: word list memory. WCST: Wisconsin card sorting test. Between group comparisons by means of independent sample t-test. [a] p <0.05 compared with controls. [b] p <0.05 compared with NA-FTD. [c] p <0.05 compared with AD.

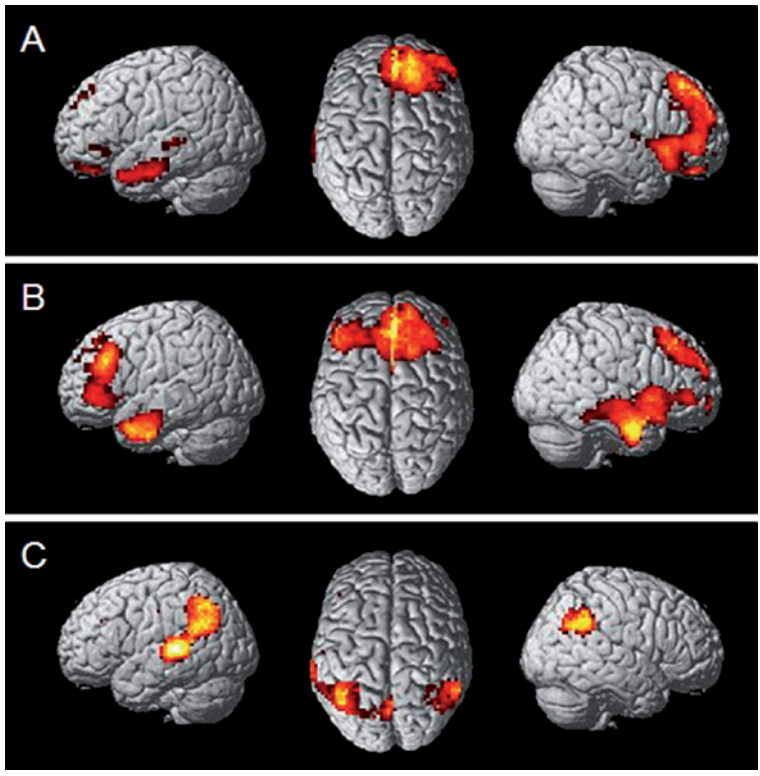

Figure 1 Regional hypoperfusion in A) NA-FTD patients; B) A-FTD patients and C) AD patients relative to controls, p <0.001 not corrected for multiple comparisons.

A direct comparison between NA-FTD and A-FTD revealed significant lower perfusion in the right parahippocampal gyrus at a threshold of p <0.001 not corrected for multiple comparisons in A-FTD relative to NA-FTD. To examine this difference more closely, we used a threshold of p <0.005 not corrected for multiple comparisons and found lower perfusion in the right parahippocampal gyrus, fusiform gyrus and the middle temporal gyrus in A-FTD relative to NA-FTD (Figure 2, Table 3). We verified whether this subtle difference could be related to cognitive functioning by extracting mean perfusion within this region, and subsequently correlating the extracted mean perfusion within this region in all FTD patients (amnestic and non amnestic together) with cognitive tests, MMSE and CDR; and found a significant correlation with the memory domain of the CDR ($r = -0.454$, $p = 0.034$ $r^2 = 0.21$).

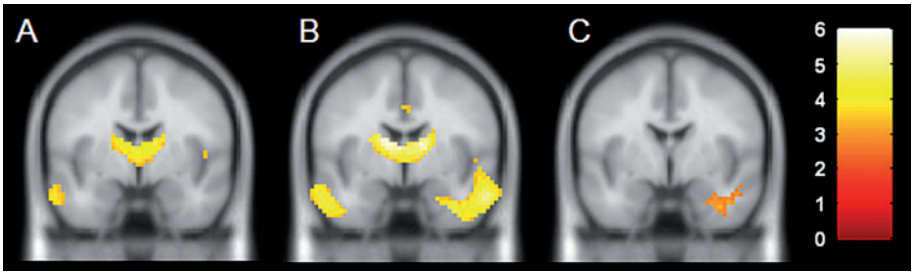

Figure 2 Regional hypoperfusion in A) NA-FTD patients and B) A-FTD patients relative to controls p <0.001 not corrected for multiple comparisons, C) A-FTD relative to NA-FTD, p <0.005 not corrected for multiple comparisons.

DISCUSSION

In the present retrospective study our aim was to examine perfusion differences in FTD patients with and without episodic memory impairment. We found significant lower perfusion in the right temporal lobe, including the parahippocampal gyrus, fusiform gyrus and middle temporal gyrus in FTD patients with episodic memory disorders as compared with FTD patients without episodic memory disorders. Mean perfusion within these regions correlated with CDR memory scores in the full cohort of FTD patients. In comparison with A-FTD patients, NA-FTD patients and controls, AD patients showed hypoperfusion in the posterior temporal gyrus and parietal lobule.

Results of the present study support the notion that verbal episodic memory can be impaired in bvFTD (Graham et al., 2005; Hornberger et al., 2010; Pasquier et al., 2001). The extent of impairment in FTD relative to AD varies between studies using a verbal episodic memory task (Binetti et al., 2000; Glosser et al., 2002; Wicklund et al., 2006; Wittenberg et al., 2008). While some studies reported better encoding and retrieval ability in FTD (Binetti et al., 2000; Glosser et al., 2002; Wicklund et al., 2006; Wittenberg et al., 2008), others found encoding and retrieval to be equally impaired in both FTD and AD patients (Gregory et al., 1997; Pasquier et al., 2001; Wicklund et al., 2006).

Table 3 MNI coordinates of areas of significant regional hypoperfusion in patient groups relative to other patient groups

Anatomical location	MNI coordinates			T	Z	Cluster size
	X	Y	Z			
Regional hypoperfusion in NA-FTD relative to A-FTD*						
-						
Regional hypoperfusion in NA-FTD relative to AD						
Orbital gyrus R	3	48	-24	5.94	5.08	3837
Medial frontal gyrus R	6	48	15	5.90	5.05	
Superior frontal gyrus R	18	45	42	5.54	4.81	
Inferior frontal gyrus R	39	24	0	5.19	4.57	
Anterior cingulate gyrus R	3	30	27	4.90	4.37	
Middle frontal gyrus R	30	33	-15	4.65	4.18	
Regional hypoperfusion in A-FTD relative to NA-FTD*						
Parahippocampal gyrus R	33	-9	-30	3.30	3.10	126
Fusiform gyrus R	36	-3	-33	3.18	3.01	
Middle temporal gyrus	51	-6	-21	3.15	2.98	
Regional hypoperfusion in A-FTD relative to AD						
Cingulate gyrus L	-6	24	30	5.58	4.84	4450
Caudate nucleus L	-12	9	12	5.41	4.72	
Orbital gyrus R	9	51	-24	5.11	4.52	
Superior frontal gyrus R	15	57	-12	4.91	4.37	
Middle temporal gyrus R	48	3	-33	4.86	4.33	
Inferior frontal gyrus R	42	24	3	4.84	4.32	
Medial frontal gyrus R	3	21	-21	4.83	4.31	
Caudate nucleus R	18	15	3	4.74	4.25	
Inferior temporal gyrus R	45	-6	-36	4.72	4.23	
Fusiform gyrus R	54	-9	-30	4.66	4.19	
Parahippocampal gyrus R	33	-15	-30	4.49	4.06	
Insula	48	12	3	4.37	3.97	
Superior temporal gyrus L	-39	12	-36	4.72	4.23	331
Inferior temporal gyrus L	-60	-9	-27	3.57	3.33	
Regional hypoperfusion in AD relative to NA-FTD						
Middle temporal gyrus R	54	-75	12	5.33	4.67	289
Middle occipital gyrus R	27	-96	18	4.70	4.22	
Angular gyrus R	48	-69	33	3.43	3.21	
Inferior parietal lobule L	-45	-63	48	4.72	4.23	628
Precuneus L	-45	-75	33	4.15	3.80	
Middle temporal gyrus L	-48	-78	24	3.64	3.39	
Angular gyrus L	-51	-66	30	3.53	3.30	
Precuneus R	24	-51	48	4.03	3.71	49
Regional hypoperfusion in AD relative to A-FTD						
Precuneus L	-12	-66	27	4.83	4.31	1115
Cuneus L	-15	-72	15	3.95	3.64	
Middle temporal gyrus L	-33	-69	21	3.89	3.59	
Inferior parietal lobule L	-30	-45	39	3.65	3.40	
Supramarginal gyrus L	-39	-42	33	3.54	3.31	
Precuneus R	12	-69	27	3.40	3.19	199
Middle temporal gyrus R	-51	-36	3	3.99	3.68	74

Significance at threshold p <0.001 not corrected for multiple comparisons. * Significance at threshold p <0.005 not corrected for multiple comparisons. NA-FTD: non amnestic bvFTD. A-FTD: amnestic bvFTD.

Conflicting results may partly be explained by methodological differences, e.g. the use of different study populations (Binetti et al., 2000) and differences in the design of the verbal episodic memory tests (Glosser et al., 2002; Gregory et al., 1997; Hornberger et al., 2010). In addition, memory impairment in FTD has been attributed to disrupted executive control and retrieval strategy resulting from frontal deterioration, and FTD patients would hypothetically benefit from the use of structured forced choice formats. In the present study we found no evidence for this hypothesis as first, A-FTD and AD patients show equal performance on the forced choice format recognition tests, which is in line with other studies (Glosser et al., 2002; Pennington et al., 2011), and second we found no significant differences in frontal hypoperfusion between A-FTD and NA-FTD, not even at a lenient threshold.

Our findings of significant lower right temporal lobe perfusion in FTD patients with episodic memory impairment as compared to those without, has not been reported before, as to our knowledge no other studies carried out quantitative neuroimaging analysis between FTD patients with and without episodic memory disorders. There is a general consensus that the medial temporal lobe (MTL) is the primary neural substrate of episodic memory (Nyberg et al., 1996; Scoville and Milner, 1957). Although MTL or hippocampal involvement is usually not associated with FTD, several studies have reported hippocampal atrophy or atrophy of the entorhinal cortex in FTD (Broe et al., 2003; Hodges, 2001), even to the same extent as AD (Hodges, 2001; Laakso et al., 2000). Furthermore, an association between these findings and episodic memory functioning in FTD was encountered (Lavenu et al., 1998; Soderlund et al., 2008). In our study, right medial temporal lobe perfusion correlated with the CDR memory score in all FTD patients. The fact that cognitive tests, in particular memory tests, did not correlate with perfusion measures can be attributed to one single outlier with normal memory functioning yet with MTL hypoperfusion. Pennington et al. (2011) used a semi-quantitative scale of atrophy in a limited number of regions, and found that in FTD immediate and delayed recall did not correlate with atrophy, whereas recognition memory was associated with orbitofrontal atrophy. The lack of a correlation with MTL regions may be explained by the use of a semi-quantitative scale to rate atrophy, which is not as sensitive as the quantitative method used in the present study. A recent PET study in A-FTD using a quantitative method reported posterior region involvement (Bastin et al., 2012). It has been known that hippocampal and posterior parietal regions are interconnected (Pandya et al., 1981), and precuneus or posterior cingulate gyrus involvement was shown to play a role in memory network functioning (Greicius et al., 2003). However, in the present study we found no evidence for posterior hypoperfusion in A-FTD patients.

An interesting issue is whether the observed memory deficits in bvFTD are due to topographical heterogeneity in bvFTD or merely reflect an advanced stage of bvFTD. Whitwell et al. (2009) distinguished four subtypes of bvFTD based on a hierarchical cluster analysis of grey matter volumes, and found memory primarily associated with a temporal-dominant cluster. In this line of reasoning, A-FTD patients could represent an anatomical subtype of FTD, with prominent right temporal lobe involvement. Right temporal FTD as anatomic variant of FTD, either presents with bvFTD or semantic dementia; with inappropriate behavior as most common finding in right temporal bvFTD, and difficulty recognizing faces (prosopagnosia) or word-finding difficulties associated with SD (Edwards-Lee et al., 1997; Josephs et al., 2009; Miller et al., 1995; Mychack et al., 2001). We excluded all patients with SD in the present study. Furthermore, apathy was the most common clinical presentation in our group of A-FTD, which is an uncommon clinical presentation of the temporal variant bvFTD (Josephs et al., 2009). In line with Seeley et al. (2008), the finding of right temporal lobe differences in A-FTD patients as compared to NA-FTD patients could possibly indicate a more advanced disease stage. Seeley et al. (2008) claimed that memory impairment reflects an advanced stage in which eventually the medial temporal lobe is affected and thereby the extent of right hemisphere involvement, including the right hippocampus, exceeded left hemispheric involvement in terms of atrophy. Further support for this hypothesis is the fact that A-FTD patients had a longer disease duration as compared with NA-FTD patients. Even though some studies have reported the occurrence of overt memory impairment early in the disease process (Graham et al., 2005), we consider our results as an expression of disease severity.

We found AD to be associated with hypoperfusion in the posterior parietotemporal cortex with a relative absence of medial temporal lobe involvement, which is in line with the literature (Karas et al., 2007; Kemp et al., 2003; Varma et al., 2002). Posterior hypoperfusion on SPECT is thought to be either the result of direct amyloid deposition in presenile AD (Braak and Braak, 1991b; Mormino et al., 2011; Shin et al., 2011), or a reflection of a disconnection of efferent fibres projecting from the medial temporal structures in somewhat older AD cases. Functional neuroimaging studies have shown episodic memory-related activation in the parietal cortex (Cabeza et al., 2008; Konishi et al., 2000) in particular the cuneus and precuneus (Cavanna and Trimble, 2006; Fletcher et al., 1995; Wagner et al., 2005). Together with the adjacent posterior cingulate cortex, the precuneus is furthermore known to be involved in the default mode network, a highly connected network of brain regions showing consistently greater activation during rest 'default' conditions than during experimental conditions, known to play a role in memory (Greicius et al., 2003).

The novelty of the present paper lies in the fact that we used a quantitative method to explore the differences between bvFTD patients with and without episodic memory impairment. Previous studies with a similar aim used mostly semi-quantitative methods (Lavenu et al., 1998; Pennington et al., 2011), or investigated all FTD patients instead of subdividing them into patients with and without episodic memory impairment (Soderlund et al., 2008). We acknowledge that our study has some potential drawbacks. First, our study groups were small, which can affect our results and limit the generalizability of our findings to the FTD and AD population at large. Therefore, a second limitation of the present study is the absence of information on CSF markers in a large proportion of patients and controls. A lower tau/ $A\beta_{42}$ ratio however, was found in a subset of FTD patients, supporting the clinical diagnosis. *APOE* genotyping might be informative as it is known to be a risk factor for AD; however, *APOE* genotyping will not be helpful in diagnosis setting or differential diagnosis in the individual patient (Duara et al., 1999). In addition, it is important to state that more than half of the FTD patients in our cohort had a definite diagnosis FTD, either by neuropathological confirmation or by the presence of *MAPT* or *Progranulin* gene mutations. A final limitation of the present study is the use of a lenient threshold not corrected for multiple comparisons to obtain within and between group differences. This was done to grasp the full extent of the functional differences in the patient groups and to elucidate subtle group differences in perfusion (Lieberman & Cunningham, 2009). It is important to note however, that by using a threshold that is not corrected for multiple comparisons, Type I errors, or false-positive findings increase. Our results, in particular the between group results, should therefore be interpreted with caution and should be confirmed within a larger FTD patient cohort.

In this study we compared functional neuroimaging results in FTD patients with episodic memory impairment and FTD patients without episodic memory impairment, showing significant lower perfusion in the right temporal lobe in amnestic FTD patients. Our results highlight the fact that although current diagnostic criteria emphasize the relative preservation of memory in bvFTD (Neary et al., 1998; Rascovsky et al., 2011), memory disturbances can be present in bvFTD. We postulate that these memory disturbances are related to right temporal lobe dysfunctioning and may represent disease progression.

REFERENCES

Andel R, McCleary CA, Murdock GA, Fiske A, Wilcox RR, Gatz M. Performance on the CERAD Word List Memory task: a comparison of university-based and community-based groups. Int J Geriatr Psychiatry 2003; 18: 733-739.

Ashburner J, Friston KJ. Nonlinear spatial normalization using basis functions. Hum Brain Mapp 1999; 7: 254-266.

Bastin C, Feyers D, Souchay C, Guillaume B, Pepin JL, Lemaire C, *et al.* Frontal and posterior cingulate metabolic impairment in the behavioural variant of frontotemporal dementia with impaired autonoetic consciousness. Hum Brain Mapp 2012; 33: 1268-1278.

Bian H, Van Swieten JC, Leight S, Massimo L, Wood E, Forman M, *et al.* CSF biomarkers in frontotemporal lobar degeneration with known pathology. Neurology 2008; 70: 1827-1835.

Binetti G, Locascio JJ, Corkin S, Vonsattel JP, Growdon JH. Differences between Pick disease and Alzheimer disease in clinical appearance and rate of cognitive decline. Arch Neurol 2000; 57: 225-232.

Braak H, Braak E. Demonstration of amyloid deposits and neurofibrillary changes in whole brain sections. Brain Pathol 1991a; 1: 213-216.

Braak H, Braak E. Neuropathological stageing of Alzheimer-related changes. Acta Neuropathol 1991b; 82: 239-259.

Brand N, Jolles J. Learning and retrieval rate of words presented auditorily and visually. J Gen Psychol 1985; 112: 201-210.

Broe M, Hodges JR, Schofield E, Shepherd CE, Kril JJ, Halliday GM. Staging disease severity in pathologically confirmed cases of frontotemporal dementia. Neurology 2003; 60: 1005-1011.

Cabeza R, Ciaramelli E, Olson IR, Moscovitch M. The parietal cortex and episodic memory: an attentional account. Nat Rev Neurosci 2008; 9: 613-625.

Cavanna AE, Trimble MR. The precuneus: a review of its functional anatomy and behavioural correlates. Brain 2006; 129: 564-583.

Claus JJ, van Harskamp F, Breteler MM, Krenning EP, van der Cammen TJ, Hofman A, *et al.* Assessment of cerebral perfusion with single-photon emission tomography in normal subjects and in patients with Alzheimer's disease: effects of region of interest selection. Eur J Nucl Med 1994; 21: 1044-1051.

Duara R, Barker W, Luis CA. Frontotemporal dementia and Alzheimer's disease: differential diagnosis. Dement Geriatr Cogn Disord 1999; 10 (suppl 1): 37-42.

Edwards-Lee T, Miller BL, Benson DF, Cummings JL, Russell GL, Boone K, *et al.* The temporal variant of frontotemporal dementia. Brain 1997; 120 (Pt 6): 1027-1040.

Fletcher PC, Frith CD, Baker SC, Shallice T, Frackowiak RS, Dolan RJ. The mind's eye--precuneus activation in memory-related imagery. Neuroimage 1995; 2: 195-200.

Frisoni GB, Testa C, Sabattoli F, Beltramello A, Soininen H, Laakso MP. Structural correlates of early and late onset Alzheimer's disease: voxel based morphometric study. J Neurol Neurosurg Psychiatry 2005; 76: 112-114.

Friston K, Holmes A, K. W, Poline J, Frith C, Frackowiak R. Statistical parametrical maps in functional imaging: a general linear approach. Hum Brain Mapp 1995; 2: 189-210.

Glosser G, Gallo JL, Clark CM, Grossman M. Memory encoding and retrieval in frontotemporal dementia and Alzheimer's disease. Neuropsychology 2002; 16: 190-196.

Graham A, Davies R, Xuereb J, Halliday G, Kril J, Creasey H, *et al.* Pathologically proven frontotemporal dementia presenting with severe amnesia. Brain 2005; 128: 597-605.

Gregory CA, Orrell M, Sahakian B, Hodges JR. Can frontotemporal dementia and Alzheimer's disease be differentiated using a brief battery of tests? Int J Geriatr Psychiatry 1997; 12: 375-383.

Greicius MD, Krasnow B, Reiss AL, Menon V. Functional connectivity in the resting brain: a network analysis of the default mode hypothesis. Proc Natl Acad Sci U S A 2003; 100: 253-258.

Grossman M, Farmer J, Leight S, Work M, Moore P, Van Deerlin V, *et al.* Cerebrospinal fluid profile in frontotemporal dementia and Alzheimer's disease. Ann Neurol 2005; 57: 721-729.

Hodges JR. Frontotemporal dementia (Pick's disease): clinical features and assessment. Neurology 2001; 56: S6-10.

Hodges JR, Davies RR, Xuereb JH, Casey B, Broe M, Bak TH, *et al.* Clinicopathological correlates in frontotemporal dementia. Ann Neurol 2004; 56: 399-406.

Hornberger M, Piguet O, Graham AJ, Nestor PJ, Hodges JR. How preserved is episodic memory in behavioural variant frontotemporal dementia? Neurology 2010; 74: 472-479.

Josephs KA, Whitwell JL, Knopman DS, Boeve BF, Vemuri P, Senjem ML, *et al.* Two distinct subtypes of right temporal variant frontotemporal dementia. Neurology 2009; 73: 1443-1450.

Karas G, Scheltens P, Rombouts S, van Schijndel R, Klein M, Jones B, *et al.* Precuneus atrophy in early-onset Alzheimer's disease: a morphometric structural MRI study. Neuroradiology 2007; 49: 967-976.

Kemp PM, Holmes C, Hoffmann SM, Bolt L, Holmes R, Rowden J, *et al.* Alzheimer's disease: differences in technetium-99m HMPAO SPECT scan findings between early onset and late onset dementia. J Neurol Neurosurg Psychiatry 2003; 74: 715-719.

Kim EJ, Cho SS, Jeong Y, Park KC, Kang SJ, Kang E, *et al.* Glucose metabolism in early onset versus late onset Alzheimer's disease: an SPM analysis of 120 patients. Brain 2005; 128: 1790-1801.

Konishi S, Wheeler ME, Donaldson DI, Buckner RL. Neural correlates of episodic retrieval success. Neuroimage 2000; 12: 276-286.

Laakso MP, Frisoni GB, Kononen M, Mikkonen M, Beltramello A, Geroldi C, *et al.* Hippocampus and entorhinal cortex in frontotemporal dementia and Alzheimer's disease: a morphometric MRI study. Biol Psychiatry 2000; 47: 1056-1063.

Lavenu I, Pasquier F, Lebert F, Pruvo JP, Petit H. Explicit memory in frontotemporal dementia: the role of medial temporal atrophy. Dement Geriatr Cogn Disord 1998; 9: 99-102.

Lieberman MD, Cunningham WA. Type I and Type II error concerns in fMRI research: re-balancing the scale. SCAN 2009; 4: 423-428.

McKhann G, Drachman D, Folstein M, Katzman R, Price D, Stadlan EM. Clinical diagnosis of Alzheimer's disease: report of the NINCDS-ADRDA Work Group under the auspices of Department of Health and Human Services Task Force on Alzheimer's Disease. Neurology 1984; 34: 939-944.

McKhann GM, Albert MS, Grossman M, Miller B, Dickson D, Trojanowski JQ. Clinical and pathological diagnosis of frontotemporal dementia: report of the Work Group on Frontotemporal Dementia and Pick's Disease. Arch Neurol 2001; 58: 1803-1809.

Miller BL, Darby AL, Swartz JR, Yener GG, Mena I. Dietary changes, compulsions and sexual behaviour in frontotemporal degeneration. Dementia 1995; 6: 195-199.

Mormino EC, Smiljic A, Hayenga AO, Onami SH, Greicius MD, Rabinovici GD, *et al.* Relationships between beta-amyloid and functional connectivity in different components of the default mode network in aging. Cereb Cortex 2011; 21: 2399-2407.

Morris JC, Heyman A, Mohs RC, Hughes JP, van Belle G, Fillenbaum G, *et al.* The Consortium to Establish a Registry for Alzheimer's Disease (CERAD). Part I. Clinical and neuropsychological assessment of Alzheimer's disease. Neurology 1989; 39: 1159-1165.

Mychack P, Kramer JH, Boone KB, Miller BL. The influence of right frontotemporal dysfunction on social behaviour in frontotemporal dementia. Neurology 2001; 56: S11-15.

Neary D, Snowden JS, Gustafson L, Passant U, Stuss D, Black S, *et al.* Frontotemporal lobar degeneration: a consensus on clinical diagnostic criteria. Neurology 1998; 51: 1546-1554.

Nishimiya M, Matsuda H, Imabayashi E, Kuji I, Sato N. Comparison of SPM and NEUROSTAT in voxelwise statistical analysis of brain SPECT and MRI at the early stage of Alzheimer's disease. Ann Nucl Med 2008; 22: 921-927.

Nyberg L, McIntosh AR, Houle S, Nilsson LG, Tulving E. Activation of medial temporal structures during episodic memory retrieval. Nature 1996; 380: 715-717.

Pandya DN, Van Hoesen GW, Mesulam MM. Efferent connections of the cingulate gyrus in the rhesus monkey. Exp Brain Res 1981; 42: 319-330.

Pasquier F, Grymonprez L, Lebert F, Van der Linden M. Memory impairment differs in frontotemporal dementia and Alzheimer's disease. Neurocase 2001; 7: 161-171.

Pennington C, Hodges JR, Hornberger M. Neural correlates of episodic memory in behavioural variant frontotemporal dementia. J Alzheimers Dis 2011; 24: 261-268.

Rascovsky K, Hodges JR, Knopman D, Mendez MF, Kramer JH, Neuhaus J, *et al.* Sensitivity of revised diagnostic criteria for the behavioural variant of frontotemporal dementia. Brain 2011; 134: 2456-2477.

Scoville WB, Milner B. Loss of recent memory after bilateral hippocampal lesions. J Neurol Neurosurg Psychiatry 1957; 20: 11-21.

Seelaar H, Kamphorst W, Rosso SM, Azmani A, Masdjedi R, de Koning I, *et al.* Distinct genetic forms of frontotemporal dementia. Neurology 2008; 71: 1220-1226.

Seelaar H, Klijnsma KY, de Koning I, van der Lugt A, Chiu WZ, Azmani A, *et al.* Frequency of ubiquitin and FUS-positive, TDP-43-negative frontotemporal lobar degeneration. J Neurol 2010; 257: 747-753.

Seelaar H, Rohrer JD, Pijnenburg YA, Fox NC, van Swieten JC. Clinical, genetic and pathological heterogeneity of frontotemporal dementia: a review. J Neurol Neurosurg Psychiatry 2011; 82: 476-486.

Seeley WW, Crawford R, Rascovsky K, Kramer JH, Weiner M, Miller BL*, et al.* Frontal paralimbic network atrophy in very mild behavioural variant frontotemporal dementia. Arch Neurol 2008; 65: 249-255.

Shin J, Kepe V, Small GW, Phelps ME, Barrio JR. Multimodal Imaging of Alzheimer Pathophysiology in the Brain's Default Mode Network. Int J Alzheimers Dis 2011; 2011: 687945.

Soderlund H, Black SE, Miller BL, Freedman M, Levine B. Episodic memory and regional atrophy in frontotemporal lobar degeneration. Neuropsychologia 2008; 46: 127-136.

Soonawala D, Amin T, Ebmeier KP, Steele JD, Dougall NJ, Best J*, et al.* Statistical parametric mapping of (99m)Tc-HMPAO-SPECT images for the diagnosis of Alzheimer's disease: normalizing to cerebellar tracer uptake. Neuroimage 2002; 17: 1193-1202.

van de Pol LA, Hensel A, van der Flier WM, Visser PJ, Pijnenburg YA, Barkhof F*, et al.* Hippocampal atrophy on MRI in frontotemporal lobar degeneration and Alzheimer's disease. J Neurol Neurosurg Psychiatry 2006; 77: 439-442.

Van Laere KJ, Versijpt J, Koole M, Vandenberghe S, Lahorte P, Lemahieu I*, et al.* Experimental performance assessment of SPM for SPECT neuroactivation studies using a subresolution sandwich phantom design. Neuroimage 2002; 16: 200-216.

Varma AR, Adams W, Lloyd JJ, Carson KJ, Snowden JS, Testa HJ*, et al.* Diagnostic patterns of regional atrophy on MRI and regional cerebral blood flow change on SPECT in young onset patients with Alzheimer's disease, frontotemporal dementia and vascular dementia. Acta Neurol Scand 2002; 105: 261-269.

Verhage F. Intelligentie en leeftijd: onderzoek bij Nederlanders van twaalf tot zevenenzeventig jaar [Intelligence and age: Research on Dutch people aged twelve to seventy-seven years old]. Assen: Van Gorcum 1964.

Wagner AD, Shannon BJ, Kahn I, Buckner RL. Parietal lobe contributions to episodic memory retrieval. Trends Cogn Sci 2005; 9: 445-453.

Whitwell JL, Przybelski SA, Weigand SD, Ivnik RJ, Vemuri P, Gunter JL*, et al.* Distinct anatomical subtypes of the behavioural variant of frontotemporal dementia: a cluster analysis study. Brain 2009; 132: 2932-2946.

Wicklund AH, Johnson N, Rademaker A, Weitner BB, Weintraub S. Word list versus story memory in Alzheimer disease and frontotemporal dementia. Alzheimer Dis Assoc Disord 2006; 20: 86-92.

Wittenberg D, Possin KL, Rascovsky K, Rankin KP, Miller BL, Kramer JH. The early neuropsychological and behavioural characteristics of frontotemporal dementia. Neuropsychol Rev 2008; 18: 91-102.

Yakushev I, Landvogt C, Buchholz HG, Fellgiebel A, Hammers A, Scheurich A*, et al.* Choice of reference area in studies of Alzheimer's disease using positron emission tomography with fluorodeoxyglucose-F18. Psychiatry Res 2008; 164: 143-153.

Chapter 3.2

Brain perfusion patterns in familial frontotemporal lobar degeneration

Harro Seelaar
Janne M. Papma
Gaëtan Garraux
Inge de Koning
Ambroos E.M. Reijs
Roelf Valkema
Annemieke J.M. Rozemuller
Eric Salmon
John C. van Swieten

Neurology 2011; 77(4): 384-392

ABSTRACT

Introduction

Frontotemporal lobar degeneration (FTLD) is a clinically, genetically and pathologically heterogeneous disorder. The aim of this study was to compare clinical features and perfusion patterns on SPECT of patients with familial FTLD-TDP and *MAPT* mutations.

Methods

Patients were included if they had *MAPT* or *GRN* mutations, positive family history with pathologically-proven FTLD in the patient or first-degree relative, or were part of FTD-MND families. All patients and ten age- and gender-matched controls underwent measurement of brain perfusion using ^{99m}Tc-HMPAO SPECT. We used SPM8 to perform image processing and voxel based group analyses ($p < 0.001$, not corrected for multiple comparisons). Gender and age were included as nuisance variables in the design matrices.

Results

Of the 29 patients with familial FTLD, 19 had familial FTLD-TDP (*GRN* mutations in six), and 10 had *MAPT* mutations. At clinical presentation, familial FTLD-TDP patients were older at onset ($p = 0.030$) and had more memory deficits ($p = 0.011$), whereas *MAPT* had more naming deficits ($p < 0.001$) and obsessive-compulsive behavior ($p = 0.001$). The between group SPECT analyses revealed significantly less perfusion in the right frontal lobe, precuneus, cuneus and inferior parietal lobule in familial FTLD-TDP, whereas significantly less perfusion was found in the left temporal and inferior frontal gyri in *MAPT*. Post-hoc analysis of familial FTLD-TDP with unknown genetic defect (UGD) versus *MAPT* patients revealed less perfusion in the right frontal and parietal lobe.

Discussion

Familial FTLD-TDP shows relatively more posterior hypoperfusion, including the precuneus and inferior parietal lobule, possibly related to significant memory impairment. *MAPT* patients were characterized by impaired perfusion of the temporal regions and naming deficits.

INTRODUCTION

Frontotemporal lobar degeneration (FTLD) is clinically characterized by a variable clinical presentation of progressive behavioral, language and executive dysfunction (McKhann et al., 2001). Two major gene defects have been found in familial FTLD; mutations in the *microtubule associated protein tau* (*MAPT*) and *progranulin* (*GRN*) genes (Baker et al., 2006; Cruts et al., 2006; Hutton et al., 1998). However, there still remain one or more familial forms of FTLD with unknown gene defect (UGD), in particular familial FTLD with motor neuron disease (Rohrer et al., 2009; Seelaar et al., 2008). *MAPT* is associated with FTLD with tau-positive inclusions (FTLD-tau), whereas *GRN* and familial forms with unknown genetic defect are associated with ubiquitin- and TDP-43 positive inclusions (FTLD-TDP) (Rohrer et al., 2009; Seelaar et al., 2008). Clinically, disinhibition, obsessive-compulsive behavior, and semantic deficits occur in *MAPT* (Pickering-Brown et al., 2008; Seelaar et al., 2008), versus apathy, social withdrawal, non-fluent speech, word finding difficulties and episodic memory deficits in patients with familial FTLD-TDP with and without *GRN* mutations (Pickering-Brown et al., 2008; Seelaar et al., 2008; van Swieten and Heutink, 2008). Voxel based morphometry (VBM) on MRI has shown symmetrical and predominantly temporofrontal atrophy in *MAPT* mutations versus asymmetrical frontotemporoparietal atrophy in *GRN* mutations (Rohrer et al., 2010; Whitwell, 2009). Functional imaging using SPECT has also revealed asymmetrical frontotemporoparietal hypoperfusion in patients with *GRN* mutations, whereas perfusion patterns in *MAPT* patients have not been investigated yet (Cruchaga et al., 2009; Le Ber et al., 2008; Masellis et al., 2006). We aim to investigate differences in brain perfusion on ^{99m}Tc-HMPAO SPECT scans of patients with familial FTLD-TDP (*GRN* and UGD) and *MAPT* mutations by using statistical parametrical mapping (SPM8).

METHODS

Participants

Patients with FTD were included in the study since 1994 (Rosso et al., 2003; Seelaar et al., 2008), after referral to the outpatient clinic department of the Erasmus MC – University Medical Center Rotterdam, the Netherlands. Detailed clinical history was obtained from spouses and first-degree relatives using a checklist of behavioral and cognitive changes, and motor symptoms. Age at onset was defined as the age at which the first symptoms were observed by a close relative or caregiver. Extrapyramidal and MND signs in neurological examination were separately noted. Family history, obtained by using a structured questionnaire, was defined positive if patients had at least one first-degree relative with dementia, parkinsonism, or MND, irrespective of their age at onset. A group

of ten age and gender matched controls without neurological or cognitive disorders were selected. This study was approved by the medical ethics committee of the Erasmus MC. For each patient, a spouse or first-degree relative gave written informed consent.

Inclusion criteria

We included patients with a positive family history, an available ^{99m}Tc-HMPAO SPECT scan, and at least one of the following characteristics: 1) confirmed neuropathological diagnosis of FTLD in patient or a first-degree relative, 2) positive DNA screening for *MAPT* or *GRN* mutations, 3) being part of a family with FTD-MND and therefore suggestive for FTLD-TDP pathology.

Clinical features

The presence of apathy, disinhibition, obsessive-compulsive behavior, memory deficits, word finding difficulties, economy of speech, comprehension deficits, naming deficits and motor neuron disease was scored as absent or present. Severity of dementia at time of SPECT scan was assessed using the Clinical Dementia Rating scale (CDR) (Morris, 1993). Memory impairment not explained by language deficits, included losing objects, forgetting appointments or previous conversations. We scored memory impairment on a three-point scale: 0) forgetfulness absent or rarely present without interaction of daily life, 1) forgetfulness was sometimes present, interfering mildly with daily life, 2) forgetfulness often to very often present, moderately or severely interacting with daily life.

Neuropsychological data

Neuropsychological evaluation was performed in 21 patients and ten controls. The test battery included the Mini-Mental State Examination (MMSE), Trail Making Test (TMT) A and B, Stroop I, II and III, the Dutch 15-Word Verbal Learning Test (15-WVLT), Boston Naming Test, Phonological or letter (DAT) fluency, semantic fluency (animals and occupations), Clock Drawing long or short, and orientation for time and place. T-scores were attained, corrected for age, sex and education, based on Dutch norms.

Structural imaging data

The presence and severity of frontal, temporal and parietal atrophy on structural imaging data (CT or MRI) were reviewed and scored by two investigators over the last 15 years, as: 0) no atrophy, 1) mild atrophy, 2) moderate or severe atrophy. In case of disagreement, a third observer with neuroradiological expertise was asked for his evaluation.

Genetic screening

Mutation screening of all exons and exon-intron regions of *MAPT*, *GRN* and *CHMP2B* genes were performed in all patients as previously described (Seelaar et al., 2008).

Pathology

Brain autopsy was carried out in 12 patients and of two first degree relatives included in this study according to the Legal and Ethical Code of Conduct of the Netherlands Brain Bank. The pathology protocols have been described before (Seelaar et al., 2008; Seelaar et al., 2010; Seelaar et al., 2007). A panel of antibodies including AT-8, ubiquitin, TDP-43 and FUS were used for the diagnoses made by the neuropathologist (AJMR). FTLD-TDP cases were classified in line with Sampathu et al. (2006).

^{99m}Tc-HMPAO SPECT scanning and image processing

Brain perfusion ^{99m}Tc-hexamethyl propylene amine oxime (^{99m}Tc-HMPAO) SPECT scans were exclusively performed at the department of nuclear medicine of the Erasmus MC. SPECT scans were acquired on a Prism 3000XP Philips (Picker) three-headed system, with a fan-beam collimator. Acquisition was performed after injection of 740 MBq ^{99m}Tc-HMPAO whilst resting in a quiet room. Duration of scanning was 30 minutes. A 128x128 pixel matrix and approximately 7 mm resolution for the Picker camera, as estimated by the manufacturer, was used for image acquisition with 120 projections (40 steps of 3^{o}, and 20 seconds per step) with pixel size and slice thickness of 3.56 mm. Image reconstruction was performed by a ramp-filtered back projection and three-dimensionally smoothed with a Metz Filter. After gross manual image reorientation and approximate definition of the image center point, the SPECT scans were spatially processed using Statistical Parametric Mapping (SPM8, Wellcome Trust Centre for Neuroimaging, London, UK) implemented in Matlab 7.4.0 (MathWorks, Natick, MA, USA). SPECT scans were normalized with respect to the MNI atlas with a 12-parameter affine transformation followed by non-linear transformations and a trilinear interpolation. Dimensions of the resulting voxel were 3x3x3 mm. For every subject, estimation of individual SPECT normalization parameters was constrained by a source weighting image. This method is used to correct for registering lesioned or abnormal brains. All spatially normalized images were visually checked to make sure that SPECT scans were not misregistrated with the SPM8 SPECT template. Images were then smoothed by a Gaussian filter of 16 mm FWHM that was limited to measured brain tissue. For SPECT data, smoothing with at least twice the FWHM of the imaging system was shown to provide optimal detection sensitivity (Van Laere et al., 2002), and is not unusual in pathological brains studied with SPECT and PET (Kim et al., 2005). Voxel based image analyses were conducted using

SPM8 in the framework of the general linear model (Friston et al., 1995). We compared relative perfusion using proportional scaling by cerebral global mean values to control for individual variation in ^{99m}Tc-HMPAO uptake. The method of using a regional reference (Yakushev et al., 2008), was not suitable for our data since we were unable to obtain a reference area where perfusion was relatively preserved in all groups. Group comparisons of spatially normalized and smoothed images were performed on a voxel-by-voxel basis using a full factorial design. Age and gender were entered as nuisance variables in the design matrix. We performed the following contrasts: Familial FTLD-TDP minus controls; *MAPT* minus controls, familial FTLD-TDP minus *MAPT* inclusively masked at a very liberal threshold of $p < 0.05$ by familial FTLD-TDP minus controls; *MAPT* minus familial FTLD-TDP inclusively masked ($p < 0.05$) for *MAPT* minus controls. Significance level was set at $p < 0.001$, not corrected for multiple comparisons, with at least 20 contiguous voxels either with or without masking.

Statistical analysis

SPSS 15.0 for Windows (SPSS, Chicago, Ill. U.S.A.) was used for statistical analysis of clinical and demographic data. Data of age at onset, age at SPECT, time between onset and time of SPECT were analyzed using independent sample t-test. The Chi-square test was used to analyze differences between gender, clinical and structural neuroimaging parameters. The non-parametric Mann-Whitney *U* test was used to analyze neuropsychological data. A p value < 0.05 was considered statistically significant.

RESULTS

Clinical data

A group of 29 patients was included in this study and consisted of 19 patients with familial FTLD-TDP and 10 patients with *MAPT* mutations. Of the 19 familial FTLD-TDP patients, six had a *GRN* gene mutation (Ser82ValfsX174 in five from one family, Gln125X in one) with pathological confirmation in one (FTLD-TDP, type 3) (Sampathu et al., 2006). The other 13 patients came from 10 families, seven were pathologically diagnosed as FTLD-TDP type 2 (Sampathu et al., 2006), four had a first-degree relative with pathologically confirmed FTLD-TDP, and the remaining two patients were part of a large FTD-MND family without pathological confirmation. The *MAPT* mutation group consisted of ten patients from two families (P301L in eight, G272V in two) and brain specimens were available in four cases. There were no patients with FTLD-tau pathology and a positive family history without a *MAPT* mutation.

Table 1 Demographic, clinical and structural imaging data of familial FTLD-TDP, *MAPT* and controls

	Familial FTLD-TDP (n=19)	*MAPT* (n=10)	Controls (n=10)	P-value*
Male : Female	11 : 8	5 : 5	6 : 4	0.569
CDR, median (range)	1.0 (0.5-2)	1.0 (0.5-3)	-	1.000
Age at onset, yrs (sd)	56.9 (8.9)	49.8 (5.9)	-	**0.030**
Age at SPECT, yrs (sd)	59.4 (9.4)	52.1 (6.3)	56.7 (7.8)	**0.039**
Time onset till SPECT, yrs (sd)	2.4 (1.6)	2.3 (1.3)	-	0.869
Age at death, yrs (sd)	64.3 (10.6) (n=14)	58.6 (7.5) (n=10)	-	0.154
FTD subtype				
bvFTD (%)	15 (79)	10 (100)	-	1.000
FTD-MND (%)	4 (21)	0 (0)	-	0.268
Clinical presentation				
Apathy (%)	15 (79)	8 (80)	-	1.000
Disinhibition (%)	17 (84)	8 (80)	-	0.592
Obsessive-Compulsive (%)	3 (16)	8 (80)	-	**0.001**
Memory impairment (%)	16 (84)	3 (30)	-	**0.011**
Language				
Word-finding difficulties (%)	10 (53)	3 (30)	-	0.433
Economy of speech (%)	10 (53)	2 (20)	-	0.126
Comprehension deficits (%)	0 (0)	2 (20)	-	0.111
Naming deficits (%)	0 (0)	6 (60)	-	**<0.001**
Apraxia (%)	4 (21)	0 (0)	-	0.268
Parkinsonism (%)	4 (21)	1 (10)	-	0.633
Motor neuron disease (%)	4 (21)	0 (0)	-	0.268
Atrophy on structural imaging				
Frontal atrophy				
0 (%)	0 (0)	1 (10)	-	0.161
+ (%)	10 (47)	1 (10)	-	**0.025**
++ (%)	9 (53)	8 (80)	-	0.090
Temporal atrophy				
0 (%)	1 (6)	1 (10)	-	0.632
+ (%)	10 (47)	2 (20)	-	0.215
++ (%)	8 (47)	7 (70)	-	0.153
Parietal atrophy				
0 (%)	2 (12)	5 (50)	-	**0.018**
+ (%)	12 (59)	4 (40)	-	0.233
++ (%)	5 (29)	1 (10)	-	0.303

Values are unadjusted means (standard deviations) or number of participants (%). CDR: clinical dementia rating scale. FTLD: frontotemporal lobar degeneration. MND: motor neuron disease. Atrophy is rated as: 0, no atrophy; +, mild atrophy; ++, moderate-to-severe atrophy. *Familial FTLD-TDP compared with *MAPT*; independent sample t-test or Chi square test.

Demographical, clinical and structural imaging data of familial FTLD-TDP, *MAPT* and controls are summarized in Table 1. Patients with *MAPT* mutations were younger at time of SPECT-scan. MND (bulbar in three) was present in four patients of the familial FTLD-TDP. Memory impairment was more often present in familial FTLD-TDP, whereas obsessive-compulsive behavior and naming deficits were more often present in *MAPT* (Table 1). Neuropsychological data revealed differences on the Boston Naming Test when *MAPT* was compared with familial FTLD-TDP (p = 0.019), without differences (using t-scores) in other cognitive domains. All neuropsychological data and analyses between the two distinct patient groups compared with controls are presented in Table 2.

Table 2 Neuropsychological data of familial FTLD-TDP, *MAPT* and controls.

	n	FTLD-TDP	n	*MAPT*	n	Controls	P-value*
MMSE	14	21.9 (12-30)[b]	5	23.4 (14-28)[b]	10	28.6 (27-30)	0.559
Processing Speed							
Trail Making Test A, sec †	14	88.8 (30-179)[b]	7	82.6 (38-179)	9	42.0 (22-60)	0.585
Stroop I, sec †	12	74.0 (50-109)	6	73.8 (34-109)	8	58.5 (41-91)	0.820
Executive Function							
Trail Making Test B, sec †	14	218.9 (127-258)[b]	7	200.3 (57-258)	9	126.2 (48-258)	0.856
Stroop III , sec †	12	215.6 (94-281)[a]	6	191.7 (90-281)	8	130.9 (79-208)	0.358
WCST, concepts	13	1.8 (0-6)[b]	6	1.7 (0-6)[a]	10	4.5 (1-6)	0.918
Memory							
15-WVLT IR, max 75	10	23.8 (9-38)[b]	4	33.3 (9-43)	9	41.9 (25-62)	0.142
15-WVLT DR, max 15	10	4.8 (0-10)	4	6.5 (0-11)	8	7.6 (3-13)	0.454
Language							
Boston naming test, max 60	8	48.9 (36-56)[a]	5	32.2 (24-45)[b]	9	54.6 (39-59)	**0.019**
Phonological Fluency DAT	11	10.2 (0-27)[c]	5	12.4 (0-51)	9	29.7 (22-40)	0.320
Semantic Fluency Animal	15	10.7 (1-25)[b]	7	7.4 (0-22)[b]	7	22.3 (15-37)	0.210
Semantic Fluency Occupations	15	7.3 (1-17)[c]	7	5.7 (0-17)[b]	7	15.1 (8-22)	0.407
Visuo-constructive function							
Clock drawing long, max. 14	6	12.0 (8-14)	0	-	7	12.7 (12-14)	-
Clock drawing short, max. 3	9	2.0 (0-3)	6	2.2 (0-3)	0	-	0.607
Orientation							
Orientation time, max 5	15	3.3 (0-5)[a]	6	3.7 (0-5)	10	4.7 (3-5)	0.677
Orientation place, max 5	15	4.2 (1-5)	6	4.2 (0-5)	10	4.9 (4-5)	0.569

Values are unadjusted means. Range of each test is given between brackets. WCST: Wisconsin card sorting test. WVLT: Word verbal learning test. IR: Immediate recall. DR: Delayed recall. † Higher scores indicate worse performance * Familial FTLD-TDP versus *MAPT.* Differences between groups by ANOVA, followed by Mann-Whitney *U* test: [a] p <0.05 compared with controls. [b] p <0.01 compared with controls. [c] p <0.001 compared with controls.

Perfusion comparisons

On SPECT, familial FTLD-TDP patients compared with controls ($p < 0.001$ not corrected for multiple comparisons) showed relative hypoperfusion of both frontal lobes, the precentral gyrus, the right superior temporal gyrus, left and right inferior parietal lobule, left postcentral gyrus, caudate and thalamus (Figure 1). *MAPT* patients compared with controls showed left bifrontal and bitemporal gyrus, caudate and thalamus hypoperfusion (Figure 1).

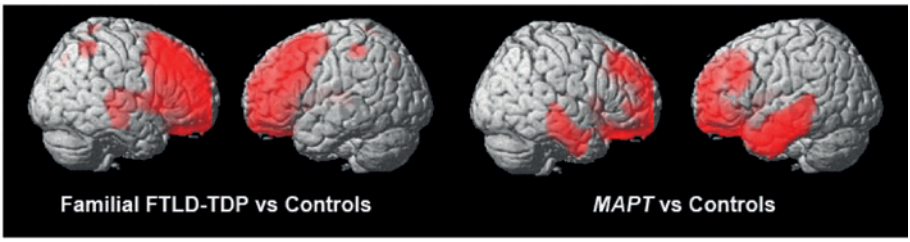

Figure 1 Perfusion pattern of familial FTLD-TDP and *MAPT* compared with controls at $p < 0.001$ not corrected for multiple comparisons.

Familial FTLD-TDP directly compared with *MAPT* showed relative hypoperfusion of the right and left precuneus, right cuneus, precentral gyrus, inferior parietal lobule, inferior frontal and middle frontal gyri, cingulate gyrus, lingual gyrus and cerebellum. Hypoperfusion of the left hemisphere was found in the cingulate gyrus and middle frontal gyrus (Figure 2, Table 3). To confirm that these differences occurred in brain areas where perfusion was indeed lower than in controls, the same analysis was carried out while inclusively masking by the contrast familial FTLD-TDP compared with controls ($p < 0.05$). When masked at this liberal threshold, all regions except the left precuneus and cerebellum remained significant (Table 3).

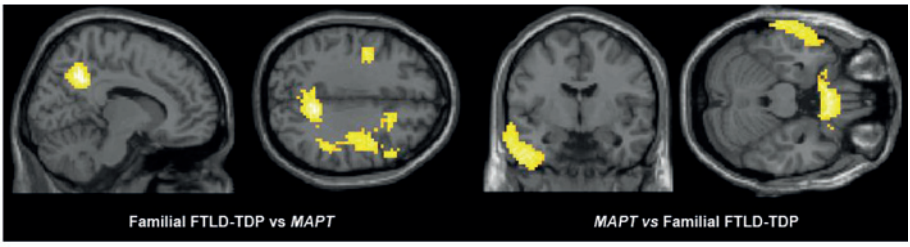

Figure 2 Perfusion pattern of familial FTLD-TDP compared with *MAPT* at $p < 0.001$ not corrected for multiple comparisons.

Comparing *MAPT* mutations and familial FTLD-TDP directly, hypoperfusion was found of the left inferior, middle and superior temporal gyri, right inferior and medial gyri, right rectal gyrus and left inferior occipital gyrus (Figure 2). All temporal and frontal regions remained significant after inclusively masking by the contrast *MAPT* compared with controls (at $p < 0.05$, Table 3).

Table 3 Brain regions with relative hypoperfusion in familial FTLD-TDP compared with *MAPT*

	MNI coordinates			
	x	y	z	Z
Familial FTLD-TDP (n=19) compared with *MAPT* (n=10)				
Precentral Gyrus R, BA 6*	42	-4	37	3.74
Cingulate Gyrus L, BA 24	-12	5	40	3.69
Inferior Frontal Gyrus R, BA 9*	54	20	28	3.65
Middle Frontal gyrus R, BA 46*	48	17	25	3.60
Inferior Parietal Lobule R, BA 40*	45	-52	58	3.50
Precuneus R, BA 7*	9	-64	40	3.45
Precuneus L, BA 31	-6	-52	37	3.44
Middle Frontal L, BA 6	-24	-10	49	3.43
Cingulate Gyrus R, BA 32*	18	23	37	3.41
Lingual Gyrus R, BA 19	18	-64	-2	3.41
Cuneus R, BA 7*	6	-70	31	3.21
***MAPT* (n=10) compared with familial FTLD-TDP n=19)**				
Medial Frontal Gyrus R, BA 25†	3	20	-20	4.10
Rectal gyrus R, BA 11†	3	23	-26	3.96
Inferior Temporal Gyrus L, BA 20†	-51	-4	-38	3.97
Inferior Occipital Gyrus L, BA 18	-33	-97	-14	3.89
Middle Temporal Gyrus L, BA 21†	-63	2	-20	3.64
Superior Temporal Gyrus L, BA 38†	-30	11	-29	3.38
Inferior Frontal Gyrus L, BA 47†	27	23	-23	3.20

* Areas that remained significant after masking by Familial FTLD-TDP compared with Controls. † Areas that remained significant after masking by *MAPT* compared with controls. BA: Brodmann area.

Post-hoc analyses

To determine whether posterior cortical hypoperfusion in familial FTLD-TDP was not driven by *GRN* gene mutations, we distinguished between familial FTLD-TDP group with *GRN* gene mutations (n = 6) and those with unknown genetic defect (UGD) (n = 13). This yielded a relative hypoperfusion bifrontally, including precentral gyrus, in right middle temporal lobe, right precuneus, superior parietal lobule, inferior parietal lobule, thalamus and caudate nucleus in the FTLD-TDP UGD compared with controls (Figure 3). Compared with *MAPT* mutations, FTLD-TDP UGD showed a relative hypoperfusion in the right precentral gyrus, middle frontal gyrus, right and left inferior frontal gyrus, right precuneus, cuneus, and superior parietal lobule (Figure 3, Table 4). When familial FTLD-TDP UGD was directly compared with *GRN* and vice versa, no differences of relative hypoperfusion were found.

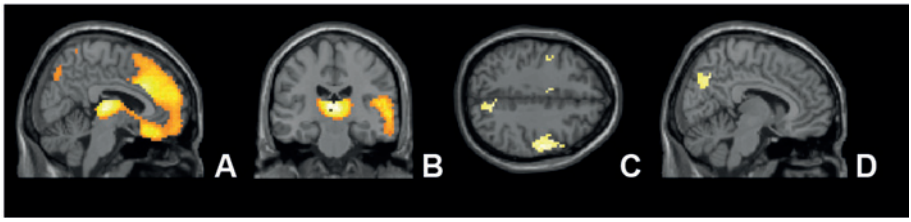

Figure 3 Familial FTLD-TDP UGD compared with controls and *MAPT.* A) and B) Familial FTLD-TDP UGD versus controls. C) and D) Familial FTLD-TDP UGD compared with *MAPT*, masked by familial FTLD-TDP UGD compared with controls at p <0.001 not corrected for multiple comparisons.

Table 4 Brain regions with relative hypoperfusion in familial FTLD-TDP UGD compared with *MAPT*

	MNI coordinates			
	x	y	z	Z
Precentral Gyrus R, BA 6*	57	-7	43	3.79
Middle Frontal Gyrus R, BA 6*	48	2	40	3.62
Cerebellum L	-12	-58	-8	3.53
Postcentral Gyrus R, BA 2	48	-28	31	3.51
Lingual Gyrus R, BA 19	18	-64	-2	3.48
Inferior Frontal Gyrus R, BA 9	54	20	28	3.46
Superior Parietal Lobule R, BA 7*	36	-55	64	3.46
Cuneus R, BA 7*	6	-70	31	3.44
Middle Frontal Gyrus R, BA 46*	48	17	25	3.38
Precuneus R, BA 7*	6	-73	37	3.31
Cingulate Gyrus L, BA 24	-12	-5	40	3.26
Precentral Gyrus L, BA 6	-36	-4	40	3.22
Inferior Frontal Gyrus L, BA 9	-48	-1	25	3.14

* Areas that remained significant after masking by Familial FTLD-TDP with unknown genetic defect (UGD) versus controls. BA: Brodmann area.

To correct for severity of atrophy and CDR score, we entered these possible confounding covariates in the design matrix. We found that hypoperfusion of the right precuneus, cuneus, cingulate gyrus, inferior parietal lobule, precentral gyrus, inferior and middle frontal gyri remained significant in the familial FTLD-TDP group compared with *MAPT* group. In the opposite analysis, only relative hypoperfusion of the rectal gyrus was found in the *MAPT* compared with familial FTLD-TDP, while the relative hypoperfusion of the temporal lobe was not present anymore after accounting for atrophy. In the analyses familial FTLD-TDP UGD compared with *MAPT*, and familial FTLD-TDP UGD compared with *GRN* and vice versa, all previous found regions remained significantly hypoperfused.

Memory deficits were significantly more often present in familial FTLD-TDP, whereas obsessive-compulsive behavior and naming deficits were more present in *MAPT*. We entered the score on memory deficits, obsessive-compulsive behavior, and naming deficits of the 29 patients in three different matrices, with age and gender as nuisance variables. Memory deficits were negatively correlated with relative hypoperfusion of the posterior cingulate and precuneus, right middle frontal gyrus, right inferior parietal lobule, right cerebellum and right midbrain (Figure 4). This means that a greater memory deficit was associated with lower perfusion in these areas. Obsessive-compulsive behavior did not correlate with any brain region. Naming deficits were correlated with the left temporal lobe and rectal gyrus. An analysis with memory as categorical variable between patients with severe and without memory problems, revealed relative hypoperfusion in the previous described brain regions, plus the left middle frontal gyrus.

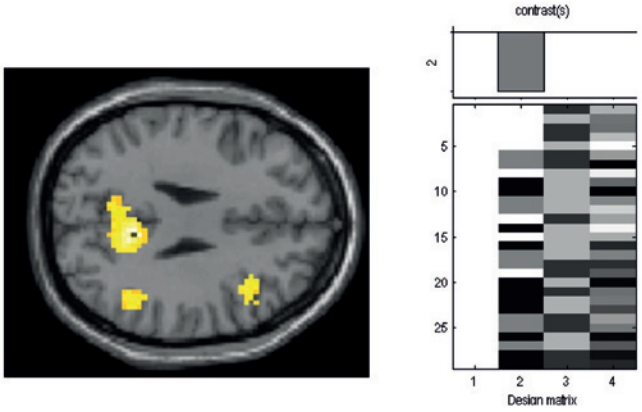

Figure 4 Correlation with memory performance in 29 FTLD patients. Correlation of memory deficits ($p < 0.001$ not corrected for multiple comparisons) with perfusion levels in posterior cingulate, precuneus, right inferior parietal lobule and right middle frontal gyrus projected on a SPM8 canonical single subject template.

DISCUSSION

The present study comparing familial FTLD-TDP and *MAPT* has demonstrated relative hypoperfusion in the right frontal and posterior cortical regions in familial FTLD-TDP patients compared with *MAPT* mutations, whereas vice versa relative hypoperfusion was found in the left lateral temporal lobe and medial frontal gyrus in *MAPT* mutations.

The observation of relative hypoperfusion in the posterior cortical regions, predominantly right-sided, in familial FTLD-TDP (including six patients with *GRN* mutations) is in line with earlier observations in patients with *GRN* gene mutations (Le Ber et al., 2008; Rohrer et al., 2010; Whitwell, 2009), although most of the present patients with familial FTLD-TDP had no *GRN* mutations. However, parietal lobe and posterior cingulate atrophy on MRI, has

also been reported in patients with clinical bvFTD and different underlying pathologies (Whitwell et al., 2009c), as well as in patients with FTLD-MND linked to chromosome 9 (Family VSM-20) (Boxer et al., 2011). In addition, VBM-studies did not show differences between patients with FTLD-tau and FTLD-TDP (Grossman et al., 2007; Kim et al., 2007; Pereira et al., 2009; Whitwell, 2009; Whitwell et al., 2009b). Therefore it will be important in future imaging studies to perform group analyses based on clinical, genetic (sporadic and familial) and pathological status to get explicit information on hypoperfusion and atrophy patterns in FTLD subgroups.

A higher frequency of memory deficits and lower scores on immediate recall memory task were found in familial FTLD-TDP compared with controls, and not compared with *MAPT* mutations possibly due to the small sample size of *MAPT* patients. These memory deficits correlated with precuneus hypoperfusion. This cortical region together with the posterior cingulate is comprised in Papez' circuit and related to episodic memory functioning (Bastin et al., 2012; Kobayashi et al., 2008). Atrophy and hypoperfusion of these cortical regions are frequently described in mild cognitive impairment and early stage of Alzheimer's disease (AD) (Matsuda, 2007; Salmon et al., 2008), and in patients with *GRN* gene mutations (Rohrer et al., 2010; Whitwell, 2009). Our results showed that the occurrence of memory problems also applies for FTLD-TDP with unknown genetic defect.

Another novel finding in the present study is the relative hypoperfusion of the precentral gyrus in familial FTLD-TDP compared with controls and *MAPT* mutations, which might be explained by the frequent occurrence of clinical MND in these patients (Guedj et al., 2007; Habert et al., 2007). Sparing of the precentral gyrus in *MAPT* is in line with the absence of MND in FTLD-tau (van Swieten and Heutink, 2008). It is still unclear why in familial FTLD-MND some family members develop FTD and others MND or both (Seelaar et al., 2007). There may be a certain threshold of precentral hypoperfusion associated with the development of clinical MND, and this hypoperfusion might be considered as an early biomarker in familial FTD-MND.

The finding of predominantly left-sided bifrontotemporal hypoperfusion in *MAPT* mutations corresponds with the clinical and neuropsychological profile of bvFTD with naming deficits in these patients (Rohrer et al., 2010; Whitwell, 2009; Whitwell et al., 2009a). We confirmed in our study the suggestion that *MAPT* mutations not affecting the splicing of exon 10 have anterolateral temporal and frontal atrophy, as the majority of our patients had a P301L mutation (Whitwell et al., 2009a). In contrast to this, *MAPT* mutations that affect exon 10 splicing and thus influence the alternative splicing of tau pre-messenger RNA were found to have a more medial temporal gray matter loss,

which suggests a possible association between mutation function and atrophy in *MAPT* (Whitwell et al., 2009a).

A shortcoming of our study was that patients might have had their eyes open or closed during scanning. Despite this, we think that the hypoperfusion of the cuneus and precuneus hypoperfusion in the familial FTLD-TDP group compared with *MAPT* mutations is a real finding, and presume that eyes were closed or open randomly distributed between groups. A second shortcoming was the relatively small number of patients with full neuropsychological assessment. Therefore, the results of the correlation analyses have to be interpreted with caution. A third shortcoming is that we could not determine brain regions with increased perfusion in our analyses, as the global normalization method we used did not allow increases of perfusion in areas unaffected by pathology. Finally, although SPECT measures may be confounded by atrophy, a voxel-by-voxel correction for atrophy could not be performed due to the different scanners used for structural imaging. Newer tools in functional brain imaging may help to differentiate FTLD subtypes in the future, especially the development of specific binding tracers in PET. The Pittsburgh Compound-B (PIB) tracer enables to differentiate between FTLD and Alzheimer's disease (Rabinovici et al., 2007), but to date there are no specific tracers available to diagnose FTLD or differentiate its pathological subtypes during life with more certainty. Future studies will focus on the earliest changes in these patients, and which functional molecular networks are affected in the pathogenesis of FTLD-TDP and FTLD-tau. These studies, including PET and functional MRI, will hopefully become sensitive enough to detect the earliest changes in presymptomatic mutation carriers to serve as biomarkers for disease progression in future therapeutic studies. Whether the outcomes of familial FTLD cases can be implemented for sporadic FTLD has yet to be elucidated.

REFERENCES

Baker M, Mackenzie IR, Pickering-Brown SM, Gass J, Rademakers R, Lindholm C, *et al.* Mutations in progranulin cause tau-negative frontotemporal dementia linked to chromosome 17. Nature 2006; 442: 916-919.

Bastin C, Feyers D, Souchay C, Guillaume B, Pepin JL, Lemaire C, *et al.* Frontal and posterior cingulate metabolic impairment in the behavioural variant of frontotemporal dementia with impaired autonoetic consciousness. Hum Brain Mapp 2012; 33: 1268-1278.

Boxer AL, Mackenzie IR, Boeve BF, Baker M, Seeley WW, Crook R, *et al.* Clinical, neuroimaging and neuropathological features of a new chromosome 9p-linked FTD-ALS family. J Neurol Neurosurg Psychiatry 2011; 82: 196-203.

Cruchaga C, Fernandez-Seara MA, Seijo-Martinez M, Samaranch L, Lorenzo E, Hinrichs A, *et al.* Cortical atrophy and language network reorganization associated with a novel progranulin mutation. Cereb Cortex 2009; 19: 1751-1760.

Cruts M, Gijselinck I, van der Zee J, Engelborghs S, Wils H, Pirici D, *et al.* Null mutations in progranulin cause ubiquitin-positive frontotemporal dementia linked to chromosome 17q21. Nature 2006; 442: 920-924.

Friston KJ, Holmes AP, Worsley KJ, Poline JB, Frith CD, Frackowiak RSJ. Statistical parametrical maps in functional imaging: a general linear approach. Hum Brain Mapp 1995; 2: 189-210.

Grossman M, Libon DJ, Forman MS, Massimo L, Wood E, Moore P, *et al.* Distinct antemortem profiles in patients with pathologically defined frontotemporal dementia. Arch Neurol 2007; 64: 1601-1609.

Guedj E, Le Ber I, Lacomblez L, Dubois B, Verpillat P, Didic M, *et al.* Brain spect perfusion of frontotemporal dementia associated with motor neuron disease. Neurology 2007; 69: 488-490.

Habert MO, Lacomblez L, Maksud P, El Fakhri G, Pradat JF, Meininger V. Brain perfusion imaging in amyotrophic lateral sclerosis: extent of cortical changes according to the severity and topography of motor impairment. Amyotroph Lateral Scler 2007; 8: 9-15.

Hutton M, Lendon CL, Rizzu P, Baker M, Froelich S, Houlden H, *et al.* Association of missense and 5'-splice-site mutations in tau with the inherited dementia FTDP-17. Nature 1998; 393: 702-705.

Kim EJ, Cho SS, Jeong Y, Park KC, Kang SJ, Kang E, *et al.* Glucose metabolism in early onset versus late onset Alzheimer's disease: an SPM analysis of 120 patients. Brain 2005; 128: 1790-1801.

Kim EJ, Rabinovici GD, Seeley WW, Halabi C, Shu H, Weiner MW, *et al.* Patterns of MRI atrophy in tau positive and ubiquitin positive frontotemporal lobar degeneration. J Neurol Neurosurg Psychiatry 2007; 78: 1375-1378.

Kobayashi S, Tateno M, Utsumi K, Takahashi A, Saitoh M, Morii H, *et al.* Quantitative analysis of brain perfusion SPECT in Alzheimer's disease using a fully automated regional cerebral blood flow quantification software, 3DSRT. J Neurol Sci 2008; 264: 27-33.

Le Ber I, Camuzat A, Hannequin D, Pasquier F, Guedj E, Rovelet-Lecrux A, *et al.* Phenotype variability in progranulin mutation carriers: a clinical, neuropsychological, imaging and genetic study. Brain 2008; 131: 732-746.

Masellis M, Momeni P, Meschino W, Heffner R, Jr., Elder J, Sato C, *et al.* Novel splicing mutation in the progranulin gene causing familial corticobasal syndrome. Brain 2006; 129: 3115-3123.

Matsuda H. Role of neuroimaging in Alzheimer's disease, with emphasis on brain perfusion SPECT. J Nucl Med 2007; 48: 1289-1300.

McKhann GM, Albert MS, Grossman M, Miller B, Dickson D, Trojanowski JQ. Clinical and pathological diagnosis of frontotemporal dementia: report of the Work Group on Frontotemporal Dementia and Pick's Disease. Arch Neurol 2001; 58: 1803-1809.

Morris JC. The Clinical Dementia Rating (CDR): current version and scoring rules. Neurology 1993; 43: 2412-2414.

Pereira JM, Williams GB, Acosta-Cabronero J, Pengas G, Spillantini MG, Xuereb JH, *et al.* Atrophy patterns in histologic vs clinical groupings of frontotemporal lobar degeneration. Neurology 2009; 72: 1653-1660.

Pickering-Brown SM, Rollinson S, Du Plessis D, Morrison KE, Varma A, Richardson AM, *et al.* Frequency and clinical characteristics of progranulin mutation carriers in the Manchester frontotemporal lobar degeneration cohort: comparison with patients with MAPT and no known mutations. Brain 2008; 131: 721-731.

Rabinovici GD, Furst AJ, O'Neil JP, Racine CA, Mormino EC, Baker SL, *et al.* 11C-PIB PET imaging in Alzheimer disease and frontotemporal lobar degeneration. Neurology 2007; 68: 1205-1212.

Rohrer JD, Guerreiro R, Vandrovcova J, Uphill J, Reiman D, Beck J, *et al.* The heritability and genetics of frontotemporal lobar degeneration. Neurology 2009; 73: 1451-1456.

Rohrer JD, Ridgway GR, Modat M, Ourselin S, Mead S, Fox NC, *et al.* Distinct profiles of brain atrophy in frontotemporal lobar degeneration caused by progranulin and tau mutations. Neuroimage 2010; 53: 1070-1076.

Rosso SM, Donker Kaat L, Baks T, Joosse M, de Koning I, Pijnenburg Y, *et al.* Frontotemporal dementia in The Netherlands: patient characteristics and prevalence estimates from a population-based study. Brain 2003; 126: 2016-2022.

Salmon E, Lekeu F, Garraux G, Guillaume B, Magis D, Luxen A, *et al.* Metabolic correlates of clinical heterogeneity in questionable Alzheimer's disease. Neurobiol Aging 2008; 29: 1823-1829.

Sampathu DM, Neumann M, Kwong LK, Chou TT, Micsenyi M, Truax A, *et al.* Pathological heterogeneity of frontotemporal lobar degeneration with ubiquitin-positive inclusions delineated by ubiquitin immunohistochemistry and novel monoclonal antibodies. Am J Pathol 2006; 169: 1343-1352.

Seelaar H, Kamphorst W, Rosso SM, Azmani A, Masdjedi R, de Koning I, *et al.* Distinct genetic forms of frontotemporal dementia. Neurology 2008; 71: 1220-1226.

Seelaar H, Klijnsma KY, de Koning I, van der Lugt A, Chiu WZ, Azmani A, *et al.* Frequency of ubiquitin and FUS-positive, TDP-43-negative frontotemporal lobar degeneration. J Neurol 2010; 257: 747-753.

Seelaar H, Schelhaas HJ, Azmani A, Kusters B, Rosso S, Majoor-Krakauer D, *et al.* TDP-43 pathology in familial frontotemporal dementia and motor neuron disease without Progranulin mutations. Brain 2007; 130: 1375-1385.

Van Laere KJ, Versijpt J, Koole M, Vandenberghe S, Lahorte P, Lemahieu I, *et al.* Experimental performance assessment of SPM for SPECT neuroactivation studies using a subresolution sandwich phantom design. Neuroimage 2002; 16: 200-216.

van Swieten JC, Heutink P. Mutations in progranulin (GRN) within the spectrum of clinical and pathological phenotypes of frontotemporal dementia. Lancet Neurol 2008; 7: 965-974.

Whitwell JL. Jack CR, Boeve BF, Senjem ML, Baker M, Rademakers R, *et al*. Voxel-based morphometry patterns of atrophy in FTLD wit mutations in MAPT or PGRN. Neuroimage 2009; 72: 813-820.

Whitwell JL, Jack CR, Jr., Boeve BF, Senjem ML, Baker M, Ivnik RJ, *et al.* Atrophy patterns in IVS10+16, IVS10+3, N279K, S305N, P301L, and V337M MAPT mutations. Neurology 2009a; 73: 1058-1065.

Whitwell JL, Jack CR, Jr., Senjem ML, Parisi JE, Boeve BF, Knopman DS, *et al.* MRI correlates of protein deposition and disease severity in postmortem frontotemporal lobar degeneration. Neurodegener Dis 2009b; 6: 106-117.

Whitwell JL, Przybelski SA, Weigand SD, Ivnik RJ, Vemuri P, Gunter JL, *et al.* Distinct anatomical subtypes of the behavioural variant of frontotemporal dementia: a cluster analysis study. Brain 2009c; 132: 2932-2946.

Yakushev I, Landvogt C, Buchholz HG, Fellgiebel A, Hammers A, Scheurich A, *et al.* Choice of reference area in studies of Alzheimer's disease using positron emission tomography with fluorodeoxyglucose-F18. Psychiatry Res 2008; 164: 143-153.

Chapter 3.3

Midcingulate involvement in progressive supranuclear palsy and tau-positive frontotemporal dementia

Wang Zheng Chiu
Janne M. Papma
Inge de Koning
Laura Donker Kaat
Harro Seelaar
Ambroos E.M. Reijs
Roelf Valkema
Djo Hasan
Agnita J.W. Boon
John C. van Swieten

Journal of Neurology, Neurosurgery & Psychiatry 2012; 83(9): 910-915.

ABSTRACT

Introduction

Progressive supranuclear palsy (PSP) patients often exhibit cognitive decline and behavioral changes during the disease course. In a subset, these symptoms may be the presenting manifestation, and can be similar to those in frontotemporal dementia (FTD). However, correlation studies between quantitative imaging measures and detailed neuropsychological assessment are scarce. Our aim is to investigate the functional role of affected brain regions in cognition in PSP compared to controls and subsequently examine these regions in FTD patients with known tau pathology (FTD-tau).

Methods

Twenty-one PSP patients, 27 healthy controls, and 11 FTD-tau patients were enrolled**.** All participants underwent neuropsychological testing and perfusion ^{99m}Tc-HMPAO SPECT. Regression slope analyses were performed in SPM to find significant associations between neuropsychological test results and brain perfusion.

Results

PSP patients showed hypoperfusion in the midcingulate cortex of which the posterior part correlated with Stroop III and Weigl. In FTD-tau patients, midcingulate cortex involvement was located more anterior and correlated with Stroop III and Wisconsin Card Sorting Test concepts. The degree of hypoperfusion in the anterior- and midcingulate cortex in the disorders differed in the subgenual anterior cingulate cortex only.

Discussion

The posterior part of the midcingulate cortex is prominently involved in the neurodegenerative process of PSP, and the severity of its hypoperfusion correlated with the extent of executive dysfunction. In FTD-tau, this cognitive domain was associated with anterior midcingulate cortex involvement. The degree of hypoperfusion in these regions did not differ between PSP and FTD-tau. These observations provide insight into the role of the cingulate cortex in cognitive dysfunction in these neurodegenerative disorders and warrant further investigations.

INTRODUCTION

Progressive supranuclear palsy (PSP) is a neurodegenerative disorder characterized by early postural instability, supranuclear gaze palsy, parkinsonism, pseudobulbar palsy and cognitive decline (Litvan et al., 1996a; Steele et al., 1964). PSP patients often exhibit mental slowness and a dysexecutive syndrome, as well as behavioral changes, commonly considered as frontal-subcortical dementia (Albert et al., 1974). The cognitive dysfunction in PSP has a significant effect on the quality of life of patients, for which effective therapeutic interventions are lacking (Schrag et al., 2003). In a subset of PSP patients, the cognitive and behavioral symptoms may even be the predominant presenting manifestation, and can be similar to those observed in the behavioral variant of frontotemporal dementia (bvFTD) (Donker Kaat et al., 2007). Overlap between PSP and FTD is further emphasized by tau-positive inclusions in the brain, which characterize PSP, but are also found in a large subset of bvFTD patients, denoted as frontotemporal degeneration with tau pathology (FTD-tau). Various brain imaging modalities, including ^{99m}Tc-HMPAO SPECT, ^{18}F-fluorodeoxyglucose (FDG)-PET and MRI, have found involvement of the caudate nuclei, thalamus and midbrain in PSP (Blin et al., 1990; Cordato et al., 2005; Eckert et al., 2008; Johnson et al., 1992; Josephs et al., 2011; Paviour et al., 2006). In addition, frontal brain regions and specifically the cingulate cortex have shown involvement in PSP as well as in FTD (Guedj et al., 2008; Salmon et al., 1997; Teune et al., 2010; Varrone et al., 2007; Williams et al., 2005). However, the few published cognition-imaging correlation studies in PSP lacked quantitative imaging measures (Johnson et al., 1992), extensive neuropsychological assessment (Blin et al., 1990; Cordato et al., 2005; Groschel et al., 2004; Josephs et al., 2011), or detailed division of cortical areas (Paviour et al., 2006). We sought to overcome these limitations by determining perfusion measures on ^{99m}Tc-HMPAO SPECT using statistical parametric mapping (SPM), and correlating these with neuropsychological test scores. Our aim is to elucidate the functional role of affected brain regions in cognition in PSP compared to healthy controls, in order to gain insight into the underlying mechanisms of cognition in this disorder. To assess the specificity of regions that are affected in PSP, we specifically examined these areas in FTD-tau as well.

METHODS

Participants

PSP patients, with subjective cognitive complaints, were recruited between 2002 and 2010 by nationwide referral to the outpatient department of the Erasmus MC – University Medical Center Rotterdam, the Netherlands, as part of a large longitudinal study (Chiu et al., 2010; Donker Kaat et al., 2007). FTD patients were recruited in a similar fashion

(Rosso et al., 2003). All patients were examined by either the research physician (WZC) or a neurologist (AJWB and JvS). Detailed clinical history was obtained from patients and their family members, and by reviewing medical records. The neurologic examinations were performed according to a standard protocol. Structural neuroimaging of patients was reviewed by the investigators to exclude other structural causes. The clinical diagnosis of all patients was established in a consensus meeting according to the National Institute for Neurological Diseases and Stroke-Society for PSP (NINDS-SPSP) criteria (Litvan et al., 1996a), and the Lund and Manchester criteria for FTD (1994). All PSP patients in the current study were typical Richardson's syndrome cases (10 probable and 11 possible cases). The PSP rating scale (PSPRS) quantified the measure of disability in PSP patients (Golbe and Ohman-Strickland, 2007). According to the Diagnostic and Statistical Manual of Mental Disorders Fourth Edition (DSM-IV), one PSP patient was found to suffer from prolonged periods of a depressed mood and suicidal thoughts but without intent, and without vegetative symptoms other than apathy. Healthy controls were recruited from the Rotterdam Elderly Study and had no neurological disorders or abnormalities at neurological and neuropsychological examination (Claus et al., 1994). In the current study, FTD patients consisted of a subset of patients described in a previous study of our group (Chiu et al., 2010). FTD-tau patients were selected for this study and comprise 4 pathologically proven tau-positive FTD patients without and 7 FTD patients with *MAPT* mutations (2 G272V and 5 P301L) that underwent ^{99m}Tc-HMPAO SPECT scan and neuropsychological examination. As was the case in our previous study, FTD-tau patients were significantly younger than PSP patients (Chiu et al., 2010). The PSP, FTD and Rotterdam Elderly studies were approved by the medical ethics committee of the Erasmus MC, all participants or first-degree relatives signed informed consent. Neuropsychological testing and ^{99m}Tc-HMPAO SPECT scans of patients were part of the diagnostic workup.

Neuropsychological assessment

The neuropsychological test battery for all patients and controls, carried out by a single experienced clinical neuropsychologist (IdK), included the Mini-Mental State Examination (MMSE), the Dutch version of the Rey Auditory Verbal Learning Test (15-WVLT Test) or Word List Memory Test (CERAD), Trail Making Test (TMT) A and B, the Stroop Color-Word Test, phonological fluency (DAT), and semantic fluency (animals and occupations). Higher scores on the TMT and Stroop tests corresponds to worse performance. Additional tests for patients consisted of the Boston Naming Test, Wisconsin Card Sorting Test or Weigl Color-Form Sorting Test. Differences in test batteries between patients and controls are due to the clinical setting in which PSP and FTD patients were assessed as opposed to the Rotterdam Elderly Study. Education was categorized according to the system of Verhage (1964), which consists of 7 increasing levels of education.

^{99m}Tc-HMPAO SPECT scanning and image processing

^{99m}Tc-HMPAO SPECT brain perfusion scans of all participants were exclusively carried out at the department of Nuclear Medicine of the Erasmus Medical Center. After injection of 740 MBq ^{99m}Tc-HMPAO, SPECT scans of PSP and bvFTD patients were acquired on a Prism 3000XP Philips (Picker) three-headed system, with a fan-beam collimator. Only controls that underwent SPECT imaging using the same three-head camera were selected from the Rotterdam Elderly Study (Claus et al., 1994). On average, scans were started 20 minutes after injection of ^{99m}Tc-HMPAO while resting in a quiet room. Duration of scanning was 30 minutes. One hundred-twenty projections (3 x 40 steps of 3°, and 20 seconds per step) were acquired. Image reconstruction was performed by a ramp-filtered back projection and three-dimensionally smoothing with a Metz Filter. No attenuation and scatter correction was performed. After gross manual image reorientation and approximate definition of the image centre point (anterior commisure), the SPECT scans were spatially processed using Statistical Parametric Mapping (SPM5; Wellcome Trust Center for Neuroimaging, London, UK) implemented in Matlab 7.9.0 (MathWorks, Natick, MA, USA). The effect of differences in spatial resolution was minimized by masking the images. SPECT images in native space were resliced into the same orientation, and spatially normalized onto the SPM5 MNI SPECT brain template with a 12-parameter affine transformation followed by non-linear transformations and a trilinear interpolation. Dimensions of the resulting voxel were 3 x 3 x 3 mm. In this normalization step estimation of individual SPECT normalization parameters were constrained by a source weighting image. This method is used to correct for registering lesioned brains. Hereafter, images were smoothed using a Gaussian filter of 16 mm full width at half maximum (FWHM), limited to measured brain tissue. For SPECT data, smoothing with at least twice the FWHM of the imaging system was shown to provide good detection sensitivity (Van Laere et al., 2002), and is used in pathological brain studies with SPECT and PET (Kim et al., 2005). Voxel based image analyses were conducted within the framework of the General Linear Model as provided by SPM (Friston et al., 1995). Proportional scaling to the mean global image intensity was used to remove confounding effects due to variations in individual ^{99m}Tc-HMPAO uptake (Acton and Friston, 1998). We performed two group analyses. In the first analysis we compared PSP, FTD-tau and controls in a full factorial design with gender as nuisance variable. We chose not to adjust for age in this analysis, as we expected patients to exhibit decreased perfusion, which likely reflects underlying disease and not effects of age, seeing that patients were younger than controls. The results of the full factorial design were thresholded at $p < 0.05$, Family Wise Error (FWE) correction for multiple comparisons. The contrasts PSP vs. controls and FTD-tau vs. controls were used to define an overlapping ROI, i.e. deteriorated regions involved in both conditions. Group analysis in PSP showed significant hypoperfusion of the anterior cingulate cortex (ACC) and midcingulate cortex (MCC) relative to controls. To

assess the association between these regions and cognitive dysfunction in PSP as well as FTD-tau, we performed a second group analysis. The design matrix of this ANCOVA model contained SPECT scans of both patient groups as dependent variable and regressors for group and neuropsychological data per patient group. We correlated neuropsychological data with perfusion in PSP and FTD-tau separately within a ROI comprising the entire ACC and MCC. We then performed F-test interaction analyses of neuropsychological data and group, within a ROI of overlapping hypoperfusion in PSP and FTD-tau relative to controls consisting of a part of the MCC (Figure 1 B), to make inferences on differences in regression slope between the patient groups in a region that was affected in both conditions. Results of the slope and interaction analyses were thresholded at the liberal threshold of $p < 0.005$, not corrected for multiple comparisons, to ensure that even subtle differences between these patient groups would be noted. Post hoc, peak values of regions with significant regression slopes or interaction effect were used to extract individual proportional perfusion within a 5 mm radius of the peak voxel, using the Matlab toolbox MarsBaR (Brett et al., 2002). These perfusion measures were subsequently exported to SPSS to examine and visualize these effects. In a post hoc analysis we examined hypoperfusion of the cingulate cortex in PSP and FTD-tau more carefully by performing the contrast PSP vs. FTD-tau and vice versa within a ROI of the entire ACC and MCC. MNI anatomical labelling of significant clusters was performed using WFU Pickatlas software extension to SPM5 (Functional MRI laboratory – Wake Forest University School of Medicine, Winston Salem). The various subregions of the cingulate cortex are designated according to the four-region model as proposed by Vogt et al. (2005). MNI coordinates were assigned to specific parts of the MCC following subregion division of the cingulate cortex by Yu et al. (2011).

Statistical analysis

SPSS 15.0 for Windows (SPSS, Chicago, Illinois, USA) was used for statistical analysis. Age at examination, gender and education levels were analyzed by independent sample t-test or Chi-square test, whereas ANOVA was used for analysis of neuropsychological data, followed by independent sample t-test. For reasons explained above, we did not adjust for age in between group comparisons. Perfusion measures were entered as regressors in a stepwise regression analysis, with neuropsychological data as dependent variables, adjusted for demographical data. A p value <0.05 was considered statistically significant.

RESULTS

Characteristics of patients and healthy controls are summarized in Table 1. The mean PSPRS score of <30 in 19 PSP patients reflects an early and mild disease stage. Two patients were recruited before the introduction of the PSPRS.

Table 1 Characteristics of PSP, FTD and controls

	Controls (n = 27)	PSP (n = 21)	FTD-tau (n = 11)	P-value
Age at examination	76.3 (5.8)	69.1 (5.5)	54.8 (7.6)	**<0.001**
Male gender, n (%)	13 (48.1)	12 (57.1)	4 (36.4)	0.531
Education	3.8 (1.5)	4.5 (1.7)	4.0 (1.5)	0.297
Disease duration at examination	-	3.4 (1.3)	3.0 (1.4)	0.341

Values are unadjusted means (standard deviations) or number of participants (%). PSP: progressive supranuclear palsy. FTD: frontotemporal dementia. Differences between groups by means of ANOVA.

Cognitive function and cerebral perfusion in PSP

PSP patients performed significantly worse than controls on all examined cognitive domains of memory, attention and concentration, executive function, and language (Table 2).

Table 2 Neuropsychological results in PSP, FTD-tau and controls

	n	PSP	n	FTD-tau	n	Controls	P-value
MMSE	20	25.7 (3.0)	7	23.6 (4.0)	27	27.7 (2.1)	**0.001**[a]
Memory							
Learning (%)	21	37.1 (12.0)	10	32.6 (20.0)	26	63.0 (13.9)	**<0.001**[a]
Delayed Recall (%)	21	35.2 (13.7)	10	24.3 (27.7)	26	63.1 (18.5)	**<0.001**[a]
Attention and concentration							
TMT A	21	93.9 (42.2)	11	94.6 (66.3)	25	58.1 (25.1)	**0.009**[a]
Stroop I	16	100.4 (29.0)	9	80.6 (29.0)	23	47.7 (6.7)	**<0.001**[a]
Stroop II	16	118.4 (32.4)	9	105.9 (34.6) 34.6	23	66.1 (14.8)	**<0.001**[a]
Executive function							
TMT B	21	274.3 (111.1)	11	221.2 (69.2)	24	122.8 (54.6)	**<0.001**[a]
Stroop III	16	211.2 (111.1)	9	202.2 (93.8)	23	128.6 (47.0)	**0.001**[a]
WCST, concepts	17	3.1 (1.8)	9	1.8 (2.5)	-	-	0.146
Weigl	12	8.1 (2.8)	6	4.3 (5.5)	-	-	0.167
Language							
Semantic fluency	21	17.4 (5.3)	11	11.7 (10.9)	24	34.5 (9.1)	**<0.001**[a]
Phonological fluency	21	14.3 (11.9)	9	10.6 (17.6)	26	37.7 (13.8)	**<0.001**[a]
Boston Naming Test	18	47.8 (5.1)	5	32.2 (11.2)	-	-	**0.034**[b]

Values are unadjusted means (standard deviations). PSP: progressive supranuclear palsy. FTD: frontotemporal dementia. TMT: trail making test. MMSE: mini mental state examination. Differences between groups by means of ANOVA, followed by independent sample t-test: [a] $p < 0.05$ between patients and controls. [b] $p < 0.05$ between PSP and FTD-tau.

SPM analysis with a threshold of p <0.05, FWE correction for multiple comparisons, yielded relative hypoperfusion in PSP patients compared to controls in predominantly the ACC and MCC (Figure 1 A). A more lenient analysis p <0.001 not corrected for multiple comparisons resulted in widespread relative hypoperfusion in frontal regions, cerebellum, basal ganglia and midbrain. Based on the results from the p <0.05 FWE correction for multiple comparisons analysis of PSP patients vs. controls, we restricted analyses of the ANCOVA model to the ACC and MCC. Regression slope analyses yielded significant result for the executive tests Stroop III (MNI X, Y, Z = -15 6 39) and Weigl (MNI X, Y, Z = 6 3 45) only, indicating significant associations between these test results and perfusion in the posterior part of the MCC. The magnitudes of these associations were post hoc assessed in SPSS by correlating extracted perfusion measures with Stroop III (adjusted $r^2 = 0.245$, $\beta = -0.543$, $p = 0.03$) and Weigl (adjusted $r^2 = 0.418$, $\beta = 0.686$, $p = 0.014$).

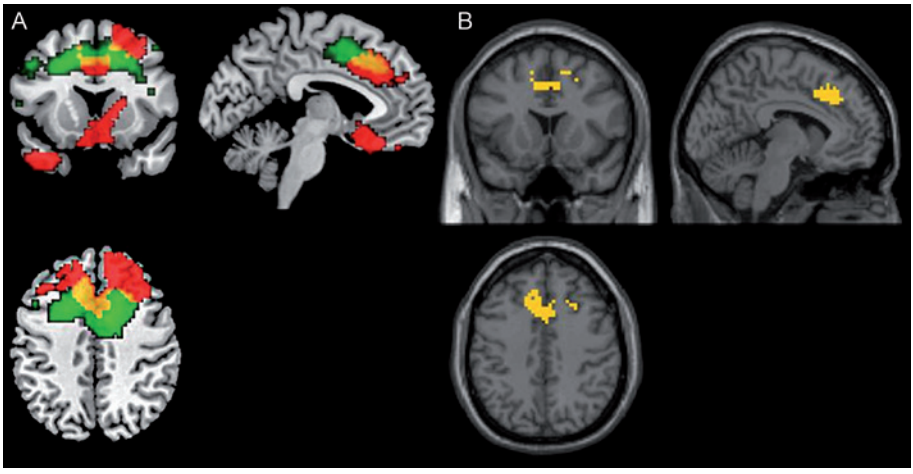

Figure 1 A) Hypoperfusion in PSP (green) and FTD-tau (red) and overlap in hypoperfusion (yellow). B) ROI based on the overlap of hypoperfusion between PSP and FTD. Results shown at p <0.05 FWE correction for multiple comparisons.

Cognitive function and cerebral perfusion in FTD-tau

FTD-tau patients performed worse than controls but equal to PSP patients on MMSE and all subtests of the examined cognitive domains. Only scores on the Boston Naming Test were significantly worse in FTD-tau patients (Table 2). The stringent corrected analysis revealed relative hypoperfusion in frontal, cingulate and temporal regions in FTD-tau patients compared to controls (Figure 1 A). Regression slope analyses in the ACC and MCC ROI yielded significant results in the anterior part of the MCC for the executive tests Stroop III (MNI X, Y, Z = 6 30 27) and WCST (MNI X, Y, Z = 3 33 27) only (p <0.005 not corrected for multiple comparisons), with the following magnitudes for Stroop III (adjusted $r^2 = 0.638$, $\beta = -0.826$, $p = 0.006$) and WCST (adjusted $r^2 = 0.662$, $\beta = 0.839$, $p = 0.005$).

PSP vs. FTD-tau

To assess whether there is a difference in slope in regions that are involved in both PSP and FTD-tau between the disorders, we performed a group-by-neuropsychological test interaction analysis in an overlap ROI (Figure 1 B). This showed that the disorders differed significantly on only one of the executive tests, namely Weigl, in the posterior part of the MCC (MNI X, Y, Z = 9 12 42); PSP patients had a significantly steeper slope than FTD-tau patients (Figure 2). Comparison of anterior- and midcingulate hypoperfusion between PSP and FTD-tau patients revealed differences in the subgenual part of the ACC (sACC) only, at a stringent threshold, with higher perfusion values in PSP patients.

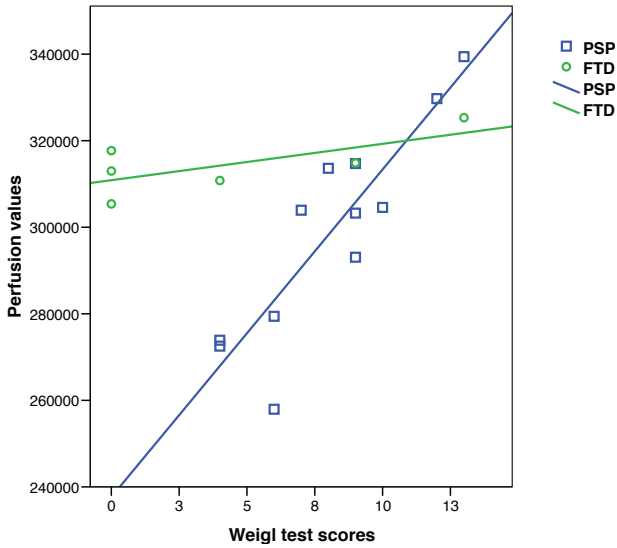

Figure 2 Significant difference in regression slopes between PSP and FTD-tau on the Weigl test in the posterior part of the midcingulate cortex (coordinate MNI X, Y, Z; 9, 12, 42).

DISCUSSION

The present study revealed prominent hypoperfusion in the posterior part of the MCC in PSP patients compared to controls using quantitative SPM analysis. This hypoperfusion correlated with the extent of executive dysfunction, as was the case for hypoperfusion in the anterior part of the MCC in FTD-tau patients. The degree of anterior- and midcingulate hypoperfusion in the disorders differed in the sACC only.

The robust finding of cingulate involvement in PSP patients in the present study has also been described by other investigators (Cordato et al., 2005; Salmon et al., 1997; Teune et al., 2010; Varrone et al., 2007). Salmon et al. (1997) detected impairment of glucose

metabolism in the MCC in 10 PSP patients compared to healthy controls, and patients with Alzheimer's disease. Involvement of the MCC was also found in PSP patients compared to Parkinson's disease patients (Varrone et al., 2007), whereas similar findings were reported in FTD compared to Alzheimer's disease patients and controls (Varrone et al., 2002). However, the functional role of the cingulate cortex in PSP and FTD remained speculative as correlation with neuropsychological evaluation was not performed in these studies.

We found that hypoperfusion in the posterior part of the MCC correlates to impairment of specific frontal functions in PSP. Several studies have linked frontal involvement to executive dysfunction and behavioral changes (Blin et al., 1990; Cordato et al., 2005; Josephs et al., 2011; Paviour et al., 2006), but these studies did not distinguish between different regions of the frontal lobe (Paviour et al., 2006), or correlated frontal regions to a more global measure as Frontal Behavioral Inventory (FBI) instead of specific frontal tests (Blin et al., 1990; Cordato et al., 2005; Josephs et al., 2011). Furthermore, compared to these studies our PSP patients have been evaluated early in the disease course. Only Blin et al. (1990) had a comparable mean disease duration at examination of 3.1 years. In addition to the correlation of executive function with the posterior part of the MCC in PSP patients, we found this cognitive domain to be associated with the anterior part of the MCC in FTD-tau patients. This observation is in line with a very recent structure based meta-analysis by Torta and Cauda (2011) who have found multiple portions of the cingulate cortex activated for executive tasks, adding to the notion of multifunctionality of parts of the cingulate cortex.

The difference in anterior- and midcingulate hypoperfusion patterns between PSP and FTD patients when compared to controls was also found by other investigators; the posterior part of the MCC was predominantly affected in PSP compared to controls, whereas the most affected part of the cingulate in FTD compared to controls was located more anterior. However, direct comparison of cingulate involvement between PSP and FTD was not assessed in their study (Teune et al., 2010). Our observation that the extent of hypoperfusion in the cingulate cortex in PSP did not differ from that in FTD-tau, except for the sACC, emphasizes a remarkable degree of involvement of anterior- and midcingulate regions in PSP. This is in accordance with another study that has found reduced cingulate cortex metabolism to differentiate PSP from Parkinson's disease (Klein et al., 2005). The regression slope in the overlapping region between PSP and FTD-tau was similar for both disorders, except for the Weigl. Based on this observation, a differential effect on the Weigl may exist, but further studies with larger sample sizes are needed to confirm this.

An interesting issue is whether the correlation in PSP might reflect the impairment of cortical-subcortical connections. The frontal hypometabolism in PSP is thought to be either secondarily caused by damage to subcortical projections, which disrupt cortical-subcortical circuits, or the primary accumulation of cortical tau pathology. The MCC in a post mortem cohort of 24 PSP patients showed neurodegenerative involvement reflected by variable tau pathology, despite the visually assessed absence of neuronal loss (Chiu et al., 2010). These observations are similar to findings by Schofield et al. (2011), adding to the growing evidence for cortical tau pathology being at least in part directly responsible for the impaired functionality. The cingulate cortex also plays a role in social cognition (Fujiwara et al., 2007), which may be explained by the exclusive presence of von Economo neurons (VENs) in the cingulate cortex and frontal insula. Selective loss of VENs has been found in bvFTD (Seeley et al., 2006), and the question is whether the impaired recognition of negative emotions in PSP (Ghosh et al., 2009) is related to changes in the number of VENs. Future studies are needed to investigate the involvement of VENs in the cingulate cortex in PSP.

A limitation of the current study is the lack of pathological confirmation in our PSP patients. The NINDS-SPSP criteria however have shown a good positive predictive value of diagnosing typical cases of PSP (Litvan et al., 1996b). Secondly, our sample of FTD-tau patients with full neuropsychological data and a perfusion scan is relatively small. Another limitation is that controls are slightly older than PSP patients. However, this means that the observed findings in PSP patients are likely an underestimate rather than an overestimate of the difference in hypoperfusion between PSP and controls, as aging is accompanied by regionally selective reduction of cortical perfusion (Chen et al., 2011). Another issue is a larger difference in age between PSP and FTD patients. This is inherent to the underlying disorders, as FTD is characterized by a presenile onset.

In conclusion, we have gained insight into the involvement and the role of the MCC in cognition in PSP. The extent of hypoperfusion in this region in PSP did not differ from that in FTD-tau, and was in both disorders correlated to executive function. Our observations support the idea that further investigations into the role of this intriguing region in PSP especially, but also FTD, are warranted, as the cingulate cortex has not been a focus in PSP research. Understanding this region may prove key to finding a treatment for cognitive symptoms in these neurodegenerative disorders.

REFERENCES

Clinical and neuropathological criteria for frontotemporal dementia. The Lund and Manchester Groups. J Neurol Neurosurg Psychiatry 1994; 57: 416-418.

Acton PD, Friston KJ. Statistical parametric mapping in functional neuroimaging: beyond PET and fMRI activation studies. Eur J Nucl Med 1998; 25: 663-667.

Albert ML, Feldman RG, Willis AL. The 'subcortical dementia' of progressive supranuclear palsy. J Neurol Neurosurg Psychiatry 1974; 37: 121-130.

Blin J, Baron JC, Dubois B, Pillon B, Cambon H, Cambier J, *et al.* Positron emission tomography study in progressive supranuclear palsy. Brain hypometabolic pattern and clinicometabolic correlations. Arch Neurol 1990; 47: 747-752.

Brett M, Anton J, Valabregue R, Poline JP. Region of interest analysis using an SPM toolbox. 8th International conference on functional mapping of the human brain. June 2002 Sendai, Japan 2002.

Chen JJ, Rosas HD, Salat DH. Age-associated reductions in cerebral blood flow are independent from regional atrophy. Neuroimage 2011; 55: 468-478.

Chiu WZ, Kaat LD, Seelaar H, Rosso SM, Boon AJ, Kamphorst W, *et al.* Survival in progressive supranuclear palsy and frontotemporal dementia. J Neurol Neurosurg Psychiatry 2010; 81: 441-445.

Claus JJ, van Harskamp F, Breteler MM, Krenning EP, van der Cammen TJ, Hofman A, *et al.* Assessment of cerebral perfusion with single-photon emission tomography in normal subjects and in patients with Alzheimer's disease: effects of region of interest selection. Eur J Nucl Med 1994; 21: 1044-1051.

Cordato NJ, Duggins AJ, Halliday GM, Morris JG, Pantelis C. Clinical deficits correlate with regional cerebral atrophy in progressive supranuclear palsy. Brain 2005; 128: 1259-1266.

Donker Kaat L, Boon AJ, Kamphorst W, Ravid R, Duivenvoorden HJ, van Swieten JC. Frontal presentation in progressive supranuclear palsy. Neurology 2007; 69: 723-729.

Eckert T, Tang C, Ma Y, Brown N, Lin T, Frucht S, *et al.* Abnormal metabolic networks in atypical parkinsonism. Mov Disord 2008; 23: 727-733.

Friston KJ, Holmes AP, Worsley KJ, Poline JP, Frith CD, Frackowiak RSJ. Statistical parametric mapping in functional imaging: a general linear approach. Human Brain Mapping 1995; 2: 189-210.

Fujiwara H, Hirao K, Namiki C, Yamada M, Shimizu M, Fukuyama H, *et al.* Anterior cingulate pathology and social cognition in schizophrenia: a study of gray matter, white matter and sulcal morphometry. Neuroimage 2007; 36: 1236-1245.

Ghosh BC, Rowe JB, Calder AJ, Hodges JR, Bak TH. Emotion recognition in progressive supranuclear palsy. J Neurol Neurosurg Psychiatry 2009; 80: 1143-1145.

Golbe LI, Ohman-Strickland PA. A clinical rating scale for progressive supranuclear palsy. Brain 2007; 130: 1552-1565.

Groschel K, Hauser TK, Luft A, Patronas N, Dichgans J, Litvan I, *et al.* Magnetic resonance imaging-based volumetry differentiates progressive supranuclear palsy from corticobasal degeneration. Neuroimage 2004; 21: 714-724.

Guedj E, Allali G, Goetz C, Le Ber I, Volteau M, Lacomblez L, *et al.* Frontal Assessment Battery is a marker of dorsolateral and medial frontal functions: A SPECT study in frontotemporal dementia. J Neurol Sci 2008; 273: 84-87.

Johnson KA, Sperling RA, Holman BL, Nagel JS, Growdon JH. Cerebral perfusion in progressive supranuclear palsy. J Nucl Med 1992; 33: 704-709.

Josephs KA, Whitwell JL, Eggers SD, Senjem ML, Jack CR, Jr. Gray matter correlates of behavioural severity in progressive supranuclear palsy. Mov Disord 2011; 26: 493-498.

Kim EJ, Cho SS, Jeong Y, Park KC, Kang SJ, Kang E, *et al.* Glucose metabolism in early onset versus late onset Alzheimer's disease: an SPM analysis of 120 patients. Brain 2005; 128: 1790-1801.

Klein RC, de Jong BM, de Vries JJ, Leenders KL. Direct comparison between regional cerebral metabolism in progressive supranuclear palsy and Parkinson's disease. Mov Disord 2005; 20: 1021-1030.

Litvan I, Agid Y, Calne D, Campbell G, Dubois B, Duvoisin RC, *et al.* Clinical research criteria for the diagnosis of progressive supranuclear palsy (Steele-Richardson-Olszewski syndrome): report of the NINDS-SPSP international workshop. Neurology 1996a; 47: 1-9.

Litvan I, Hauw JJ, Bartko JJ, Lantos PL, Daniel SE, Horoupian DS, *et al.* Validity and reliability of the preliminary NINDS neuropathologic criteria for progressive supranuclear palsy and related disorders. J Neuropathol Exp Neurol 1996b; 55: 97-105.

Paviour DC, Price SL, Jahanshahi M, Lees AJ, Fox NC. Longitudinal MRI in progressive supranuclear palsy and multiple system atrophy: rates and regions of atrophy. Brain 2006; 129: 1040-1049.

Rosso SM, Donker Kaat L, Baks T, Joosse M, de Koning I, Pijnenburg Y, *et al.* Frontotemporal dementia in The Netherlands: patient characteristics and prevalence estimates from a population-based study. Brain 2003; 126: 2016-2022.

Salmon E, Van der Linden MV, Franck G. Anterior cingulate and motor network metabolic impairment in progressive supranuclear palsy. Neuroimage 1997; 5: 173-178.

Schofield EC, Hodges JR, Macdonald V, Cordato NJ, Kril JJ, Halliday GM. Cortical atrophy differentiates Richardson's syndrome from the parkinsonian form of progressive supranuclear palsy. Mov Disord 2011; 26: 256-263.

Schrag A, Selai C, Davis J, Lees AJ, Jahanshahi M, Quinn N. Health-related quality of life in patients with progressive supranuclear palsy. Mov Disord 2003; 18: 1464-1469.

Seeley WW, Carlin DA, Allman JM, Macedo MN, Bush C, Miller BL, *et al.* Early frontotemporal dementia targets neurons unique to apes and humans. Ann Neurol 2006; 60: 660-667.

Steele JC, Richardson JC, Olszewski J. Progressive Supranuclear Palsy. A Heterogeneous Degeneration Involving the Brain Stem, Basal Ganglia and Cerebellum with Vertical Gaze and Pseudobulbar Palsy, Nuchal Dystonia and Dementia. Arch Neurol 1964; 10: 333-359.

Teune LK, Bartels AL, de Jong BM, Willemsen AT, Eshuis SA, de Vries JJ, *et al.* Typical cerebral metabolic patterns in neurodegenerative brain diseases. Mov Disord 2010; 25: 2395-2404.

Torta DM, Cauda F. Different functions in the cingulate cortex, a meta-analytic connectivity modeling study. Neuroimage 2011; 56: 2157-2172.

Van Laere KJ, Versijpt J, Koole M, Vandenberghe S, Lahorte P, Lemahieu I, *et al.* Experimental performance assessment of SPM for SPECT neuroactivation studies using a subresolution sandwich phantom design. Neuroimage 2002; 16: 200-216.

Varrone A, Pagani M, Salvatore E, Salmaso D, Sansone V, Amboni M, *et al.* Identification by [99mTc]ECD SPECT of anterior cingulate hypoperfusion in progressive supranuclear palsy, in comparison with Parkinson's disease. Eur J Nucl Med Mol Imaging 2007; 34: 1071-1081.

Varrone A, Pappata S, Caraco C, Soricelli A, Milan G, Quarantelli M, *et al.* Voxel-based comparison of rCBF SPET images in frontotemporal dementia and Alzheimer's disease highlights the involvement of different cortical networks. Eur J Nucl Med Mol Imaging 2002; 29: 1447-1454.

Verhage F. Intelligentie en leeftijd: onderzoek bij Nederlanders van twaalf tot zevenenzeventig jaar [Intelligence and age: Research on Dutch people aged twelve to seventy-seven years old]. Assen: Van Gorcum 1964.

Vogt BA. Pain and emotion interactions in subregions of the cingulate gyrus. Nat Rev Neurosci 2005; 6: 533-544.

Williams GB, Nestor PJ, Hodges JR. Neural correlates of semantic and behavioural deficits in frontotemporal dementia. Neuroimage 2005; 24: 1042-1051.

Yu C, Zhou Y, Liu Y, Jiang T, Dong H, Zhang Y, *et al.* Functional segregation of the human cingulate cortex is confirmed by functional connectivity based neuroanatomical parcellation. Neuroimage 2011; 54: 2571-2581.

Chapter 4

General discussion

Dementia refers to a clinical syndrome defined by the deterioration of cognitive functions and accompanying impairment of activities of daily living. This syndrome can be caused by a number of brain diseases, of which Alzheimer's disease (AD) is the most common cause, followed by vascular dementia at old age and frontotemporal dementia (FTD) at young onset.

To diagnose the specific brain diseases underlying dementia early in the disease course becomes increasingly important with the development of new treatment strategies directed at specific pathological substrates, as well as increasing knowledge regarding the prognosis of dementia subtypes. Early diagnosis or differentiation is hampered however, first by a lack of knowledge regarding the effects of pathological subtypes either in isolation or co-existing with other pathological subtypes, and second, by the fact that disorders causing dementia may overlap in clinical and cognitive symptoms. Functional and advanced structural neuroimaging techniques enable us to address these issues in prodromal and early stages of dementia. The specific aim of this thesis was twofold:

1. To study the effects of cerebral small vessel disease on brain functioning and structural connectivity in mild cognitive impairment, using functional MRI and diffusion tensor imaging.

2. To study patterns of impaired brain perfusion underlying cognitive symptoms in early onset AD, FTD and progressive supranuclear palsy, using perfusion single-photon emission computed tomography.

Functional and structural neuroimaging in mild cognitive impairment

Cerebral small vessel disease in mild cognitive impairment

Mild cognitive impairment (MCI) is a clinical concept that defines a transitional stage between normal aging and dementia. MCI patients are characterized by cognitive impairment and have an increased risk of dementia, with estimated yearly progression rates between 10 and 15 percent (DeCarli, 2003a; Petersen, 2004). Although MCI is a heterogeneous condition in terms of underlying etiology, presentation and prognosis, clinically most MCI patients present with an episodic memory disorder, either isolated or as the foremost presenting feature (Tabert et al., 2006). In those patients, AD is the main clinical outcome, and memory disorders are related to AD neuropathological changes affecting the medial temporal lobe (Petersen et al., 2006). In older people, AD pathology is often accompanied by cerebrovascular pathology, in particular cerebral small vessel disease (CSVD) (Jellinger and Attems, 2005; Petersen et al., 2006). CSVD is a fairly common

condition in the elderly population, and is known to affect the microvessels supplying the white matter and subcortical grey matter regions. Although it is hard to directly visualize cerebrovascular pathology in the smallest vessels in vivo, parenchymal lesions caused by small vessel damage can be ascertained on MRI as white matter hyperintensities (WMH) and lacunar infarcts (Pantoni, 2010). The presence of CSVD is traditionally associated with frontal lobe functional interference resulting in executive dysfunction and impaired processing speed (Cummings, 1993; Pugh and Lipsitz, 2002). More recently, CSVD has been related to impairment in other cognitive domains, including episodic memory (Luchsinger et al., 2009; Nordahl et al., 2005; Villeneuve et al., 2011). This is reflected in recently proposed criteria for prodromal vascular cognitive impairment (VCI), i.e. vascular MCI, in which amnestic subtypes are considered (Gorelick et al., 2011). The mechanisms through which CSVD contributes to cognitive symptoms at the MCI stage however, are still a matter of debate.

Early alterations in brain functioning and white matter structure can be studied by means of multimodal neuroimaging techniques like functional MRI (fMRI) and diffusion tensor imaging (DTI). fMRI is a technique that measures brain function by detecting temporally related changes in the blood flow in active brain regions. Standardized cognitive performance during fMRI enables us to study and localize transient brain activation directly resulting from a specific cognitive event. DTI is an advanced structural MRI technique that can reveal changes in white matter microstructure and allows mapping of the brain's structural connectivity (Hagmann et al., 2007). These advanced MRI techniques may aid in unraveling the mechanisms and role of CSVD in MCI.

Criteria for MCI and VCI

The use of a construct that classifies subjects in an intermediate stage between normal aging and dementia has some important benefits, as it offers the opportunity for an early diagnosis, may guide research into the development of early pathophysiological changes, and aids the identification of at-risk subjects for future disease modifying treatments. MCI is the most used prodromal dementia concept nowadays (Petersen, 2004). While originally developed to define prodromal AD cases, the concept was broadened to identify the prestages of other dementia subtypes as well. Vascular cognitive impairment (VCI) includes the prodromal stage of vascular dementia, as this umbrella concept applies to all cognitive impairment with a presumed vascular cause (Hachinski, 1994). Recently, new criteria have been developed for prodromal AD, 'MCI due to AD' (Albert et al., 2011), and prodromal vascular dementia, vascular MCI (VaMCI) (Gorelick et al., 2011). In **Chapter 2.1** we show that these proposed criteria are not easy to operationalize in a clinical cohort. Furthermore, by aiming to be mutually exclusive, the criteria for prodromal AD and VaD

disregard the fact that cerebrovascular and Alzheimer pathology may co-exist in patients with cognitive impairment who do not fulfill the criteria for dementia (Jellinger, 2006; Jellinger and Attems, 2005). Distinguishing this mixed prodromal group from the pure cerebrovascular or pure neurodegenerative causes of cognitive impairment aids clinical research regarding the prognosis and proper treatment of these patients, as well as research into the influence of different pathology types on cognitive and clinical symptoms and underlying brain structure and function. The latter was one of the major goals of this thesis. In the studies regarding MCI described in this thesis, we selected patients on the basis of the commonly used criteria of Petersen (2004), and subdivided MCI patients into those with and without CSVD on the basis of T1 and T2 weighted MRI findings.

Functional and structural neuroimaging in MCI: the effects of CSVD

To investigate the mechanisms through which CSVD affects cognitive functioning in MCI, we used task based fMRI and DTI. In **Chapter 2.2** and **Chapter 2.3** we describe the results of task based fMRI studies. Although MCI patients with and without CSVD had a similar neuropsychological profile with prominent episodic memory deficits, they were shown to differ with respect to underlying brain (de)activation patterns. The extent of vascular burden in MCI patients with CSVD was found to be inversely related to hippocampal activation during episodic memory encoding, even after adjusting for hippocampal volume (**Chapter 2.2**). This finding supports the idea that CSVD interference is not restricted to the frontal lobe. In **Chapter 2.3**, discussing the results of a working memory related fMRI task, this idea was taken a step further, as we found that MCI patients with CSVD had impaired deactivation within posterior brain regions known to be involved in the default mode network (DMN). The DMN includes a number of interconnected brain regions, active during rest and actively suppressed during cognitive functioning. Deactivation failure and diminished functional connectivity between these regions were previously shown in MCI, AD and FTD (Hafkemeijer et al., 2012; Zhou et al., 2010), and postulated to underlie cognitive deterioration in these disorders. Since network functioning is thought to be highly dependent on intact white matter connections (Damoiseaux and Greicius, 2009; Teipel et al., 2010), we hypothesized that the observed changes in neural functioning in MCI patients with CSVD can, at least partly, be attributed to cerebrovascular induced white matter macrostructural and microstructural changes. In **Chapter 2.4** we examined the role of CSVD in microstructural damage within both the whole brain normal appearing white matter as well as normal appearing white matter fiber tracts interconnecting remote DMN related regions. MCI patients with CSVD had widespread white matter microstructural damage, while in MCI patients without CSVD, microstructural damage was confined to a small region within the right perforant path, a fiber tract connecting the entorhinal cortex and the hippocampus. Focusing on DMN related fiber tracts, the cingulum along

the hippocampal gyrus, consistently showed microstructural damage in both MCI patients with and without CSVD, which was related to both ipsilateral hippocampal volume and vascular burden in the full cohort of MCI patients. Other fiber tracts subserving DMN structural connectivity, like the cingulum along the cingulate cortex and the superior longitudinal fasciculus were primarily affected in MCI patients with CSVD.

Summarizing our multimodal neuroimaging findings, CSVD in MCI affects the white matter far more extensively than can be determined on conventional MRI, and moreover influences neural functioning during cognitive performance. We postulate that the mechanism through which CSVD affects cognition, or contributes to cognitive deterioration in MCI is neural network interference, as a consequence of damaging the interconnecting fiber tracts. The fact that the extent of CSVD was negatively related to hippocampal activation as well as the microstructural white matter integrity of the cingulum along the hippocampus, supports this view. Furthermore, given the fact that the hippocampus in MCI patients with CSVD was atrophied, our findings also emphasize the probable contribution of multiple pathology types, i.e. Alzheimer and cerebrovascular pathology, in the cognitive symptoms in MCI.

Functional neuroimaging in neurodegenerative disorders

After AD, FTD is the most common subtype of presenile dementia. The clinical hallmark of AD is progressive episodic memory impairment, associated with early neuropathological processes affecting memory related structures (Braak and Braak, 1991). FTD can be clinically characterized by behavioral changes, language and executive dysfunctioning, related to neurodegeneration of the frontal and temporal lobes. Neuropathological changes in these regions include tau-positive inclusions, associated with *microtubule associated protein tau* (*MAPT*) gene mutations; or ubiquitin-positive and TDP-43 positive inclusions (frontotemporal lober degeneration-TDP, FTLD-TDP), associated with *progranulin* (*GRN*) gene mutation. Clinically, both *MAPT* and *GRN* genetic forms can result in behavioral variant FTD (bvFTD), the most common subtype of FTD (Seelaar et al., 2011). Despite clear post-mortem differentiation between bvFTD and other neurodegenerative conditions, early discrimination during life is hampered by the fact that clinical and cognitive symptomatology in bvFTD patients can overlap with AD and progressive supranuclear palsy (PSP).

Perfusion single-photon emission computed tomography (SPECT), using the tracer technetium-99m-labeled hexamethylpropyleneamine oxime (^{99m}Tc-HMPAO) is a well established diagnostic technique, enabling us to assess cerebral blood flow, reflecting the level of regional brain metabolism (Weih et al., 2011). Less cerebral perfusion, or

hypoperfusion, is linked to functional degradation. Quantitative comparisons of perfusion patterns between patient groups, as well as the coupling of cognitive symptoms to the degree of perfusion can aid unraveling the functional substrates of overlapping symptomatology in FTD, AD and PSP.

Perfusion SPECT: memory in FTD

Episodic memory impairment, the clinical hallmark of AD, may also occur in bvFTD, complicating an accurate clinical diagnosis. Our aim in **Chapter 3.1** was to establish the underlying functional neural substrate of episodic memory impairment in bvFTD. For this purpose, we used quantitative comparisons of ^{99m}Tc-HMPAO SPECT brain perfusion patterns in bvFTD patients with and without episodic memory impairment. We observed reduced perfusion in the right temporal lobe, including the parahippocampal gyrus, the fusiform gyrus and middle temporal gyrus in bvFTD patients with memory impairment. The degree of hypoperfusion within these regions was related to a clinical measure of memory impairment. Early onset AD patients showed the typical pattern of posterior hypoperfusion (Kemp et al., 2003). An interesting issue is whether the perfusion differences in bvFTD patients with and without memory impairment reflect disease progression or topographical heterogeneity in bvFTD (Whitwell et al., 2009). As other studies have shown that the MTL is affected at a later disease stage in bvFTD, and thereby the right hemisphere and right hippocampus exceed left hemispheric involvement in terms of atrophy (Seeley et al., 2008), we think our findings are a reflection of disease progression. However, topographical heterogeneity was observed in **Chapter 3.2** in which we subdivided FTD cases on the basis of genetical defect, i.e. familial FTLD-TDP and *MAPT* mutations. Familial FTLD-TDP patients, including 6 patients with known and 13 patients with an unknown genetic defect, had less perfusion in the parietal lobe, including the precuneus and precentral gyrus when compared with *MAPT* patients, clinically accompanied by memory complaints at presentation. *MAPT* patients showed left temporal and mediofrontal hypoperfusion on SPECT when compared with familial FTLD-TDP and clinically presented with naming deficits and obsessive-compulsive behavior. Whether the cause of memory impairment in (bv)FTD is the consequence of topographical heterogeneity, perhaps induced by genetical determined pathological differences, or is caused by disease progression, is an issue yet to be resolved. We therefore suggest future longitudinal studies by means of functional neuroimaging and neuropsychological assessment in a large cohort of bvFTD.

Perfusion SPECT patterns underlying cognitive impairment in PSP and FTD

In PSP the pathological changes consist of neuronal and glial tau positive aggregates predominantly found in basal ganglia, associated clinically with frequent falls, vertical

gaze palsy and pseudobulbar dysarthria (Kaat et al., 2011). Cognitive symptoms however, can be the foremost presenting manifestation in PSP and are similar to those observed in FTD. In **Chapter 3.3** we examined the contribution of cortical functional involvement in cognition in PSP by means of ^{99m}Tc-HMPAO perfusion SPECT, and furthermore compared the relationship between regional cortical perfusion and cognition in PSP to that in FTD-tau. We found prominent involvement of the anterior cingulate cortex and midcingulate cortex in PSP patients, of which the posterior part of the midcingulate cortex correlated with the extent of executive dysfunction. Within a region of the anterior cingulate cortex that overlapped in terms of relative hypoperfusion in PSP and FTD patients, we found a similar relationship between hypoperfusion and cognitive dysfunction, suggesting similar brain regions underlie cognitive deficits in both these neurodegenerative conditions.

Concluding, we found that while the underlying disease or pathology type can differ, clinical and cognitive symptoms may overlap as a consequence of similarities in affected brain regions.

Scientific and clinical implications

The studies in this thesis on the effects of CSVD in MCI emphasize a role of cerebrovascular changes in MCI, and may have implications for clinical practice and future research. From a clinical perspective, the opportunity arises to influence cognition and perhaps even disease progression in MCI patients with a prominent CSVD component by aggressive management of risk factors for CSVD (DeCarli, 2003b). Furthermore, the finding of similar cognitive profiles but large white matter microstructural integrity differences in MCI patients with and without CSVD, suggests that we need to go beyond MCI cognitive subtyping and take neuroimaging findings into account when making inferences on MCI etiology. It will be very informative to study MCI subtypes with and without the microstructural white matter changes longitudinally in order to determine the significance of such differences for the prognosis of cognitive dysfunction. Meanwhile, the fMRI and DTI differences in MCI patients with CSVD compared to those without CSVD emphasize the fact that future research regarding structural and functional neuroimaging in MCI cannot dismiss the significance of CSVD. A final important issue concerns the observed widespread structural DTI changes in the presence of less extensive functional changes. While the use of different MRI techniques may influence this finding, it does refute the generally held idea that functional changes always precede structural changes in early stages of disease (Masdeu et al., 2012). Rather, it suggests that structural-functional imaging sensitivity in neurodegenerative conditions should be reconsidered.

In our studies described in Chapter 3, we found that overlapping symptoms in AD, FTD and PSP can be explained by similarities in functional substrates. Clinically, these findings suggest that the clinician should be aware of atypical presentation of neurodegenerative disorders and furthermore emphasize the use of functional and structural neuroimaging and neurochemical biomarkers in the diagnosis. A good example is the use of the Pittsburg Compound-B (PIB) tracer in positron emission tomography (PET) (Klunk et al., 2004), which enables us to examine amyloid load in the brain, and subsequently aids in the differentiation between FTD and AD.

Methodological considerations

The studies regarding MCI patients described in this thesis are part of a prospective study, but have a cross-sectional design, which has implications for causal inferences. A specific drawback of cross-sectional research in MCI patients is that the prognosis in individual patients is uncertain. Although we know that the majority of MCI patients will eventually develop AD (Busse et al., 2006; Fischer et al., 2007; Tabert et al., 2006), some patients may revert back to normal in time (Ritchie, 2004). Including such 'normal' subjects may lead to an underestimation of true associations and hence impact inferences regarding underlying pathophysiology and related structural and functional patterns, as it may have led to an underestimation of results. The retrospective design of SPECT studies described in this thesis enabled us to include patients with a definite diagnosis, either by neuropathological confirmation or genetical testing. Reflecting the progression of research in FTD, very recently, a hexanucleotide repeat expansion in the *C9orf72* gene has been identified as a major cause of both sporadic and familial FTD and amyotrophic lateral sclerosis (Simon-Sanchez et al., 2011). Some patients from the group of familiar FTD in Chapter 3.2 had this *C9orf72* defect.

As mentioned before, the concept of MCI has some important benefits, but it also bears the disadvantage of applying to a heterogeneous clinical or research population. One of the causes for this heterogeneity is the fact that the most commonly used criteria for MCI are developed to identify all prodromal dementia types (Petersen, 2004). The source of MCI patients may also contribute to heterogeneity, as patients referred to outpatient clinics constitute a different group than patients identified in a population cohort (Petersen, 2010). Finally, while MCI is used as a dichotomous construct, cognitive impairment in most dementia syndromes develops gradually over time and as a consequence MCI can include both patients with an early as well as a more advanced – nearly dementia – disease state. This is an important issue in functional MRI as the degree of task based fMRI activation and resting state functional connectivity may be related to clinical disease progression in MCI patients (Celone et al., 2006; Clement and Belleville, 2010). New criteria for 'MCI due

to AD' aim to minimize the heterogeneity in MCI by using biomarkers reflecting amyloid β or neuronal injury, to come to an earlier and more accurate identification of specifically AD etiology in MCI patients (Albert et al., 2011). Longitudinal research regarding 'MCI due to AD' will increase our knowledge of the prognostic value of these biomarkers. It has to be kept in mind however, that AD pathology often co-occurs with other pathology types, and that therefore research regarding MCI patients that do not meet the criteria for 'MCI due to AD' will remain of utmost importance. Information regarding amyloid based biomarkers would have aided the studies concerning MCI in this thesis, for example when making inferences regarding the etiology in MCI patients without CSVD, and the lack of this information is an important shortcoming of our studies.

Task based fMRI has the advantage of enabling us to study the brain 'under stress' and offers us elaborate analysis possibilities. Disadvantages of the technique are intra-individual differences in brain (de)activation, moderate test-retest reliability (Hockey and Geffen, 2004), and the difficulty to distinguish between the effects of a disordered state and poor task performance (Bullmore, 2012). Controlling for task performance was one of the reasons that in the two task based fMRI studies described in this thesis we addressed slightly different sets of MCI patients. Some task designs may not be feasible in this population, or in case of further cognitive decline, within the dementia population at large. Task based fMRI is therefore suitable to make inferences on neural functioning under stress in a group of participants able to perform a cognitive task, but the above mentioned drawbacks make it that this technique is not useful in clinical practice. Within the past decade, the field of fMRI made a general shift from activation paradigms to connectivity paradigms, using resting state fMRI. This technique is optimized to detect interregional temporal correlations of BOLD signal fluctuations, thought to represent neural networks. From both a theoretical and practical point of view, resting state fMRI has some advantages over task based fMRI. Theoretically, neurodegenerative brain disorders are expected to affect large scale networks, and network phenotypes are better addressed by connectivity analysis rather than the analysis of local activity. The practical advantage of the connectivity paradigm is that it is independent of task design and task performance and therefore more suitable to apply in a patient population and better equipped to compare across studies. Although results of multiple studies have emphasized reasonable replicability of this technique within a patient population (Van Dijk et al., 2010), the technique is not useful yet at an individual level and consequently in clinical practice. Inherent to the methodology of fMRI, neural activity is measured indirectly, by assessing its effects on the local vasculature, a process referred to as neurovascular coupling. We therefore need to make a final comment concerning the use of fMRI, either task based or resting state fMRI in subjects with vascular risk factors known to affect cortical

vasoreactivity (Glodzik et al., 2011). This may lead to differences in BOLD response, and will definitely have be addressed by future research, as it could be that patients with CSVD have a reduced BOLD fMRI response, similar to that observed in stroke patients (Pineiro et al., 2002; Rossini et al., 2004).

By the use of the radioactive ^{99m}Tc-HMPAO tracer, SPECT imaging allows us to assess cerebral blood flow and thereby brain metabolism. SPECT imaging has to compete with fludeoxyglucose (FDG) PET scanning, which more directly reflects regional glucose metabolism. While SPECT imaging is widely available and less expensive, it is limited by poorer spatial resolution, and has lower sensitivity and specificity regarding early stages of disease than FDG-PET imaging. An alternative technique measuring cerebral blood flow is arterial spin labeling (ASL), a relatively new MRI technique. Though comparative studies still have to determine its value in clinical settings compared to either SPECT or PET imaging, this perfusion MRI technique is promising as it is far lower in costs as well as far more time efficient and non invasive. PET imaging on the other hand has the advantage that lately several tracers, among which PIB as most effective tracer (Klunk et al., 2004), have been developed that make it possible to identify amyloid beta load affecting the brain in vivo. While SPECT functional neuroimaging may be inferior to these new developments in functional neuroimaging (Weih et al., 2011), the advantage of SPECT functional neuroimaging in the studies described in this thesis was that we could use our SPECT data retrospectively and subsequently at the time of analysis, we had information regarding neuropathological underlying substrates in our patient groups.

fMRI and SPECT data described in this thesis were analyzed using statistical parametric mapping (SPM). The principle of SPM is to calculate a statistic, usually on the basis of the general linear model, for each independent voxel within a particular region. An important issue when using this approach is that each analysis involves as many simultaneous significance tests as there are voxels within the selected region, creating a massive multiple comparisons/testing problem. To account for this problem, and thereby reduce Type I errors, or false-positive findings, we need to make use of appropriate correction and thresholding. A standard approach within SPM is the use of family wise error (FWE) correction for multiple comparisons, a threshold correction based on Gaussian random field theory (Worsley et al., 2004), intended to result in almost no Type I errors. While this type of thresholding is preferable to avoid Type I errors as much as possible, in practice, the use of this FWE corrected thresholding may sometimes be too conservative, for example in case of low degrees of freedom. A threshold of $p<0.001$ applied at the voxel level, without correction for multiple comparisons, with a minimum cluster size of -commonly- 20 voxels is an alternative, though this threshold is more lenient towards

Type I errors. In this thesis the type of threshold correction was variable across studies, and we sometimes made use of the relatively more lenient threshold. The first reason for using the more lenient threshold was the fact that in small patient groups statistical power was not sufficient for stringent thresholding. In particular the SPECT studies described in Chapter 3.1, 3.2 and 3.3 involved small patient groups. The main reason for the small size of these patient groups was the retrospective nature of the SPECT studies in combination with the stringent inclusion criteria we applied. Patients were included if they had either a neuropathological diagnosis, positive DNA-screening or extensive follow up and furthermore available neuropsychological assessment and ^{99m}Tc-HMPAO perfusion SPECT scans were prerequisites. A second reason for the use of a more lenient threshold was the subtlety of the studied effects. For example, in Chapter 2.2 and 2.3 we compared two MCI patient groups and a control group on the basis of brain activation patterns during task-based fMRI. While brain activation patterns in AD patients are found to clearly differ from healthy age matched controls, results in MCI patients are found to be more variable and less extensive (Celone et al., 2006; Clement and Belleville, 2010). Moreover, when comparing two MCI patient groups with a quite similar clinical phenotype, we expected to find only subtle effects on fMRI. The final reason for the use of a more lenient threshold was to identify regions with subtle between group differences reflecting functional degradation as a starting point for post hoc ROI analyses, which was the case for example in Chapter 2.2. We acknowledge that using a more lenient threshold bears the risk of reporting false-positive findings, and therefore some of our results have to be interpreted with caution and furthermore will have to be confirmed within larger patient cohorts. On the other hand, Type II errors, i.e. failing to pick up true effects, may be an important drawback of focusing solely on results obtained with stringent FWE corrected thresholds in exploratory functional neuroimaging studies like the studies described in this thesis.

Future research

Advanced neuroimaging techniques in dementia research

Understanding the pathophysiological changes in AD, VaD and FTD will aid the diagnostic process and will provide clues for the development of pharmacological interventions. These changes can be studied by using advanced functional and structural neuroimaging techniques, although a combined approach of imaging modalities in future research may be necessary to understand the complete process. A good example is a multi-modal imaging approach to AD, in which functional connectivity of the DMN was found to be decreased in the same brain regions targeted by grey matter atrophy and deposition of amyloid beta (Buckner et al., 2005). The development of specific PET ligands for other pathological substrates than amyloid beta (tau, TDP43, alfa-synuclein) would definitely contribute in research regarding the effects of neuropathology on functional and structural

damage in FTD or other types of neurodegeneration like lewy body dementia. However, it is important to note that pathological subtypes often co-exist, in particular in the elderly. The effects of co-existing pathology on structural and functional brain impairment and subsequently clinical and cognitive symptomatology should therefore be a focus of future research as well.

Regarding CSVD involvement in MCI, it has yet to be elucidated whether, -as we postulate-, the presence of CSVD affects neural functioning by damaging the interconnecting white matter tracts underlying neural networks. The relationship between structure and function may not be straightforward, as indirect connections between brain regions are known to account for variance in the functional connectivity explained by direct structural connectivity. This is one of the reasons that we suggest graph theory based analysis of the brain's structural and functional networks regarding the role of CSVD in network functioning. Using graph theory, a network is defined as a set of nodes that represent important brain regions, linked by edges representing physical connections (Bullmore and Sporns, 2009). The path length refers to the minimum number of edges that must be traveled to get from one node to the other, and the most effective networks are those with a short path length. Examining the effects of macro and microstructural white matter damage and lacunar infarcts on so-called small-world architecture would give us insight into the role of CSVD in network functioning in MCI.

Advanced neuroimaging techniques in clinical practice

One of the primary aims of future research should be the clinical applicability of advanced structural and functional neuroimaging techniques in dementia, as these techniques have the potential to identify etiology and could help predict prognosis in prodromal and advanced disease stages. Standardization of clinical and research neuroimaging acquisition procedures and analysis techniques would aid this development by enabling the set up of large normative databases for multimodal imaging techniques. fMRI is a good example of a technique with high potential as biomarker used extensively in a research setting, yet with very low clinical impact. Greater clinical engagement of fMRI could be achieved by the establishment of advanced image analysis techniques that make fMRI accessible and comprehendible to clinicians. While the use of task based fMRI can be problematic as biomarker through its dependence on task performance, connectivity paradigms, and more specifically the identification of dementia subtype phenotypical network deterioration, might be useful as a biomarker. Network deterioration could be examined at an individual level by assessing phenotypical network integrity relative to more robust networks, such as the motor network, thereby accounting for intra-individual differences in BOLD fMRI response. Another potential clinical application of

fMRI is the detection of individual pharmacological effects, both on regional and network functioning. This becomes even more interesting with the recent introduction of high field 7 Tesla MRI, which increases the spatial resolution of both structural and fMRI findings considerably. Regarding advanced structural neuroimaging, DTI has shown to be far more sensitive than convential T2 FLAIR MRI, for the detection of white matter damage, however has yet to be adapted to be suitable for clinical practice. This technique could have clinical value as it offers the opportunity to identify the extent of effects of CSVD at a microstructural level, and as microstructural changes are thought to be reversible (Han et al., 2007; Maillard et al., 2012), may serve as a proxy for clinical outcome of vascular treatment effects. Research on PET tracers directed at pathological substrates underlying dementia can potentially make it possible to determine neuropathology in vivo rather than post mortem, which would obviously be of great clinical value. However, this has to be preceded by longitudinal research regarding PIB-PET related ambiguities, as amyloid deposition was found histologically detectable prior to a 'positive' PIB-PET signal, and furthermore, the ambiguous finding of healthy elderly presenting with PIB-PET positive findings and Alzheimer patients with PIB-PET negative findings, will still have to be addressed by future research.

The above described advanced neuroimaging techniques by themselves may not have sufficient sensitivity and specificity to be used as diagnostic, prognostic or biomarker in dementia. However, multi-modal imaging techniques addressing functional, structural and neuropathological substrates in dementia may be a way to enhance the clinical applicability. The recent introduction of PET-MRI scanners promotes this, as well as it promotes multi-modal neuroimaging research regarding the effects of pathological changes in structural and functional integrity in diseases underlying dementia.

REFERENCES

Albert MS, DeKosky ST, Dickson D, Dubois B, Feldman HH, Fox NC, *et al.* The diagnosis of mild cognitive impairment due to Alzheimer's disease: recommendations from the National Institute on Aging-Alzheimer's Association workgroups on diagnostic guidelines for Alzheimer's disease. Alzheimers Dement 2011; 7: 270-279.

Braak H, Braak E. Neuropathological stageing of Alzheimer-related changes. Acta Neuropathol 1991; 82: 239-259.

Buckner RL, Snyder AZ, Shannon BJ, LaRossa G, Sachs R, Fotenos AF, *et al.* Molecular, structural, and functional characterization of Alzheimer's disease: evidence for a relationship between default activity, amyloid, and memory. J Neurosci 2005; 25: 7709-7717.

Bullmore E. The future of functional MRI in clinical medicine. Neuroimage 2012; 62: 1267-1271.

Bullmore E, Sporns O. Complex brain networks: graph theoretical analysis of structural and functional systems. Nat Rev Neurosci 2009; 10: 186-198.

Busse A, Hensel A, Guhne U, Angermeyer MC, Riedel-Heller SG. Mild cognitive impairment: long-term course of four clinical subtypes. Neurology 2006; 67: 2176-2185.

Celone KA, Calhoun VD, Dickerson BC, Atri A, Chua EF, Miller SL, *et al.* Alterations in memory networks in mild cognitive impairment and Alzheimer's disease: an independent component analysis. J Neurosci 2006; 26: 10222-10231.

Clement F, Belleville S. Compensation and disease severity on the memory-related activations in mild cognitive impairment. Biol Psychiatry 2010; 68: 894-902.

Cummings JL. Frontal-subcortical circuits and human behavior. Arch Neurol 1993; 50: 873-880.

Damoiseaux JS, Greicius MD. Greater than the sum of its parts: a review of studies combining structural connectivity and resting-state functional connectivity. Brain Struct Funct 2009; 213: 525-533.

DeCarli C. Mild cognitive impairment: prevalence, prognosis, aetiology, and treatment. Lancet Neurol 2003a; 2: 15-21.

DeCarli C. Prevention of white-matter lesions through control of cerebrovascular risk factors. Int Psychogeriatr 2003b; 15 Suppl 1: 147-151.

Fischer P, Jungwirth S, Zehetmayer S, Weissgram S, Hoenigschnabl S, Gelpi E, *et al.* Conversion from subtypes of mild cognitive impairment to Alzheimer dementia. Neurology 2007; 68: 288-291.

Glodzik L, Rusinek H, Brys M, Tsui WH, Switalski R, Mosconi L, *et al.* Framingham cardiovascular risk profile correlates with impaired hippocampal and cortical vasoreactivity to hypercapnia. J Cereb Blood Flow Metab 2011; 31: 671-679.

Gorelick PB, Scuteri A, Black SE, Decarli C, Greenberg SM, Iadecola C, *et al.* Vascular contributions to cognitive impairment and dementia: a statement for healthcare professionals from the american heart association/american stroke association. Stroke 2011; 42: 2672-2713.

Hachinski V. Vascular dementia: a radical redefinition. Dementia 1994; 5: 130-132.

Hafkemeijer A, Van der Grond J, Rombouts SARB. Imaging the default mode network in aging and dementia. Biochim Biophys Acta 2012; 1822: 431-441.

Hagmann P, Kurant M, Gigandet X, Thiran P, Wedeen VJ, Meuli R, *et al.* Mapping human whole-brain structural networks with diffusion MRI. PLoS One 2007; 2: e597.

Han BS, Kim SH, Kim OL, Cho SH, Kim YH, Jang SH. Recovery of corticospinal tract with diffuse axonal injury: a diffusion tensor image study. NeuroRehabilitation 2007; 22: 151-155.

Hockey A, Geffen G. The concurrent validity and test-retest reliability of a visuospatial working memory task. Intelligence 2004; 32: 591-605.

Jellinger KA. Clinicopathological analysis of dementia disorders in the elderly--an update. J Alzheimers Dis 2006; 9: 61-70.

Jellinger KA, Attems J. Prevalence and pathogenic role of cerebrovascular lesions in Alzheimer disease. J Neurol Sci 2005; 229-230: 37-41.

Kaat DL, Chiu WZ, Boon AJ, van Swieten JC. Recent advances in progressive supranuclear palsy: a review. Curr Alzheimer Res 2011; 8: 295-302.

Kemp PM, Holmes C, Hoffmann SM, Bolt L, Holmes R, Rowden J, *et al.* Alzheimer's disease: differences in technetium-99m HMPAO SPECT scan findings between early onset and late onset dementia. J Neurol Neurosurg Psychiatry 2003; 74: 715-719.

Klunk WE, Engler H, Nordberg A, Wang Y, Blomqvist G, Holt DP, *et al.* Imaging brain amyloid in Alzheimer's disease with Pittsburgh Compound-B. Ann Neurol 2004; 55: 306-319.

Luchsinger JA, Brickman AM, Reitz C, Cho SJ, Schupf N, Manly JJ, *et al.* Subclinical cerebrovascular disease in mild cognitive impairment. Neurology 2009; 73: 450-456.

Maillard P, Carmichael O, Harvey D, Fletcher E, Reed B, Mungas D, *et al.* FLAIR and Diffusion MRI Signals Are Independent Predictors of White Matter Hyperintensities. AJNR Am J Neuroradiol 2012.

Masdeu JC, Kreisl WC, Berman KF. The neurobiology of Alzheimer disease defined by neuroimaging. Curr Opin Neurol 2012; 25: 410-420.

Nordahl CW, Ranganath C, Yonelinas AP, DeCarli C, Reed BR, Jagust WJ. Different mechanisms of episodic memory failure in mild cognitive impairment. Neuropsychologia 2005; 43: 1688-1697.

Pantoni L. Cerebral small vessel disease: from pathogenesis and clinical characteristics to therapeutic challenges. Lancet Neurol 2010; 9: 689-701.

Petersen RC. Mild cognitive impairment as a diagnostic entity. J Intern Med 2004; 256: 183-194.

Petersen RC. Does the source of subjects matter?: absolutely! Neurology 2010; 74: 1754-1755.

Petersen RC, Parisi JE, Dickson DW, Johnson KA, Knopman DS, Boeve BF, *et al.* Neuropathologic features of amnestic mild cognitive impairment. Arch Neurol 2006; 63: 665-672.

Pineiro R, Pendlebury S, Johansen-Berg H, Matthews PM. Altered hemodynamic responses in patients after subcortical stroke measured by functional MRI. Stroke 2002; 33: 103-109.

Pugh KG, Lipsitz LA. The microvascular frontal-subcortical syndrome of aging. Neurobiol Aging 2002; 23: 421-431.

Ritchie K. Mild cognitive impairment: an epidemiological perspective. Dialogues Clin Neurosci 2004; 6: 401-408.

Rossini PM, Altamura C, Ferretti A, Vernieri F, Zappasodi F, Caulo M, *et al.* Does cerebrovascular disease affect the coupling between neuronal activity and local haemodynamics? Brain 2004; 127: 99-110.

Seelaar H, Rohrer JD, Pijnenburg YA, Fox NC, van Swieten JC. Clinical, genetic and pathological heterogeneity of frontotemporal dementia: a review. J Neurol Neurosurg Psychiatry 2011; 82: 476-486.

Seeley WW, Crawford R, Rascovsky K, Kramer JH, Weiner M, Miller BL, *et al.* Frontal paralimbic network atrophy in very mild behavioral variant frontotemporal dementia. Arch Neurol 2008; 65: 249-255.

Seeley WW, Crawford RK, Zhou J, Miller BL, Greicius MD. Neurodegenerative diseases target large-scale human brain networks. Neuron 2009; 62: 42-52.

Simon-Sanchez J, Dopper EG, Cohn-Hokke PE, Hukema RK, Nicolau N, *et al.* The clinical and pathological phenotype of C9ORF72 hexanucleotide repeat expansions. Brain 2012; 135: 723-735.

Tabert MH, Manly JJ, Liu X, Pelton GH, Rosenblum S, Jacobs M, *et al.* Neuropsychological prediction of conversion to Alzheimer disease in patients with mild cognitive impairment. Arch Gen Psychiatry 2006; 63: 916-924.

Teipel SJ, Bokde AL, Meindl T, Amaro E, Jr., Soldner J, Reiser MF, *et al.* White matter microstructure underlying default mode network connectivity in the human brain. Neuroimage 2010; 49: 2021-2032.

Van Dijk KR, Hedden T, Venkataraman A, Evans KC, Lazar SW, Buckner RL. Intrinsic functional connectivity as a tool for human connectomics: theory, properties, and optimization. J Neurophysiol 2010; 103: 297-321.

Villeneuve S, Massoud F, Bocti C, Gauthier S, Belleville S. The nature of episodic memory deficits in MCI with and without vascular burden. Neuropsychologia 2011; 49: 3027-3035.

Weih M, Degirmenci U, Kreil S, Suttner G, Schmidt D, Kornhuber J, *et al.* Nuclear medicine diagnostic techniques in the era of pathophysiology-based CSF biomarkers for Alzheimer's disease. J Alzheimers Dis 2011; 26 Suppl 3: 97-103.

Whitwell JL, Przybelski SA, Weigand SD, Ivnik RJ, Vemuri P, Gunter JL, *et al.* Distinct anatomical subtypes of the behavioural variant of frontotemporal dementia: a cluster analysis study. Brain 2009; 132: 2932-2946.

Worsley KJ, Taylor JE, Tomaiuolo F, Lerch J. Unified univeriate and multivariate random field theory. Neuroimage 2004; 23:189-195.

Zhou J, Greicius MD, Gennatas ED, Growdon ME, Jang JY, Rabinovici GD, *et al.* Divergent network connectivity changes in behavioural variant frontotemporal dementia and Alzheimer's disease. Brain 2010; 133: 1352-1367.

Chapter 5

Summary/Samenvatting

SUMMARY

Dementia refers to a clinical syndrome of cognitive deterioration and difficulty in the performance of activities of daily living. The most common cause of dementia is Alzheimer's disease (AD), followed by vascular dementia (VaD) at old age and frontotemporal dementia (FTD) at young onset. Most dementia subtypes show a gradual decline in clinical and cognitive symptomatology, which enables us to identify subjects in a prodromal stage of dementia, referred to as mild cognitive impairment (MCI). MCI is characterized by cognitive deficits yet without interference with daily living. As functional neuroimaging techniques provide a means to investigate (early) alterations in brain functioning, these techniques can aid research regarding dementia subtypes and prodromal dementia stages, as discussed in **Chapter 1**, the introduction to the thesis.

In this thesis we made use of different neuroimaging techniques. A first technique is functional MRI (fMRI). This technique enables us to measure brain function by detecting temporally related changes in the blood flow in active brain regions. When using standardized cognitive performance during fMRI scanning, we can study and localize brain activation directly resulting from a specific cognitive event. An advanced structural MRI technique used in the present thesis is diffusion tensor imaging (DTI), a technique that can reveal changes in the white matter's microstructure. Perfusion single-photon emission computed tomography (SPECT), is a well established diagnostic technique, enabling us to assess cerebral blood flow, reflecting the level of regional brain metabolism. Less cerebral perfusion, or hypoperfusion, is linked to functional degradation. Quantitative comparisons of activation, white matter integrity and regional blood flow were used to unravel our specific research questions.

The focus of this thesis was twofold. In **Chapter 2** I studied the effects of cerebral small vessel disease (CSVD) on brain functioning and structural connectivity in MCI using fMRI and DTI. CSVD is a fairly common condition in elderly, which affects the small vessels of the brain supplying the white matter and deeper grey matter regions, visible on MRI as white matter hyperintensities and lacunar infarcts. CSVD contributes to cognitive and clinical symptoms in MCI, but the underlying mechanisms are unclear. **Chapter 2.1** introduces the terminology and criteria for MCI and vascular cognitive impairment and discusses the applicability of recently proposed criteria for prodromal AD and VaD. The applicability of the new criteria within a clinical cohort of MCI patients was hampered by the fact that the criteria are insufficiently specific and need further operationalization in order to use them in a clinical setting. The focus on specifically Alzheimer or cerebrovascular pathology furthermore disregards the fact that Alzheimer and cerebrovascular pathology often co-exist. **Chapter 2.2** describes the results of an episodic memory based fMRI study used to unravel the effects of CSVD on memory related brain functioning in MCI. Presence and extent of vascular burden in MCI patients related to decreased medial temporal

lobe activation, an important brain region for memory functioning. In **Chapter 2.3** we assessed a working memory related fMRI task consisting of conditions with increasing working memory load in MCI patients with and without CSVD. The presence of CSVD in MCI patients was related to impaired deactivation in a brain region known to be involved in neural network functioning. These networks exist of brain regions that are known to function collaboratively and are important in cognitive functioning. MCI patients without CSVD showed an activation pattern with 'hyperactivation' during vigilance and 'hypoactivation' at a relatively difficult -high working memory load- task. The finding of a similar cognitive profile in MCI patients with and without CSVD combined with differences in brain functioning suggests that different types of pathology can contribute to cognitive impairment through different underlying functional pathways. **Chapter 2.4** describes the results of a diffusion tensor imaging study in MCI patients, by which we studied the effects of CSVD in MCI on the normal appearing white matter microstructure of the whole brain and of fiber tracts important for neural network functioning. The presence of CSVD in MCI patients was related to widespread microstructural damage in the normal appearing white matter, whereas MCI patients without CSVD showed microstructural damage restricted to a small region within the temporal lobe. The structural integrity of the fiber tracts interconnecting remote brain regions in the neural network was affected in MCI patients with CSVD, and related to the extent of vascular burden.

Summarizing our multimodal neuroimaging findings, CSVD in MCI affects the microstructure of the white matter, and moreover influences neural functioning during cognitive performance. We postulate that the mechanism through which CSVD affects cognition, or contributes to cognitive deterioration in MCI is neural network interference, as a consequence of damaging the interconnecting fiber tracts.

In **Chapter 3** I studied patterns of impaired brain perfusion underlying cognitive symptoms in early onset AD, FTD and progressive supranuclear palsy (PSP), using perfusion single-photon emission computed tomography (SPECT). Early discrimination between these neurodegenerative conditions during life is hampered by the fact that clinical and cognitive symptomatology can overlap. **Chapter 3.1** describes a study aimed at identifying the functional substrate of episodic memory impairment in behavioral variant FTD (bvFTD). For this purpose, we quantitatively compared brain perfusion patterns in bvFTD patients with and without episodic memory impairment. BvFTD patients with memory impairment showed lower perfusion in the right temporal lobe. Perfusion within this region was related to a clinical measure of memory impairment in the entire group of bvFTD patients. In **Chapter 3.2**, we subdivided familial FTD cases on the basis of their pathological subtype and genetic defect and studied the underlying perfusion patterns and relationship with clinical features. Patients with familial FTD and TDP-43 pathology had less perfusion in the parietal lobe when compared with patients with a *MAPT* genetic

defect, while vice versa FTD patients with a *MAPT* genetic defect showed less perfusion of the left temporal and mediofrontal lobe in comparison with familial FTD cases with TDP-43 pathology. In the entire group of patients, memory impairment was related to hypoperfusion of the parietal lobe. In **Chapter 3.3** we examined the relationship between functionally affected brain regions and cognitive impairment in PSP, and compared this relationship to that in FTD-tau patients. We found a similar relationship between hypoperfusion of the anterior cingulate cortex and executive dysfunctioning in PSP and FTD patients.

Concluding, we found that while the underlying disease or pathology type can differ, clinical and cognitive symptoms may overlap as a consequence of similarities in affected brain regions.

In **Chapter 4** I describe main findings of this thesis, discuss methodological considerations and give suggestions for future research regarding functional neuroimaging in dementia.

SAMENVATTING

Dementie definieert een klinisch syndroom dat gekenmerkt wordt door cognitief verval en problemen bij het uitvoeren van alledaagse activiteiten. De ziekte van Alzheimer (AD) is de meest voorkomende oorzaak van dementie, gevolgd door vasculaire dementie (VaD) bij ouderen en door frontotemporale dementie (FTD) bij aanvang op jonge leeftijd. De meeste dementiesubtypen hebben een langzaam progressief beloop, waardoor het mogelijk is om een prodromaal dementiestadium, een fase met vroege voortekenen, te onderscheiden dat ook wel met mild cognitive impairment (MCI) of 'milde cognitieve stoornissen' aangeduid wordt. Deze patiënten tonen cognitieve (denk-) stoornissen, ernstiger dan verwacht op basis van hun leeftijd of opleidingsniveau, maar die niet interfereren met de alledaagse bezigheden. Met behulp van functionele neuro-imaging, hersenscan, technieken zijn wij in staat om veranderingen in specifiek het functioneren van het brein te onderzoeken. Deze technieken kunnen daarom gebruikt worden om onderzoek te doen naar dementiesubtypen en het prodromale stadium van dementie, zoals beschreven in **Hoofdstuk 1**, de inleiding van het proefschrift.

In dit proefschrift worden studies beschreven die gebruik hebben gemaakt van verschillende neuroimaging, of hersenscan technieken. Een eerste techniek die gebruikt is, is functionele MRI. Deze techniek maakt het mogelijk om het functioneren van het brein te onderzoeken, door veranderingen in de bloedtoevoer naar actieve hersengebieden te meten. Door tijdens het scannen gestandaardiseerde cognitieve taken uit te voeren, kunnen we specifiek kijken welke hersengebieden actief worden als het resultaat van deze taak. Een geavanceerde structurele MRI-techniek gebruikt in dit proefschrift is diffusion tensor imaging (DTI). Met behulp van DTI kunnen wij de microstructuur van de witte stof, de verbindingsbanen van het brein, onderzoeken. Een techniek die veel gebruikt wordt voor diagnostische doeleinden is single-photon emission computed tomography (SPECT). Met behulp van perfusie SPECT kunnen wij de doorbloeding van het brein in kaart brengen. Wanneer een hersengebied verminderd van bloed wordt voorzien, dan reflecteert dit een verminderd metabolisme in deze regio, wat gelijk staat aan een afname van het functioneren van de hersencellen in dit gebied. Het kwantitatief vergelijken van hersenactivatie, witte stof integriteit en doorbloeding van hersengebieden kan ons helpen om specifieke onderzoeksvragen te beantwoorden.

De focus van dit proefschrift was tweeledig. **Hoofdstuk 2** omvat studies gericht op de invloed van beschadigingen van de kleine bloedvaten van het brein, ook wel cerebral small vessel disease (CSVD) genoemd, in MCI patiënten. Deze beschadigingen komen veel voor bij oudere mensen en worden veroorzaakt door hoge bloeddruk en andere vasculaire risicofactoren. De gevolgen van CSVD kunnen gevisualiseerd worden met behulp van MRI, en vernemen wij als laesies van de witte stof, de verbindingsbanen van het brein, evenals kleine infarcten in dieper gelegen zenuwcelkernen. Deze specifieke

beschadigingen zijn geassocieerd met cognitieve en klinische achteruitgang in MCI, maar de onderliggende mechanismen zijn onduidelijk. **Hoofdstuk 2.1** introduceert de terminologie en criteria voor MCI en 'vascular cognitive impairment', in het licht van de recente ontwikkeling van nieuwe criteria voor de vroege stadia van AD en VaD. De klinische toepasbaarheid van deze nieuwe criteria wordt belemmerd door het feit dat zij niet voldoende specifiek zijn met betrekking tot het gebruik in de klinische praktijk. Daarnaast ligt de focus van de criteria op hersenbeschadigingen specifiek veroorzaakt door de ziekte van Alzheimer dan wel vasculaire factoren, en wordt daardoor het gegeven dat Alzheimer en vasculaire beschadigingen vaak gezamenlijk voorkomen genegeerd. **Hoofdstuk 2.2** beschrijft de resultaten van een geheugen-gerelateerde fMRI studie in MCI patiënten. Het doel van deze studie was het in kaart brengen van de effecten van CSVD op geheugen geassocieerd functioneren van het brein in MCI patiënten. Uit deze studie bleek dat de ernst van de witte stof beschadigingen veroorzaakt door CSVD, gerelateerd was aan verminderde activatie van de mediale temporaalkwab, een hersengebied betrokken bij het geheugen, bij patiënten met MCI en CSVD. **Hoofdstuk 2.3** betreft een fMRI studie bij MCI patiënten waarbij gebruik gemaakt is van een werkgeheugentaak bestaande uit meerdere condities met oplopende werkgeheugenbelasting. Patiënten met MCI en CSVD lieten gestoorde deactivatie zien in een regio betrokken in functionele netwerken, netwerken van hersengebieden die gezamenlijk actief worden en belangrijk worden geacht in cognitief functioneren. MCI patiënten zonder CSVD vertoonden verhoogde hersenactivatie tijdens een relatief eenvoudige werkgeheugentaak, en een verlaagde hersenactivatie tijdens een relatief moeilijke werkgeheugentaak. Dit zou kunnen wijzen op overcompensatie in hersenactivatie bij een gemakkelijke taak, en een verval van hersenactivatie bij een moeilijke taak, waarschijnlijk niet meer goed uit te voeren door MCI patiënten. Interessant hierbij is dat MCI patiënten met en zonder CSVD eenzelfde cognitief profiel vertoonden, met vooral geheugenproblemen. In het licht van de gevonden verschillen in hersenactivatie suggereren onze bevindingen dat verschillende vormen van hersenbeschadiging bij kunnen dragen aan cognitieve stoornissen in MCI patiënten. **Hoofdstuk 2.4** beschrijft de resultaten van een DTI studie waarbij gekeken is naar de effecten van CSVD in MCI op microstructurele integriteit van de normaal uitziende witte stof. Dit werd onderzocht in het gehele brein en binnen vezel/verbindingsbanen die belangrijk zijn voor het functioneren van de eerder genoemde neurale netwerken. MCI patiënten met CSVD lieten wijdverspreide microstructurele witte stof beschadiging zien. Daarentegen werden bij MCI patiënten zonder CSVD, witte stof beschadigingen alleen gevonden in een klein gebied gelokaliseerd in de temporaalkwab. De structurele integriteit van de witte stof banen die belangrijk zijn voor neuraal netwerk functioneren was vooral geassocieerd met de mate van vasculaire schade in MCI.

Wanneer wij deze bevindingen samenvatten dan hebben wij gevonden dat CSVD in MCI de microstructuur van de witte stof, of verbindingsbanen van het brein, aantast. Daarnaast kunnen wij de aanwezigheid en de ernst van de vasculaire beschadigingen

relateren aan verminderde hersenactivatie en deactivatie gedurende het uitvoeren van cognitieve taken. Wij veronderstellen dat de aanwezigheid van CSVD in MCI interfereert met het functioneren van neurale netwerken, als een consequentie van het beschadigen van de verbindingen tussen de verschillende hersengebieden die betrokken zijn in deze netwerken.

In **Hoofdstuk 3** maak ik gebruik van kwantitatieve analyses van perfusie SPECT scans om patronen van de doorbloeding van het brein onderliggend aan FTD, preseniele AD, en progressieve supranucleaire paralyse (PSP) te onderzoeken. Vroege discriminatie tussen deze ziektebeelden wordt belemmerd door het feit dat de klinische en cognitieve symptomen kunnen overlappen. Met behulp van perfusie SPECT kunnen wij deze symptomen onderzoeken in relatie tot het onderliggende perfusie of hersendoorbloedings-patroon. **Hoofdstuk 3.1** richt zich op het identificeren van het functionele substraat van episodische geheugenstoornissen in FTD patiënten met de gedragsvariant, ook wel behavioral variant FTD (bvFTD) genoemd. Hiervoor vergeleken we de perfusiepatronen van bvFTD patiënten met en zonder geheugenstoornissen. BvFTD patiënten met geheugenstoornissen vertoonden een verminderde perfusie in de rechter temporaalkwab, een hersengebied betrokken bij het geheugen. Perfusie in deze regio was gerelateerd aan een klinische maat van geheugenstoornissen in de gehele groep van bvFTD patiënten. In **Hoofdstuk 3.2** hebben wij FTD patiënten onderverdeeld op basis van hun pathologische subtype en genetische defect, en bestudeerden vervolgens het onderliggende perfusiepatroon evenals de relatie tussen perfusie en klinische karakteristieken. Patiënten met familiaire FTD en na het overlijden vastgestelde TDP-43 pathologie, vertoonden verminderde perfusie in de pariëtaalkwab wanneer zij vergeleken werden met patiënten met een *MAPT* genetisch defect. Vice versa werd verminderde perfusie van de linker temporaalkwab en de mediofrontaalkwab gevonden in FTD patiënten met een *MAPT* genetisch defect ten opzichte van patiënten met familiaire FTD en TDP-43 pathology. In de gehele groep patiënten werden geheugenstoornissen gerelateerd aan een verminderde perfusie, en dus afname van het functioneren van de zenuwcellen in de pariëtaalkwab. **Hoofdstuk 3.3** is gericht op de relatie tussen functioneel afwijkende hersengebieden en cognitiestoornissen in PSP. We vonden een zelfde relatie tussen hypoperfusie van de anterieure cingulaire cortex en executief dysfunctioneren in PSP en FTD patiënten.

Wanneer wij deze bevindingen samenvatten dan vonden wij dat alhoewel de onderliggende ziekte of het pathologietype kan verschillen, de klinisch en cognitieve symptomen alsnog kunnen overlappen doordat dezelfde hersengebieden zijn aangedaan.

In **Hoofdstuk 4** bespreek ik de belangrijkste bevindingen en methodologische aspecten van mijn proefschrift, en doe ik suggesties voor toekomstig onderzoek betreffende functionele neuroimaging in dementie.

Chapter 6

Dankwoord

In dit hoofdstuk wil ik stilstaan bij iedereen die heeft bijgedragen aan de totstandkoming van dit proefschrift gedurende de afgelopen jaren.

Om te beginnen wil ik graag alle deelnemers aan de FIND-studie bedanken. Wetenschappelijk onderzoek is onmogelijk zonder uw vrijwillige inzet en medewerking. Bedankt voor uw enthousiasme voor het onderzoek en de prettige contacten.

Mijn copromotor Niels Prins heeft een grote rol gespeeld in de totstandkoming van dit proefschrift waarvoor ik hem erg dankbaar ben. Niels ik wil je bedanken voor al het vertrouwen, en de mogelijkheden die ik gekregen heb binnen het FIND-onderzoek. Jouw enthousiasme, rust, zorgvuldigheid en betrokkenheid waren de basis van de FIND-studie en maakten onze samenwerking erg prettig. Ik hoop deze in de toekomst voort te kunnen zetten!

Ook mijn promotoren Peter Koudstaal en John van Swieten wil ik bedanken voor hun onmisbare bijdrage aan dit proefschrift en de mogelijkheden die zij voor mij creëerden binnen de Neurologie, op het raakvlak 'neurovasculair'/'neurodegeneratief'. Peter, al lag mijn onderzoek niet helemaal in jouw 'field of expertise', jouw ondersteuning was essentieel voor dit proefschrift. Vooral wat betreft het monitoren van het promotietraject, de planning en '*politieke*' zaken ben ik je veel dank verschuldigd. Hartelijk dank voor alle inspanningen en de fijne samenwerking. John, in de afgelopen jaren heb jij me niet alleen ondersteund in het onderzoek, maar heb je mij ook de kans gegeven om binnen het Alzheimercentrum zuidwest Nederland te werken. Een onwijs leuke uitdaging die ik hoop voort te mogen zetten. Jouw directheid, enthousiasme en betrokkenheid hebben de afgelopen jaren essentieel bijgedragen aan dit proefschrift, bedankt hiervoor.

De expertise, steun en betrokkenheid van Marion Smits, mijn copromotor, waren van grote waarde bij het fMRI en DTI onderzoek beschreven in dit proefschrift. De steun beperkte zich echter niet alleen tot MRI-gerelateerde zaken maar betrof ook mentale steun. Marion heel erg bedankt voor onze fijne samenwerking de afgelopen jaren!

Graag wil ik alle leden van de promotiecommissie bedanken voor hun plaats hierin en voor de kritische blik die zij op mijn proefschrift hebben geworpen: Prof.dr. Wiro Niessen, Prof. dr. Serge Rombouts, Prof.dr. Geert Jan Biessels, Prof.dr. Aad van der Lugt en Dr. Francesco Mattace Raso.

Co-auteurs van de papers beschreven in dit proefschrift ben ik erkentelijk voor hun inzet, intellectuele bijdrage en alle discussies rondom mijn artikelen. Met name wil ik

even stilstaan bij de bijdrage van Freddy van der Veen, die mij heeft geholpen met de beginselen van de fMRI ten tijde dat de FIND-studie nog mijn afstudeeronderzoek heette. Tom den Heijer wil ik speciaal bedanken voor zijn inzet en steun bij het schrijven van mijn eerste fMRI paper ('de wondere wereld van de fMRI'). Daarnaast wil ik Marius de Groot bedanken voor alle wonderen die hij met DTI kan verrichten. 'Toen onze blob een blobje was…' Na een lange aanloop/ voorbereiding, toch in zeer korte tijd een heel 'tof' artikel geschreven!

Een taak-gerelateerd fMRI onderzoek brengt veel stress met zich mee, vooral ten tijde van het scannen zelf. Daarom ben ik Sylvia Bruininks dankbaar voor haar expertise en kunde. Dankzij haar kon ik mij focussen op de deelnemers'/mijn eigen stress-levels.

Ik wil Inge de Koning en Roos de Graaf bedanken voor de ondersteuning vanuit de neuropsychologie. Onze samenwerking wat betreft de SPECT en FIND papers en de mogelijkheden die ik kreeg om neuropsychologisch onderzoek uit te voeren bij deelnemers aan de FIND-studie hebben essentieel bijgedragen aan dit proefschrift, bedankt hiervoor.

Het secretariaat van de Neurologie en Geriatrie wil ik graag bedanken voor de fijne samenwerking en alle ondersteuning.

Alle collega's van het Alzheimercentrum zuidwest Nederland, de communicatie Erasmus MC en Havenziekenhuis en het Vriendenfonds Erasmus MC wil ik bedanken voor de prettige samenwerking gedurende de afgelopen 2 jaar. Ik heb het als een voorrecht ervaren om mij naast het promoveren bezig te kunnen houden met de logistiek rondom het opzetten van het Alzheimercentrum, de invitational conference, het zorgpad en de opening.

Collega's van de Radiologie/fMRI meeting ben ik dankbaar voor alle gedeelde kennis, discussies en methodologische hulp. Met name wil ik Maartje, Ivo, Gabry en Reshmi hier noemen en natuurlijk –op speciale plek- mijn fMRI buddies Carolina en Rebecca. Thanks guys for lots and more!

Graag wil ik alle collega-onderzoekers van de 22^{e} verdieping bedanken voor de collegialiteit en gezelligheid. Specifiek wil ik stilstaan bij de bijdrage van mijn (oud) Ee2238 kamergenoten: Laura, Harro, Wan Zheng, Elise, Judy, Kirsten, Tse, Janneke en Lize. Niet alleen een mooi uitzicht op de 22^{e}; iedere dag een feestje! Bedankt voor het lachen, de thee met –vele- versnaperingen, het lafloze borrelen, maar ook de hulp en steun die ik van jullie krijg met betrekking tot langdurige analyses, schrijven van artikelen, reviewercommentaar en het Alzheimercentrum. Wan en Elise, ik ben heel erg blij dat jullie naast me staan op 7 december, ik kan me geen betere mental coaches wensen!

Alle mensen die bijgedragen hebben aan het leven ‘naast’ deze promotie wil ik hier graag enorm voor bedanken. Hierbij wil ik specifiek noemen: mijn broers Frans en Wout, tante Cora, mijn oma’s en opa; mijn allertofste jaarclub Decalitesse: Anniek, Elbrich, Francien, Inge, Jocelyn, Karin, Kim, Margo en Mieke; thuis-thuis vriendinnen: Marianne, Marianne, Karolien, Leonie; Neuroscience/vakantie/stapvriendinnetjes: Lianne, Sarah en Veroni; Grunnbuddies: Elsje, Maike, Grace, Davey en Cor Jan. Iemand die ook niet aan deze categorie mag ontbreken is Arno, ik wil jou bedanken voor alles wat we de afgelopen jaren samen hebben beleefd.

Mijn laatste woorden wil ik richten tot mijn ouders. Pap en mam bedankt voor jullie onbegrensde vertrouwen, liefde en onvoorwaardelijke steun. Jullie zijn trots op alles wat ik bereik en leven mee als dingen niet lopen zoals gepland/gewild. Ik heb enorm veel geleerd van jullie vermogen te relativeren en levensgeluk, dankjulliewel voor alles!

Janne

Alle mensen die verwacht hadden een plekje in dit dankwoord te krijgen, maar die ik desondanks niet heb genoemd wil ik bedanken voor de impliciete bijdrage die zij aan mijn proefschrift hebben geleverd.

Chapter 7

About the author

CURRICULUM VITAE

Jacomina Maria (Janne) Papma was born on July 17, 1984, in Noordoostpolder, the Netherlands, where she lived with her family until she completed secondary school at the Emelwerda College, Emmeloord, in 2002. She studied Psychology at the University of Groningen, and received her master degree with the specialization *Psychology, Brain and Behaviour* in 2007. In the same year she started the research master Behavioural and Cognitive Neuroscience at the University of Groningen. In 2009 she moved to Den Haag to carry out her major thesis research at the Erasmus MC in Rotterdam, working at the FIND project together with her supervisor Niels D. Prins. She graduated the research master Cum Laude in 2009, and started her PhD research at the department of Neurology, Erasmus MC, Rotterdam, of which the results are described in the current thesis. In addition to her research, she became responsible for the opening of the Alzheimercentrum zuidwest Nederland from January 2011 onwards.

Janne Papma will receive her PhD degree in December 2012 for her studies on functional neuroimaging in dementia. She currently lives in Rotterdam, and will continue her research into the prospective value of functional and structural neuroimaging in mild cognitive impairment at the Erasmus MC. At the same time she will be coordinator of the Alzheimercentrum zuidwest Nederland.

LIST OF PUBLICATIONS

Seelaar H, **Papma JM**, Garraux G, de Koning I, Reijs AEM, Valkema R, Rozemuller AJM, Salmon E, van Swieten JC. Brain perfusion patterns in familial frontotemporal lobar degeneration. Neurology 2011; 77(4): 384-392.

Chiu WZ, **Papma JM**, de Koning I, Donker Kaat L, Seelaar H, Reijs AEM, Valkema R, Hasan D, Boon AJW, van Swieten JC. Midcingulate involvement in progressive supranuclear palsy and tau-positive frontotemporal dementia. J Neurol Neurosurg Psychiatry 2012; 83(9): 910-915.

Raaphorst J, Beeldman E, Schmand B, Berkhout J, Linssen WH, Van den Berg LH, Pijnenburg YA, Grupstra HF, Weikamp JG, Schelhaas HJ, **Papma JM**, Van Swieten JC, De Visser M, De Haan RJ. The ALS-FTD-Q: A new screening tool for behavioral disturbances in ALS. Neurology 2012; 79 (13): 1377-1383.

Papma JM, Seelaar H, de Koning I, Hasan D, Reijs AEM, Valkema R, Prins ND, van Swieten JC. Episodic memory impairment in frontotemporal dementia: a ^{99m}Tc-HMPAO SPECT study. Curr Alzheimer Res 2012; Published online 2012 Sep 25.

IJsselstijn L, **Papma JM**, Dekker L, Calame W, Stingl C, Koudstaal P, Prins N, Sillevis Smith P, Luider T. Serum proteomics in amnestic mild cognitive impairment. Proteomics; Major revision

Papma JM, Smits M, de Koning I, Mattace Raso FU, van der Lugt A, Vrooman HA, van Swieten JC, Koudstaal PJ, van der Veen FM, Prins ND. Cerebral small vessel disease influences encoding in MCI: an episodic memory related fMRI study. J Alzheimers Dis; Major revision.

Papma JM, den Heijer T, de Koning I, Mattace Raso FU, van der Lijn F, van der Lugt A, van Swieten JC, Koudstaal PJ, Smits M, Prins ND. The influence of cerebral small vessel disease on default mode network deactivation in mild cognitive impairment. Neuroimage Clinical; Major revision.

Papma JM, de Groot M, de Koning I, Mattace Raso FU, van der Lugt A, Vernooij MW, Niessen WJ, van Swieten JC, Koudstaal PJ, Prins ND, Smits M. Cerebral small vessel disease affects white matter microstructure in mild cognitive impairment. Human Brain Mapp; Major revision.

Papma JM, Smits M, Mattace Raso FU, Niessen WJ, de Koning I, Koudstaal PJ, van Swieten JC, Prins ND. Clinical applicability of 'mild cognitive impairment due to AD' and vascular mild cognitive impairment. Submitted.

PHD PORTFOLIO

PhD student: Janne Papma
Department: Neurology
Research school: COEUR
PhD period: 2009-2012

1. Phd training

	Year	ECTS
Academic and research skills		
Scientific English writing	2010	2.0
Introduction to data analysis	2010	5.7
Workshop Endnote & Literature search	2010	0.2
COEUR PhD day	2010	0.4
Minicourse methodology and grant proposals	2011	0.4
Indepth courses/workshops		
Basic and advanced fMRI course, Maastricht	2009	1.5
ESMRMB Hands-On MRI course on DTI & fMRI, Rotterdam	2009	1.5
Cardiovascular medicine, Rotterdam	2009	1.5
Cardiovascular imaging and diagnostics, Rotterdam	2010	1.5
Statistical Parametric Mapping fMRI, London	2010	1.5
Imaging workshop for MDs, Rotterdam	2010	0.4
Principles of genetic epidemiology, Rotterdam	2011	5.0
(Inter-)national conferences/seminars		
Endo-Neuro-Psycho Meeting, Lunteren; poster	2009	0.4
Geriatriedagen, Rotterdam; oral presentation	2010	0.8
Human Brain Mapping, Barcelona; poster	2010	1.5
Dementie update 2010, Frontotemporale dementie, Amstelveen	2010	0.3
Seminar on healthy aging; Rotterdam; oral presentation	2011	0.8
Alzheimer's Association International Conference, Paris; poster	2011	1.5
Dementie update 2011, Mild Cognitive Impairment, Amstelveen	2011	0.3
Congres NWO, Brain and cognition, Utrecht	2011	0.3
8th International Conference on Frontotemporal dementia, Manchester; poster	2012	1.5
Other		
Organization and coordination Invitational conference Alzheimercentrum zuidwest Nederland	2011	3.0
Organization and coordination Opening Alzheimercentrum zuidwest Nederland	2012	7.0

2. Teaching

Supervising 2 master theses	2010-2012	3.0
Total:		**42.0**

LIST OF ABBREVIATIONS

^{99m}Tc-HMPAO	technetium-99m labeled hexamethylpropyleneamine oxime
15-WVLT	15 word verbal learning test
Aβ	Amyloid beta
ACC	Anterior cingulate cortex
AD	Alzheimer's disease
A-FTD	Amnestic frontotemporal dementia
ALS	Amyotropic lateral sclerosis
APOE	*Apolipoprotein E*
BA	Brodmann area
BOLD	Blood oxygen level dependent
bvFTD	Behavioral variant frontotemporal dementia
CDR	Clinical dementia rating scale
CGC	Cingulum along the cingulate cortex
CGH	Cingulum along the hippocampal cortex
CSF	Cerebral spinal fluid
CST	Corticospinal tract
CSVD	Cerebral small vessel disease
CVD	Cerebrovascular disease
DMN	Default mode network
DTI	Diffusion tensor imaging
FA	Fractional anisotropy
FOV	Field of view
FDG	Fludeoxyglucose
FLAIR	Fluid attenuated inversion recovery
FMI	Forceps minor
fMRI	Functional magnetic resonance imaging
FTD	Frontotemporal dementia
FTLD	Frontotemporal lobar degeneration
FWE	Family wise error
GRN	*Progranulin*
MAPT	*Microtubule associated protein tau*
MCI	Mild cognitive impairment
MCC	Midcingulate cortex
MCI-V	MCI of the vascular type
MCP	Middle cerebellar peduncle
MD	Mean diffusivity

MMSE	Mini mental state examination
MND	Motor neuron disease
MNI	Montreal Neurological Institute
MRI	Magnetic resonance imaging
MTL	Medial temporal lobe
NA-FTD	Non-amnestic frontotemporal dementia
NAWM	Normal appearing white matter
PCC	Posterior cingulate cortex
PET	Positron emission tomography
PiB	Pittsburgh Compound-B
PSP	Progressive supranuclear palsy
ROC	Receiver operation characteristic
ROI	Region of interest
SD	Semantic dementia
SLF	Superior longitudinal fasciculus
SPECT	Single photon emission computed tomography
SPM	Statistical parametric mapping
SVC	Small volume correction
TBSS	Tract based spatial statistics
TDP	TAR DNA binding protein
TE	Echo time
TI	Inversion time
TIV	Total intracranial volume
TMT	Trail making test
TR	Repetition time
UGD	Unknown gene defect
VaD	Vascular dementia
VaMCI	Vascular mild cognitive impairment
VBM	Voxel based morphometry
VCI	Vascular cognitive impairment
VCIND	Vascular cognitive impairment no dementia
WLM	Word list memory test
WMH	White matter hyperintensity